

PROVENANCE ANALYSIS BASED ON DETRITAL-ZIRCON-AGE SPECTRA OF THE LOWER CRETACEOUS FORMATIONS IN THE RYOSEKI-MONOBEGAWA AREA, OUTER ZONE OF SOUTHWEST JAPAN

Takuji IKEDA¹, Takuya HARADA¹, Yoshikazu KOUCHI¹, Sachiko MORITA¹,
Miwa YOKOGAWA¹, Koshi YAMAMOTO² and Shigeru OTOH¹

¹ Graduate School of Science and Engineering, University of Toyama, 3190 Gofuku, Toyama 930-8555, Japan

² Graduate School of Environmental Studies, Nagoya University, Furo-cho, Chikusa-ku, Nagoya, Aichi 464-8601, Japan

ABSTRACT

Detrital-zircon-age spectra of the Lower Cretaceous Monobegawa and Nankai groups in the Ryoseki–Monobe area, Southwest Japan, are studied to make a provenance analysis and evaluate previous tectonic models. We also studied, for reference, the U–Pb zircon age of igneous rock cobbles, the detrital-zircon-age spectra of sandstone cobbles, and the detrital-zircon-age spectra of a sandstone samples of the Permian basement. The results are as follows. (1) The Ryoseki Formation of the Monobegawa Group contains many Permian zircons that were presumably reworked from the Permian basement sandstone. (2) The two groups contain Early Cretaceous detrital zircons and igneous rock cobbles of some 125 Ma, suggesting active acidic volcanism in the hinterland. (3) The Yunoki Formation of the Monobegawa Group contains 18% of 460–400 Ma zircons. It is concluded that the hinterland of the two groups were the Zhejiang–Fujian provinces of South China, where 145–100 Ma and 460–400 Ma felsic igneous rocks are widely exposed.

Key words : detrital zircon, Monobegawa Group, Nankai Group, provenance analysis, sinistral strike-slip motion, Southwest Japan

池田拓司・原田拓也・高地吉一・森田祥子・横川実和・山本鋼志・大藤 茂 (2016) 碎屑性ジルコン年代分布を用いた西南日本外帯領石一物部地域下部白亜系の後背地解析. 福井県立恐竜博物館紀要 15: 33–84.

西南日本外帯高知県領石一物部地域に分布する、秩父累帯下部白亜系物部川層群及び南海層群砂岩の碎屑性ジルコンのウラン–鉛年代を検討した。また、礫岩中の砂岩礫・火成岩礫及び物部川層群基盤のペルム系砂岩のジルコン年代も検討した。結果と考察は以下の通りである。①物部川層群領石層砂岩はペルム紀ジルコンを多量に含み、これらは基盤のペルム系砂岩からリワークされたと見られる。②両層群は前期白亜紀の碎屑性ジルコンを含み、火成岩礫のジルコン年代も約 125 Maであることから、後背地では堆積と同時に活発な酸性火成活動が生じていた。③物部川層群柚ノ木層中部層砂岩は 460–400 Maのジルコンを豊富に含む。以上より、両層群は、145–100 Ma及び 460–400 Maの酸性火成岩が露出する南中国浙江省～福建省を後背地にしたと解釈した。

INTRODUCTION

Lower Cretaceous fluvial to shallow marine formations occur in the Chichibu Composite Belt in the Outer Zone of Southwest Japan. Tashiro (1985) and Tashiro and Ikeda (1987) divided them from lithofacies and faunal assemblages into the Monobegawa, Nankai, and Pre-Sotoizumi groups (Tashiro, 1985; Tashiro and Ikeda, 1987). Tashiro (1985, 1986, 1994) suggested that the

bivalve fauna of the Nankai Group (Tethyan Fauna) indicates a warmer environment than that of the Monobegawa Group (Northern-Tethyan Fauna) and that the Nankai Group formed to the south of the Monobegawa Group. Since the Nankai Group lies on the Pacific side of the Monobegawa Group, Tashiro (1985, 1986, 1994) presumed that an arc-subparallel sinistral strike-slip fault lay between the two groups and had carried the Nankai Group relatively northward by the Albian. Matsukawa and Eto (1987), on the other hand, attributed the lithofacies and faunal differences between the two groups in the Katsuura area of Tokushima Prefecture, 80 km to the east of the study area, to the differences in sedimentary environments and ocean currents

Received August 11, 2016. Accepted November 24, 2016.

Corresponding author — Takuji IKEDA

E-mail: takujiikeda2000@yahoo.co.jp

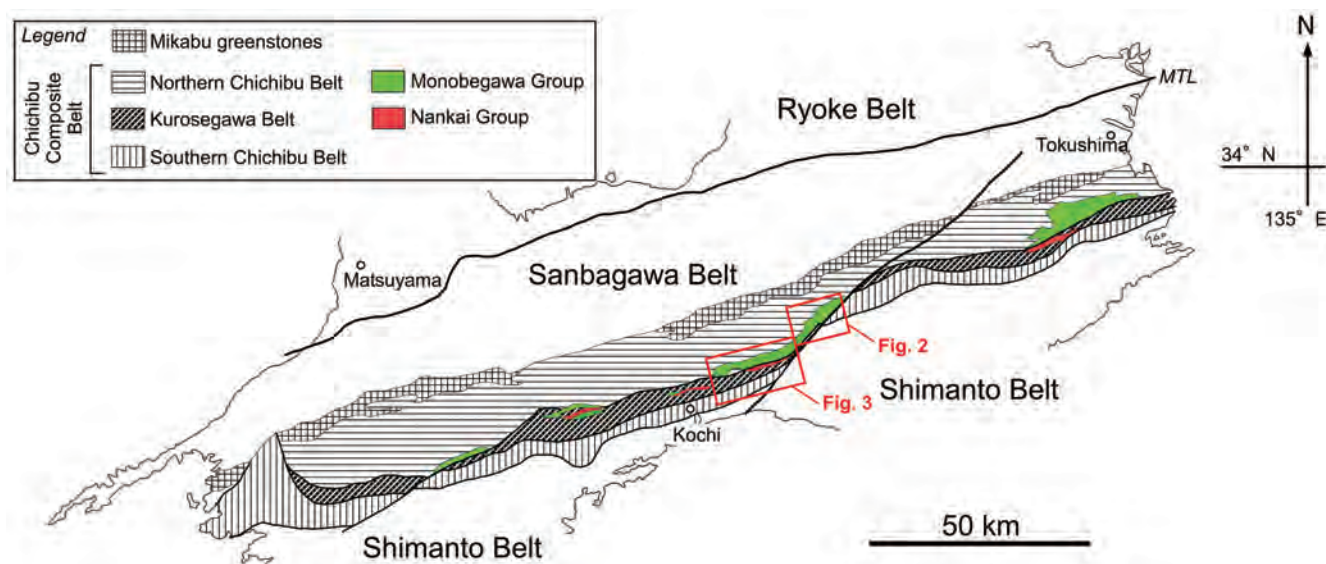


FIGURE 1. Index map showing the distribution of the Lower Cretaceous strata of the Chichibu Composite Belt and the locations of the Monobe and Ryoseki-Birafu areas drawn in Figs. 2 and 3. Modified after Yamakita (1998).

in a single sedimentary basin. They, however, also suggested a possibility of the initial separation of the basin because of the difference in clast composition of Hauterivian conglomerate in the two groups. Recent studies, reporting the presence of Tethyan–North-Tethyan mixed fauna, tend to argue that the sinistral strike-slip model only cannot explain the faunal distribution in the Monobegawa and Nankai groups (Kozai and Ishida, 2003; Kozai et al., 2007; Terabe and Matsuoka, 2009).

The Cretaceous sinistral strike-slip faulting has likely affected the distribution of Mesozoic plant fossils and major pre-Aptian geologic units of Japan. Berriasian (?)–Barremian plant fossils in the continental side of Japan (Tetori-type flora) contain many common taxa with those of Northeast China and southeast Siberia. On the other hand, Oxfordian–Barremian plant fossils in the Pacific side of Japan (Ryoseki-type flora) contain many common taxa with those of South China and the Indochina and Malay peninsulas (Kimura, 1987); the Ryoseki-type flora invaded into the continental side of Japan in the Aptian (Yabe et al., 2003). The floral contrast between the continental and Pacific sides of Japan can also be explained by an arc-parallel sinistral strike-slip fault in between that carried the geologic units with the Ryoseki-type flora relatively northward (e.g., Otoh and Yanai, 1996). The sinistral strike-slip faults can be responsible for the duplication of the pairs of pre-Aptian accretionary and non-accretionary geologic units in the continental and Pacific sides of Japan (e.g., Taira and Tashiro, 1987; Yamakita and Otoh, 2000a, b). Yamakita and Otoh (2000a, b) attributed the duplication of Permian accretionary complex (AC) in the Inner and Outer zones of Southwest Japan to the Late Cretaceous sinistral strike-slip motion along the Median Tectonic Line (MTL).

We have started provenance analysis of the Jurassic and Cretaceous formations in Japan to validate the hypothesis of the

Cretaceous strike-slip faulting. In particular, detrital zircon age spectra, which reflect the changes of provenance, paleogeography, and tectonic setting, can be a powerful tool for evaluating large-scale displacements caused by plate motion (e.g., Okawa et al., 2013). In this paper, we will present the detrital zircon age spectra of sandstone samples from all the formations of the Lower Cretaceous Monobegawa and Nankai groups in the Ryoseki–Monobe area, Outer Zone of Southwest Japan (Fig. 1). We will also provide the U–Pb zircon age of igneous rock cobbles and the detrital zircon age spectra of sandstone cobbles from the conglomerate of the two groups. Moreover, we will present the detrital zircon age spectra of two pre-Cretaceous sandstone samples of the Chichibu Composite Belt for comparison. Finally, we will compare the provenance transitions of the two groups and verify the sinistral strike-slip and other related models.

GEOLOGIC SETTING

The Chichibu Composite Belt comprises three belts: the Northern Chichibu, Kurosegawa, and Southern Chichibu belts from the continental side (from present-day north to south; Yamakita, 1998). The Northern Chichibu Belt consists of a Jurassic AC, tectonically overlying Permian AC, and the unconformably covering Lower Cretaceous Monobegawa Group. The Kurosegawa Belt consists of the following geologic bodies that have been cut and fragmented by belt-subparallel faults: pre-Jurassic metamorphic rocks, serpentinite, pre-Carboniferous basement rocks, Permian (?) chaotic rocks, Permian–Jurassic shallow marine beds, Jurassic chaotic rocks, and the Lower Cretaceous Nankai Group partly covering the Upper Jurassic–lowest Cretaceous Torinosu Group (Yamakita, 1998). The Southern Chichibu Belt consists mainly of late Early Jurassic to

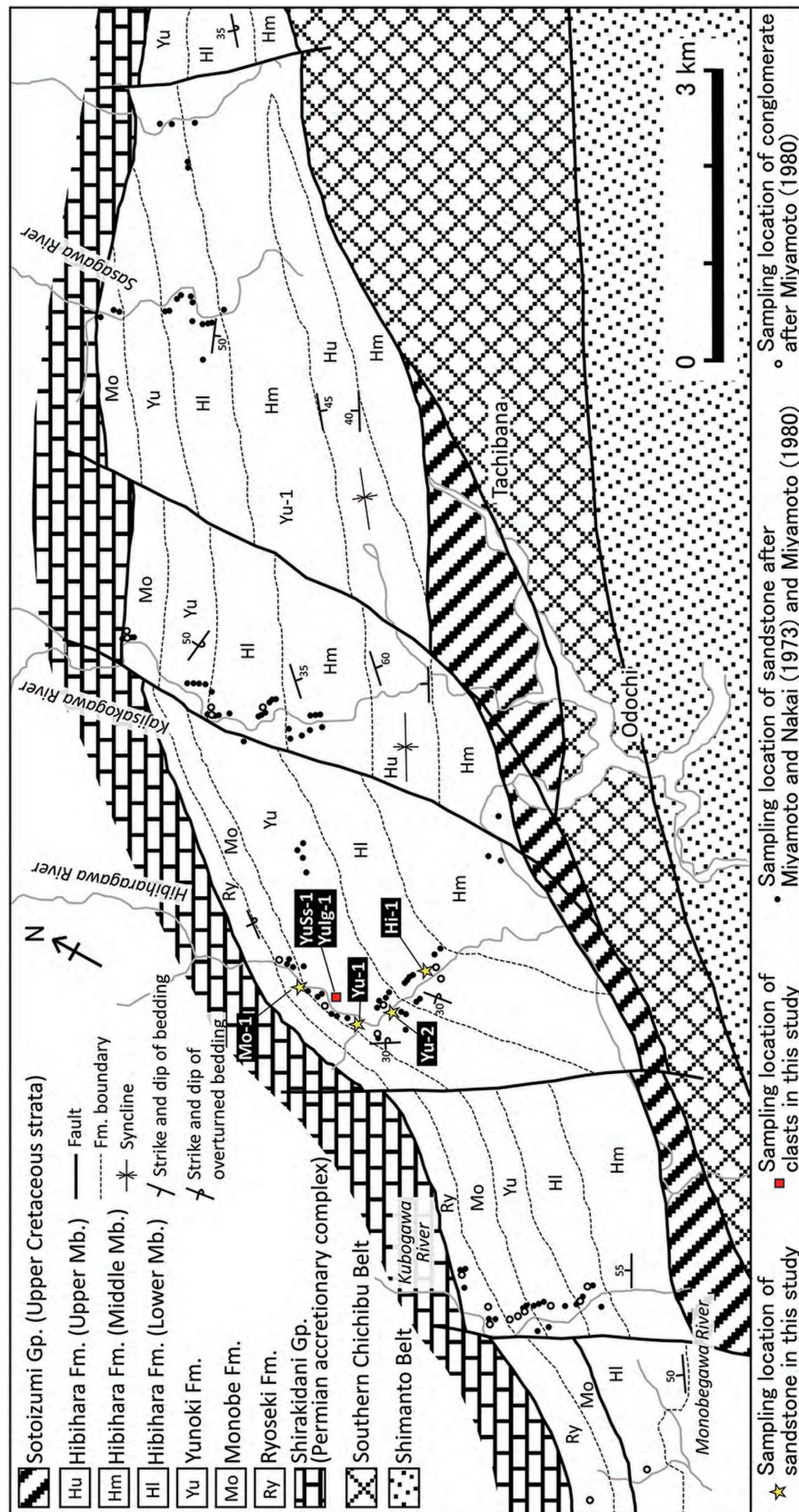


FIGURE 2. Geologic map of the Monobe area showing the sampling locations. Modified after Tashiro and Kozai (1984). Gp.: Group, Fm.: Formation, Mb.: Member.

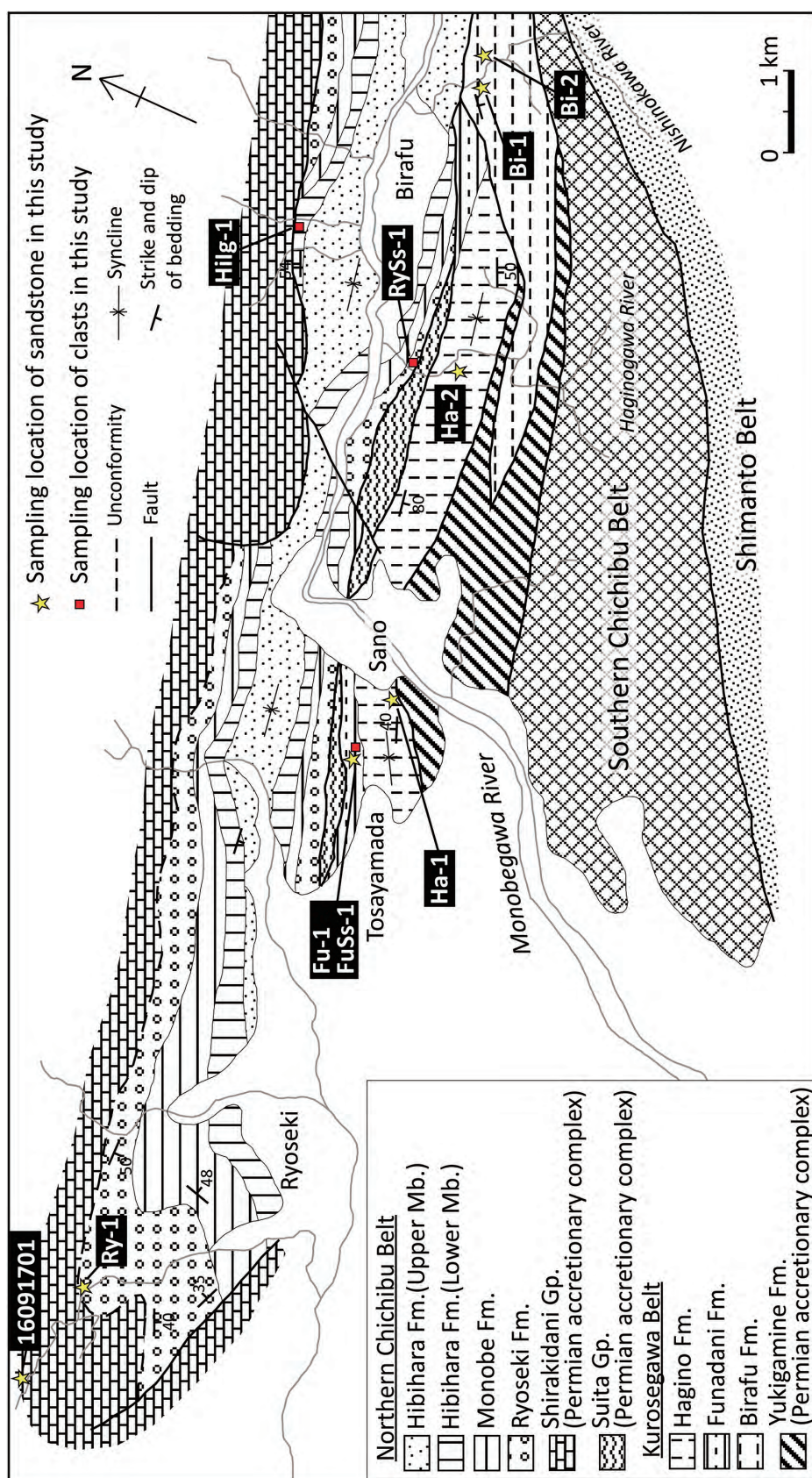


FIGURE 3. Geologic map of the Ryoseki-Birafu area showing the sampling locations. Modified after Kozai (2008). Gp.: Group, Fm.: Formation, Mb.: Member.

earliest Cretaceous AC, partly covered with the Middle Jurassic to earliest Cretaceous Naradani and Torinosu groups (Matsuoka et al., 1998).

The Monobegawa Group in the Ryoseki-Monobe area is in fault contact with or unconformably covers the Permian Shirakidani Group (AC) of the Northern Chichibu Belt on the north (Ikuma, 1980). The group is in fault contact with the Permian Suita Group, Lower Cretaceous Nankai Group, and Upper Cretaceous Sotoizumi Group on the south (Kozai et al., 2006; Hada et al., 1982; Figs. 2 and 3). The Monobegawa Group consists of the Ryoseki (Hauterivian–lowest Barremian), Monobe (Barremian), Yunoki (Aptian–lower Albian), and Hibihara (Albian) formations in ascending order and is composed mainly of siliciclastic rocks such as conglomerate, sandstone, and mudstone. Among the four formations, the Monobe Formation was originally a member of the Ryoseki Formation; Tanaka et al. (1984) separated the upper marine part of the Ryoseki Formation of the day as the Monobe Formation. The lower three formations form a conformable sequence whereas the Hibihara Formation likely covers the Yunoki Formation by disconformity (Tanaka et al., 1984; Tashiro, 1985; Fig. 4). Moreover, the Yunoki Formation does not occur in the Birafu–Ryoseki area on the west of the Kubokawa River (Kozai, 2008; Fig. 2). The Ryoseki Formation

is likely of fluvial to brackish deposits because of the abundance of red beds in the lower part and the occurrence of the Ryoseki-type flora in the upper part (Tanaka et al., 1984). The Monobe to Hibihara formations, on the other hand, are of brackish to marine deposits substantiated by abundant fossil fauna (Tashiro, 1985; Tanaka et al., 1984).

The Nankai Group in the study area consists of the Birafu (Oxfordian–Valanginian or Hauterivian), Funadani (upper Hauterivian–Barremian), and Hagino (Aptian) formations, in ascending order, and is in fault contact with the Suita and Monobegawa groups and the Permian Yukigamine Formation (Kozai et al., 2006; Fig. 3). The Nankai Group is mostly of brackish to marine deposits (Kozai and Ishida, 2000; Morino, 1993; Tashiro, 1985). There are some conflicting views on the position of the Birafu Formation. Morino et al. (1989) first defined the formation as a siliciclastic-rock formation with some Torinosu-type limestone bodies. He assigned the Birafu Formation to a member of the Nankai Group, for two reasons. First, the mudstone in the formation contained late Valanginian to Barremian radiolarians and was significantly younger than the Torinosu Group, despite the occurrence of the Torinosu-type limestone. Secondly, the formation contained many bivalve species common with those of the Nankai Group. Kozai et al. (2004), on the other

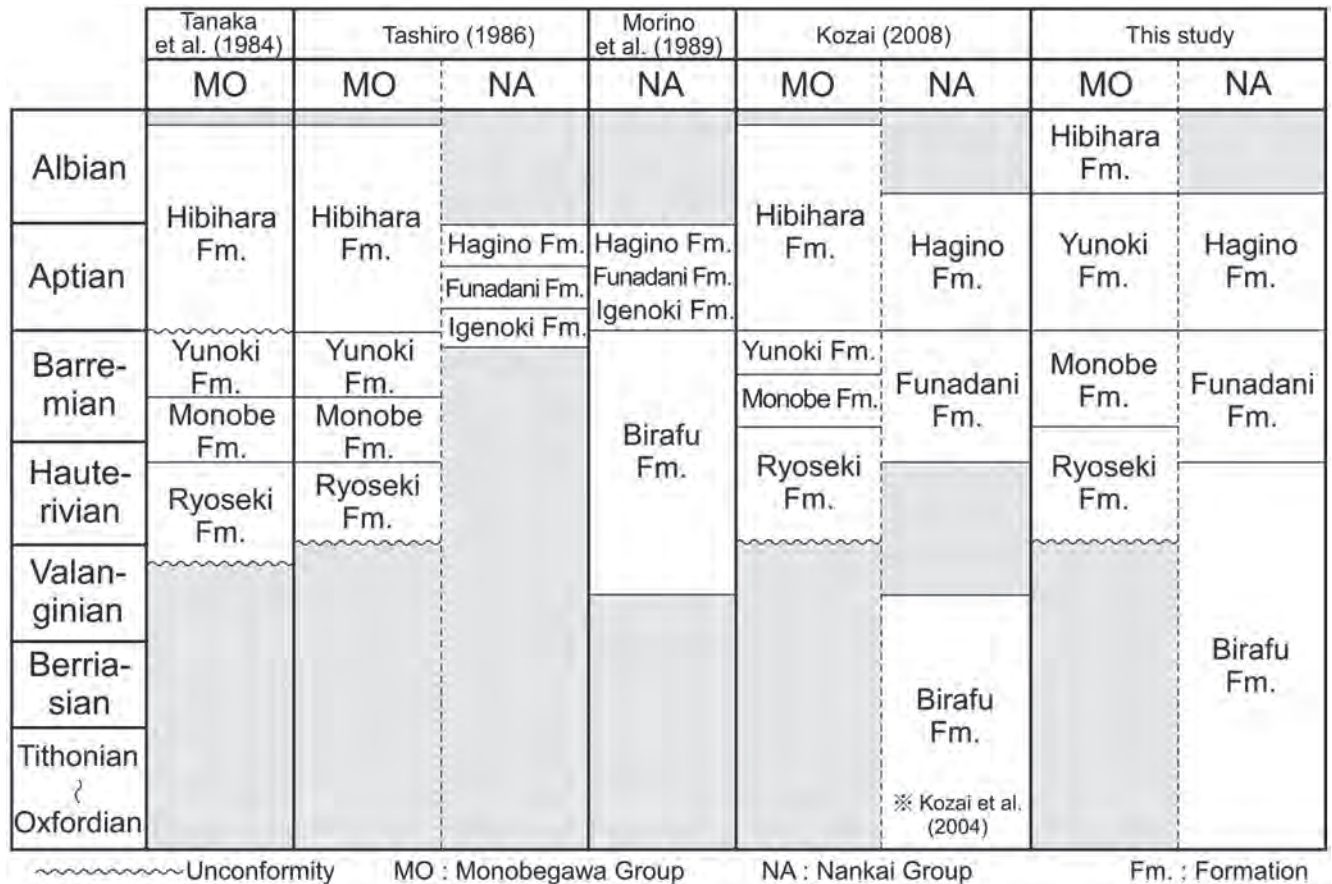


FIGURE 4. Stratigraphic correlation of the Upper Jurassic to Lower Cretaceous strata in the Ryoseki-Monobe area.

hand, separated the Birafo Formation from the Nankai Group, for three reasons. First, radiolarian and bivalve fossils indicated that the formation was of the Oxfordian to the early Valanginian and was significantly older than the Hauterivian?–Barremian Funadani Formation (Kozai, 2008), which was the oldest formation of the

Nankai Group. Secondly, the Birafo Formation is in fault contact with the Nankai Group. Finally, the southward-dipping and facing Birafo Formation is discordant in geologic structure with the Nankai Group on the north, forming a syncline. In this paper, we assign the Birafo Formation as a member of the Nankai Group

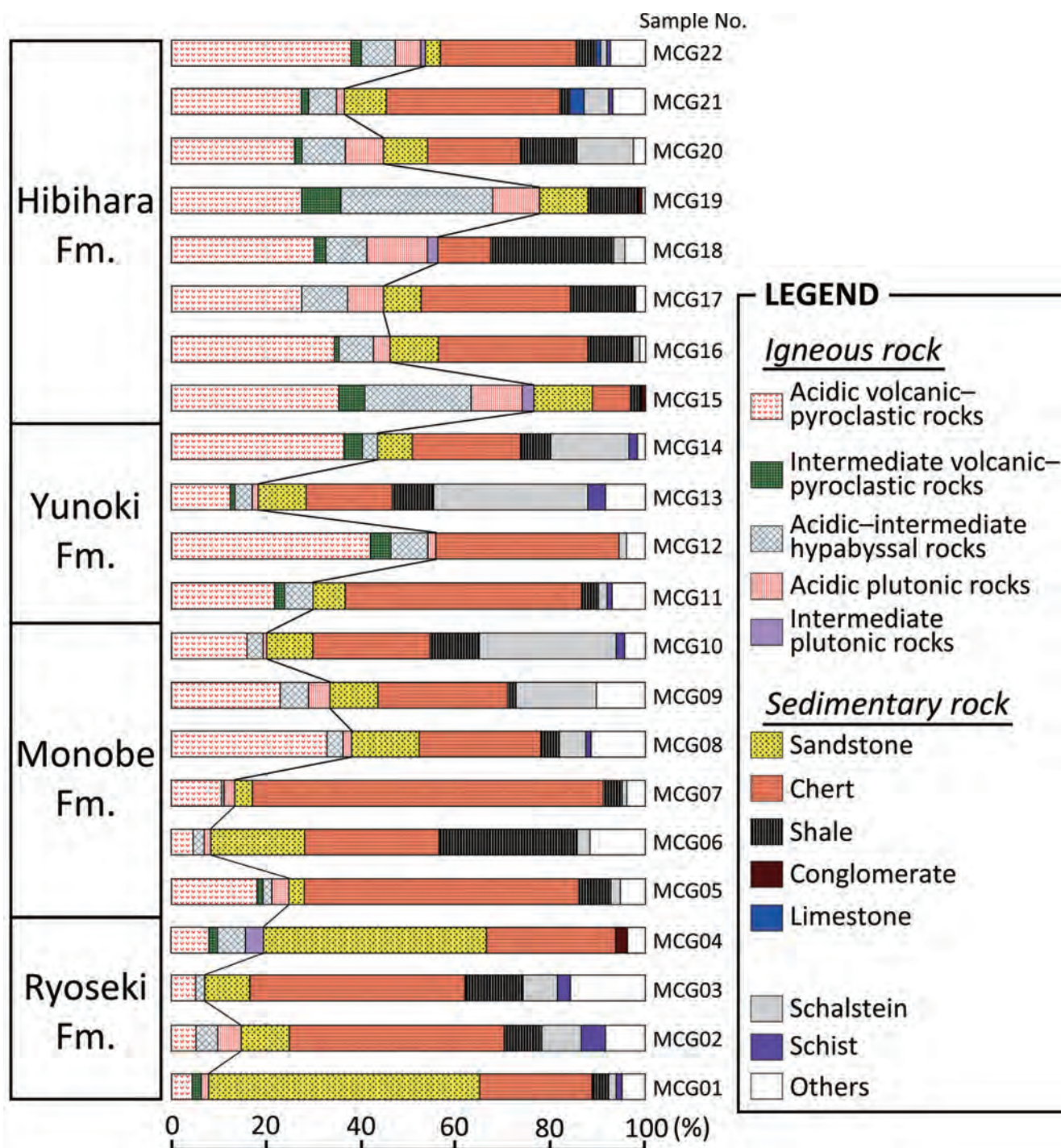


FIGURE 5. Clast compositions of the conglomerate samples from the Monobegawa Group published by Miyamoto and Nakai (1974) and Miyamoto (1980). Fm.: Formation.

from the following reasons: (1) a sandstone sample from the middle part of the Birafu Formation contains Valanginian zircons, as will be described later, and is presumably of the Valanginian or younger age; and (2) the Birafu Formation lies adjacent to the Nankai Group although a fault runs in between.

A REVIEW OF PETROGRAPHIC STUDIES OF THE LOWER CRETACEOUS CLASTIC ROCKS IN THE STUDY AREA

In this section, we will review petrographic studies of the Lower Cretaceous clastic rocks in the Ryoseki-Monobe area. Since there are differences in the distribution of each formation among the previous studies, all the sample locations of the previous studies have been plotted on the geologic map of Tashiro and Kozai (1984) and used their formation names for description.

Clast composition of conglomerates of the Monobegawa Group

Miyamoto and Nakai (1974) and Miyamoto (1980) made precise petrographic studies of the Monobegawa Group in the study area. According to the studies, the Monobegawa Group contained various kinds of clasts such as igneous-, sedimentary-, and metamorphic-rock clasts. There was a tendency that sedimentary-rock clasts prevailed in the lower part, whereas felsic-to intermediate-igneous-rock clasts increased upwards (Fig. 5). Sedimentary-rock clasts consisted mainly of chert, sandstone, and shale, among which chert clasts were most abundant. In some conglomerate horizons of the Ryoseki Formation, sandstone clasts were exceptionally more than chert clasts. The average proportion of the sedimentary-rock clasts in the Ryoseki (R), Monobe (M), Yunoki (Y), and Hibihara (H) formations was 72.8%, 59.3%, 43.1%, and 39.2%, respectively. On the other hand, the average proportion of the felsic to intermediate igneous rock clasts in the four formations was 12.5% (R), 23.1% (M), 37.1% (Y), and 54.7% (H), in ascending order. The conglomerates also contained small amounts of "schalstein" and metamorphic-rock clasts.

Sandstone modal composition of the Monobegawa Group

According to the classification of Okada (1971), the sandstone of the four formations of the Monobegawa Group was mostly assigned to lithic wacke (R; Ryoseki Formation), lithic wacke (M; Monobe Formation), lithic to feldspathic wacke (Y; Yunoki Formation), and feldspathic wacke (H; Hibihara Formation), in ascending order (Miyamoto and Nakai, 1974; Miyamoto, 1980; Fig. 6). Only one sample from the Yunoki Formation and three samples from the Hibihara Formation were assigned to arenite out of the 103 sandstone samples they studied. Thus, the greywacke type sandstone, relatively rich in the matrix, represents the Monobegawa Group. The average proportions of quartz, feldspar, rock fragments, and the matrix in the four formations were as follows. Quartz grains were 13.3% (R), 22.2% (M), 22.2% (Y), and 19.1% (H); feldspar grains were 13.8% (R), 20.8% (M), 28.8% (Y), and 37.1% (H); rock fragments were

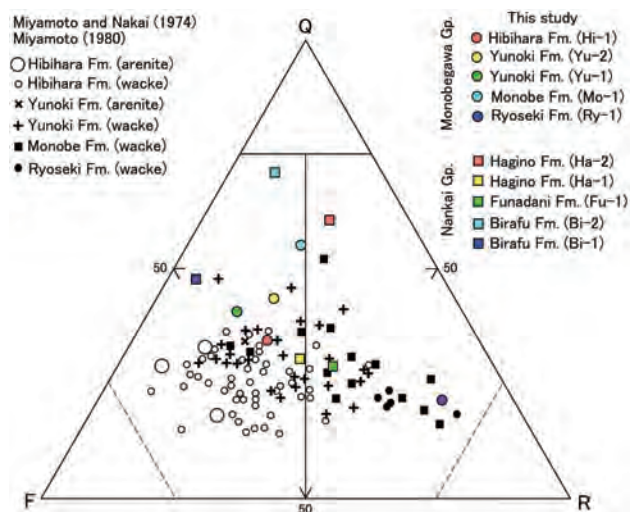


FIGURE 6. A Q-F-R diagram showing the sandstone compositions of the Monobegawa and Nankai groups provided by Miyamoto and Nakai (1974), Miyamoto (1980), and this study. Gp.: Group, Fm.: Formation, Q: quartz, F: feldspar, R: rock fragments.

36.8% (R), 32.4% (M), 22.1% (Y), and 20.0% (H); and the matrix was 36.1% (R), 24.6% (M), 26.9% (Y), and 23.8% (H). There are overall trends that the proportions of rock fragments and the matrix decrease and feldspar grains increase upwards. Miyamoto (1980) described species of rock fragments and their proportions, along the Kubokawa River route, suggesting that the ratio of sedimentary rock fragments decreased and volcanic rock fragments increased upwards (Fig. 7). The trend is concordant with the upward transition of clast proportion in conglomerates.

Lithology of the clastic rocks of the Nankai Group

Morino (1993) described that the Birafu Formation consisted mainly of mudstone and interbedded arkose sandstone and mudstone, with minor intercalations of the Torinosu-type limestone, sandstone, conglomerate, and tuff. The clasts of conglomerates were mostly pebble to granule size and consisted chiefly of greenish gray chert, with minor amounts of reddish-brown chert and granitic rocks (Morino et al., 1989). The Funadani Formation contained thick conglomerate beds having the clasts of chert and sandstone, with minor amounts of tuffaceous sandstone and limestone. The Hagino Formation was characterized by a repetitive occurrence of medium to fine sandstone, rich in arenite, and gray silty mudstone (Tashiro, 1993). Moreover, the formation in the Sano area (former Igenoki Formation; Kozai, 2008; Fig. 3) intercalated conglomerate with felsic igneous rock clasts in the bed of the Monobegawa River (Kozai and Ishida, 2000). The Nankai Group as a whole was characterized by the absence of red clastic rocks and abundance of arenite (Tashiro, 1985). Moreover, the occurrence of felsic igneous rock clasts in the conglomerate and arkose sandstone from each formation indicated the exposure of felsic igneous bodies in the provenance.

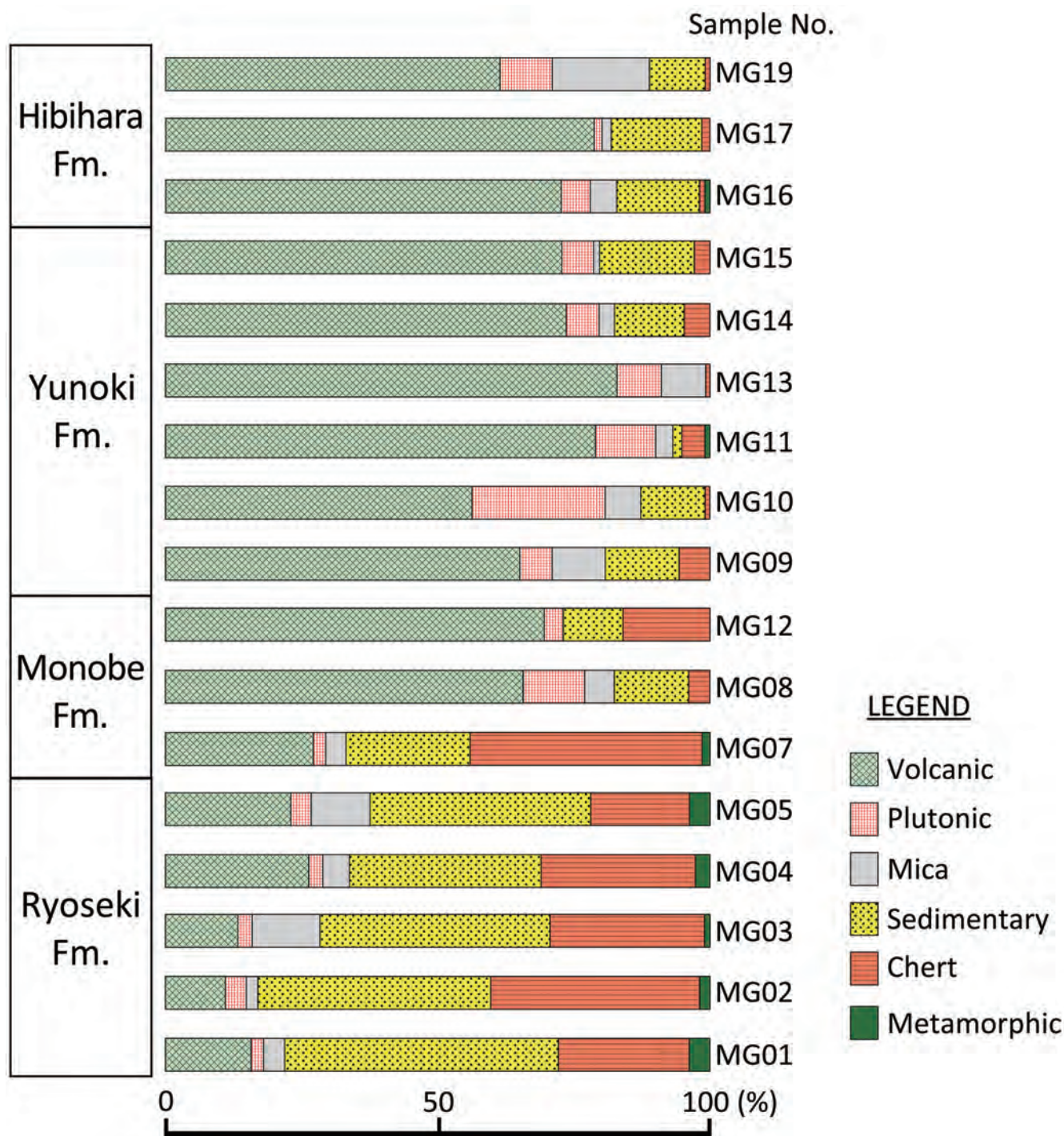


FIGURE 7. Compositions of rock fragments in sandstone samples of the Monobegawa Group published by Miyamoto and Nakai (1974) and Miyamoto (1980). Fm.: Formation.

Paleocurrent and sediment transport

Miyamoto (1980) concluded from the slump structures and sole marks developed in the Hibihara Formation in the study area that there was a land to the north (in the present coordinate) of the

sedimentary basin and that the clastic sediments were supplied from north to south. Miyamoto (1980) further proposed that Early Cretaceous igneous rock bodies that were exposed along the southern boundary of the Ryoke Belt but were completely eroded away supplied the igneous-rock clasts of the Monobegawa Group

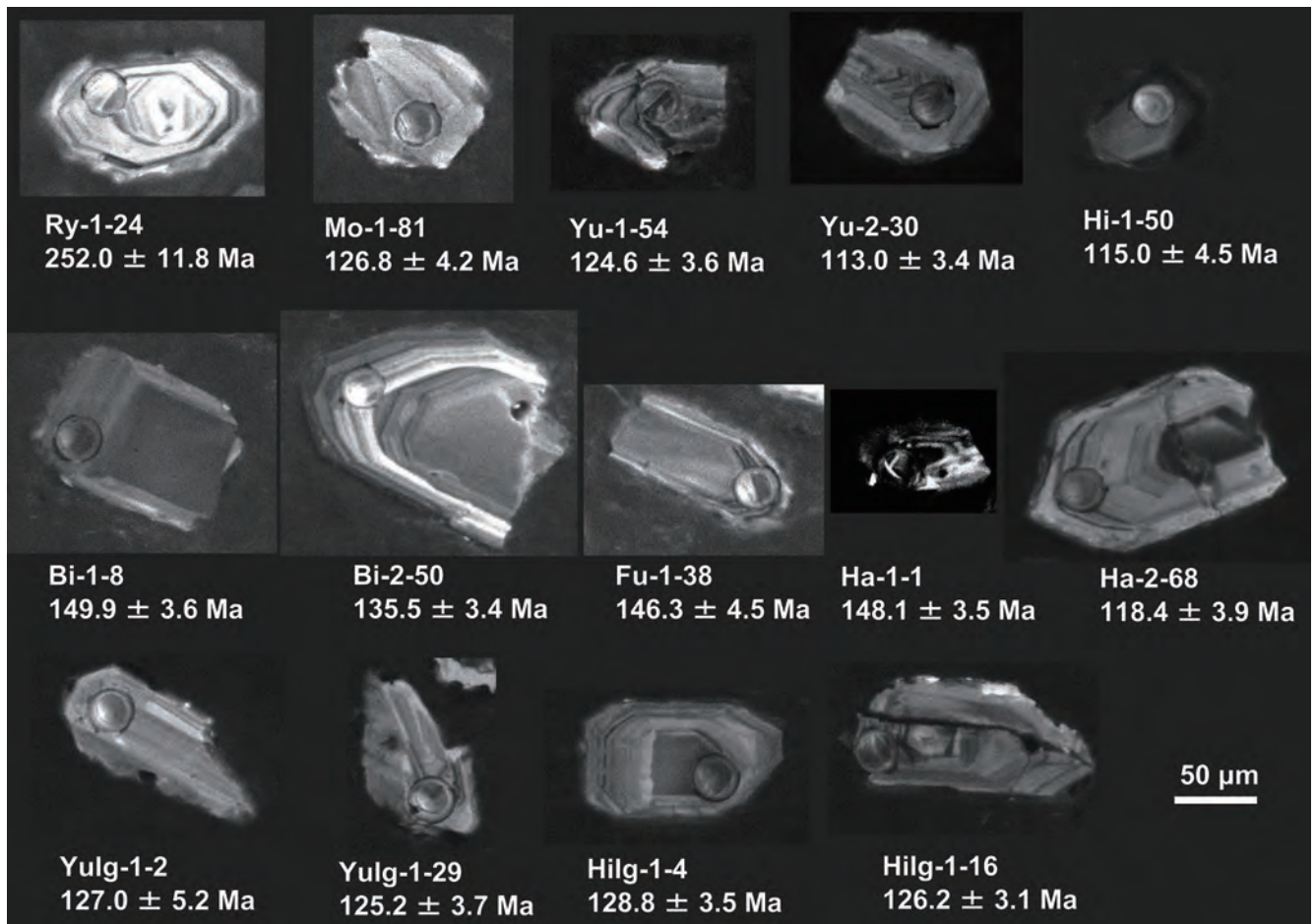


FIGURE 8. Cathodoluminescence images of some zircons analyzed in this study. For grain numbers, see Table 1.

in the study area. Kozai and Ishida (2000), on the other hand, found an Early Devonian radiolarian *Devoniglanus unicus* from a tuffaceous-sandstone clast of the Funadani Formation of the Nankai Group. Since the radiolarian species had commonly been reported from the tuffaceous sandstone in the G4 horizon of the Yokokurayama Group (Wakamatsu et al., 1990), they suggested that the clast was derived from the Siluro–Devonian of the Kurosegawa Belt.

In summary, the source of sedimentary-rock clasts in the conglomerate and sandstone of the Monobegawa Group in the study area is likely the pre-Cretaceous rocks of the Northern Chichibu Belt. The reasons are as follows: (1) the Monobegawa Group unconformably covers the Permian AC of the Northern Chichibu Belt; (2) the pre-Cretaceous AC of the Northern Chichibu Belt mainly occur on the north of the Monobegawa Group and sedimentary structures indicate the sediment supply from the north; and (3) the sediment source of the Monobegawa Group in the Katsura area has been proposed to have been the pre-Cretaceous rocks of the Northern Chichibu Belt (Ishida and Hashimoto, 1997; Matsukawa and Eto, 1987; Ogawa, 1971). A sediment source of the Nankai Group was likely a geologic entity that now constitutes

the Kurosegawa Belt (Kozai and Ishida, 2000).

SAMPLE DESCRIPTIONS

We studied the following seventeen samples: (1) five sandstone samples from the Monobegawa Group, (2) five sandstone samples from the Nankai Group, (3) three sandstone cobbles from the Ryoseki, Yunoki, and Funadani formations, (4) two igneous rock cobbles from the Yunoki and Hibihara formations, and (5) two sandstone samples from the Shingai Unit and Shirakidani Group, members of the Permian AC of the Northern Chichibu Belt. Here follows the description of the samples studied. The modal composition of a sandstone sample was measured from a thin-section using a petrological microscope and an automatic point counter. We counted five hundred points for each sandstone sample (three hundred points for each sandstone cobble) and calculated the percentages of (1) single quartz, (2) single feldspar, (3) the rock fragment, including chert fragments and mineral grains other than quartz and feldspar, and (4) matrix.

Monobegawa Group

Sandstone of the Ryoseki Formation (Sample Ry-1; 33° 37' 11.67" N, 133° 36' 39.87" E)

Sample Ry-1 of the Ryoseki Formation was collected from an exposure of the lowermost part of the formation on the northern side of Kochi Prefectural Road 269 along the Kasanokawa River (Fig. 3). The sample was of non-marine, red, ill-sorted, angular to sub-rounded, medium- to coarse-grained lithic wacke in the sense of Okada (1971), consisting of quartz (12.2%), feldspar (7.8%), rock fragments (37.2%), and matrix (42.8%). The rock fragments were mostly of sedimentary and metamorphic rocks with volcanic rocks and chert. The metamorphic rock fragments were mostly of an aggregate of elongated quartz grains with sutured grain boundaries and the longest dimensions arranging subparallel to each other (sheared quartz or stretched metamorphic quartz). Among the zircon grains we collected, 43% were euhedral, and 57% were abraded. They were mostly colorless, and only 3% were purple. The euhedral zircons had the aspect ratio of 1.2–3.0 (2.0 in average). Most of the collected zircons showed oscillatory zoning in CL images (Fig. 8).

Sandstone of the Monobe Formation (Sample Mo-1; 33° 42' 51.15" N, 133° 50' 05.49" E)

Sample Mo-1 of the Monobe Formation was collected from an exposure of the lower part of the formation along the Hibiharagawa River (Fig. 2). The sample was of light-gray, moderately- to well-sorted, sub-angular to rounded feldspathic arenite, consisting of quartz (48.1%), feldspar (20.3%), rock fragments (18.6%), and matrix (13.0%). Among the zircon grains we collected, 62% were euhedral, and 38% were abraded. They were mostly colorless, and 6% were purple or brown. The euhedral zircons had the aspect ratio of 1.0–3.3 (2.0 in average). Most of the collected zircons showed oscillatory zoning in CL images (Fig. 8).

Sandstone of the lower part of the Yunoki Formation (Sample Yu-1; 33° 42' 31.17" N, 133° 50' 01.71" E)

Sample Yu-1 of the Yunoki Formation was collected from an exposure of the Lower Marine Member (Tanaka et al., 1984) along the Hibiharagawa River (Fig. 2). The sample was of light-gray, moderately-sorted, sub-angular to sub-rounded medium-grained feldspathic arenite, consisting of quartz (38.0%), feldspar (38.8%), rock fragments (15.2%), and matrix (8.0%). Among the zircon grains we collected, 65% were euhedral, and 35% were abraded. They were mostly colorless, and 5% were purple. The euhedral zircons had the aspect ratio of 1.5–2.8 (2.1 in average). Most of the collected zircons showed oscillatory zoning in CL images (Fig. 8).

Sandstone of the middle part of the Yunoki Formation (Sample Yu-2; 33° 42' 23.83" N, 133° 50' 13.85" E)

Sample Yu-2 of the Yunoki Formation was collected from an exposure of the Middle Non-marine Member (Tanaka et al., 1984) along the Hibiharagawa River (Fig. 2). The sample was of dark-gray, ill-sorted, sub-angular to sub-rounded, fine- to very fine-grained feldspathic wacke with abundant carbonized plant fragments. The sample consisted of quartz (23.2%), feldspar

(18.2%), rock fragments (11.7%), and matrix (47.0%). Among the zircon grains we collected, 68% were euhedral, and 32% were abraded. They were mostly colorless, and 4% were purple. The euhedral zircons had the aspect ratio of 1.4–3.0 (2.1 in average). Most of the collected zircons showed oscillatory zoning in CL images (Fig. 8).

Sandstone of the Hibihara Formation (Sample Hi-1; 33° 42' 15.36" N, 133° 50' 34.28" E)

Sample Hi-1 of the Hibihara Formation was collected from an exposure of the Middle Marine Member (Tanaka et al., 1984) along the Hibiharagawa River (Fig. 2). The sample was of dark-gray, ill- to moderately-sorted, sub-angular to sub-rounded, fine- to very fine-grained feldspathic wacke, consisting of quartz (17.6%), feldspar (20.6%), rock fragments (13.0%), and matrix (48.8%). Among the zircon grains we collected, 39% were euhedral, and 61% were abraded. They were mostly colorless, and 3% were purple. The euhedral zircons had the aspect ratio of 1.3–2.8 (1.9 in average). Most of the collected zircons showed oscillatory zoning in CL images (Fig. 8).

Nankai Group

Sandstone of the lower part of the Birafu Formation (Sample Bi-1; 33° 38' 55.27" N, 133° 47' 52.38" E)

Sample Bi-1 of the Birafu Formation was collected from an exposure of the A2 Member (Kozai et al., 2004, 2006) along the Nishinokawa River (Fig. 3). The sample was of gray, moderately- to well-sorted, sub-angular to rounded, very fine-grained feldspathic arenite, consisting of quartz (43.0%), feldspar (42.6%), rock fragments (4.8%), and matrix (9.6%). Among the zircon grains we collected, 67% were euhedral, and 33% were abraded. They were mostly colorless, and only 1% were purple. The euhedral zircons had the aspect ratio of 1.5–2.7 (2.1 in average). Most of the collected zircons showed oscillatory zoning in CL images (Fig. 8).

Sandstone of the middle part of the Birafu Formation (Sample Bi-2; 33° 38' 55.66" N, 133° 48' 07.93" E)

Sample Bi-2 of the Birafu Formation was collected from an exposure of the B1 or B2 Member on the eastern side of Kochi Prefectural Road 30 along the Nishinokawa River (Fig. 3). The sample was of white, ill- to moderately-sorted, angular to rounded, coarse-grained feldspathic arenite, consisting of quartz (70.9%), feldspar (20.2%), rock fragments (8.7%), and matrix (0.2%). Among the zircon grains we collected, 62% were euhedral, and 38% were abraded. They were mostly colorless, and 7% were purple or brown. The euhedral zircons had the aspect ratio of 1.6–4.0 (2.1 in average). Most of the collected zircons showed oscillatory zoning in CL images (Fig. 8).

Sandstone of the Funadani Formation (Sample Fu-1; 33° 37' 22.79" N, 133° 41' 59.69" E)

Sample Fu-1 of the Funadani Formation was collected from an exposure near the Meoto Pond (Fig. 3). The sample was of weathered, brown, moderately-sorted, sub-angular to rounded, fine- to medium-grained lithic wacke, consisting of quartz (22.4%), feldspar (24.4%), rock fragments (32.3%), and matrix (20.9%).

Among the zircon grains we collected, 65% were euhedral, and 35% were abraded. They were mostly colorless, and 8% were purple or brown. The euhedral zircons had the aspect ratio of 1.6–3.3 (2.1 in average). Most of the collected zircons showed oscillatory zoning in CL images (Fig. 8).

Sandstone of the Hagino Formation from Sano (Sample Ha-1; 33° 37' 16.89" N, 133° 42' 42.87" E)

Sample Ha-1 of the Hagino Formation was collected from an exposure in Sano (Fig. 3). The sample was of weathered, brown, well-sorted, sub-angular to rounded, fine- to very fine-grained feldspathic wacke, consisting of quartz (22.0%), feldspar (26.2%), rock fragments (25.4%), and matrix (26.4%). Among the zircon grains we collected, 61% were euhedral, and 39% were abraded. They were mostly colorless, and 3% were brown. The euhedral zircons had the aspect ratio of 1.4–5.0 (2.4 in average). Most of the collected zircons showed oscillatory zoning in CL images (Fig. 8).

Sandstone of the Hagino Formation from Hagino (Sample Ha-2; 33° 38' 03.12" N, 133° 45' 25.74" E)

Sample Ha-2 of the Hagino Formation was collected from an exposure along the Haginogawa River in Hagino (Fig. 3). The sample was of light-gray, moderately- to well-sorted, angular to rounded, medium- to coarse-grained lithic arenite, consisting of quartz (60.8%), feldspar (14.8%), rock fragments (24.2%), and matrix (0.2%). Among the zircon grains we collected, 60% were euhedral, and 40% were abraded. They were mostly colorless, and 5% were purple or brown. The euhedral zircons had the aspect ratio of 1.4–3.4 (2.0 in average). Most of the collected zircons showed oscillatory zoning in CL images (Fig. 8).

Cobbles from conglomerate

A sandstone cobble from the Ryoseki Formation, Monobegawa Group (Sample RySs-1; 33° 38' 17.23" N, 133° 45' 23.01" E)

Sample RySs-1 was collected from an exposure of conglomerate of the Ryoseki Formation, Monobegawa Group, along the Haginogawa River (Fig. 3). The sample was of a subangular cobble of dark-gray, ill-sorted, angular to sub-rounded, coarse-grained lithic arenite, consisting of quartz (38%), feldspar (13.7%), rock fragments (37%), and matrix (11.3%). Among the zircon grains we collected, 53% were euhedral, and 47% were abraded. They were mostly colorless. The euhedral zircons had the aspect ratio of 1.3–2.7 (2.0 in average). Most of the collected zircons showed oscillatory zoning in CL images.

A sandstone cobble from the Yunoki Formation, Monobegawa Group (Sample YuSs-1; 33° 42' 43.20" N, 133° 50' 06.09" E)

Sample YuSs-1 was collected from an exposure of conglomerate of the middle part of the Yunoki Formation, Monobegawa Group, along the Hibiharagawa River (Fig. 2). The sample was of a round cobble of dark-gray, moderately-sorted, sub-angular to sub-rounded, medium- to coarse-grained feldspathic arenite, consisting of quartz (37.3%), feldspar (31.3%), rock fragments (25.3%), and matrix (6%). Among the zircon grains we collected, 56% were euhedral, and 44% were abraded. They were mostly colorless, and 8% were purple. The euhedral zircons had the aspect ratio of 1.1–2.6 (1.9 in average). Most of

the collected zircons showed oscillatory zoning in CL images.

A sandstone cobble from the Funadani Formation, Nankai Group (Sample FuSs-1; 33° 37' 21.28" N, 133° 42' 02.22" E)

Sample FuSs-1 was collected from an exposure of conglomerate of the Funadani Formation, Nankai Group, near the Meoto Pond (Fig. 3). The sample was of a subround cobble of dark-gray, ill-sorted, angular to sub-rounded, medium-grained feldspathic arenite, consisting of quartz (36.8%), feldspar (43.4%), rock fragments (10.6%), and matrix (9.3%). Among the zircon grains we collected, 68% were euhedral, and 32% were abraded. They were mostly colorless, and only 1% were purple. The euhedral zircons had the aspect ratio of 1.4–2.8 (1.7 in average). Most of the collected zircons showed oscillatory zoning in CL images.

A rhyolite cobble from the Yunoki Formation, Monobegawa Group (Sample YuIg-1; 33° 42' 43.20" N, 133° 50' 06.09" E)

Sample YuIg-1 was collected from the same exposure with sample YuSs-1 (Fig. 2). The sample was of a round cobble of rhyolite with quartz and plagioclase phenocrysts floated in a groundmass (Fig. 9a-c). Among the zircon grains we collected, 78% were euhedral, and 22% were abraded. They were mostly colorless, and 5% were purple or brown. The euhedral zircons had the aspect ratio of 1.5–3.2 (2.2 in average). Most of the collected zircons showed oscillatory zoning in CL images (Fig. 8).

A granodiorite cobble from the Hibihara Formation, Monobegawa Group (Sample HiIg-1; 33° 39' 34.69" N, 133° 46' 01.87" E)

Sample HiIg-1 was collected from an exposure of conglomerate of the Hibihara Formation, Monobegawa Group, along a northern branch of the Monobegawa River (Fig. 3). The sample was of a round cobble of granodiorite with quartz, plagioclase, and minor chlorite (Fig. 9d-f). Among the zircon grains we collected, 92% were euhedral, and 8% were abraded. They were mostly colorless, and 3% were brown. The euhedral zircons had the aspect ratio of 1.3–3.6 (2.1 in average). Most of the collected zircons showed oscillatory zoning in CL images (Fig. 8).

Pre-Cretaceous sandstone of the Northern Chichibu Belt

Sandstone of the Shingai Unit (Sample 13072103; 33° 36' 16.44" N, 133° 28' 22.83" E)

The Shingai Unit is a geologic unit of the Permian AC of the Northern Chichibu Belt, correlative to the Shirakidani Group in the Ryoseki area (Fig. 3). The Shingai Unit consists mainly of sandstone, mudstone, chert, basalt, and limestone (Wakita et al., 2007). Sample 13072103 was collected from an exposure along the Kochi Prefectural Road 33 at Kagamiimai, Kochi City. The sample was of grayish-green, moderately sorted, fine- to medium-grained lithic arenite, consisting of quartz (32.9%), feldspar (14.2%), rock fragments (52.9%), and matrix (12.8%). The rock fragments were mostly of volcanic rocks. Among the zircon grains we collected, 56% were euhedral, and 44% were abraded. They were mostly colorless, and 2% were purple or brown. Most of the collected zircons showed oscillatory zoning in CL images.

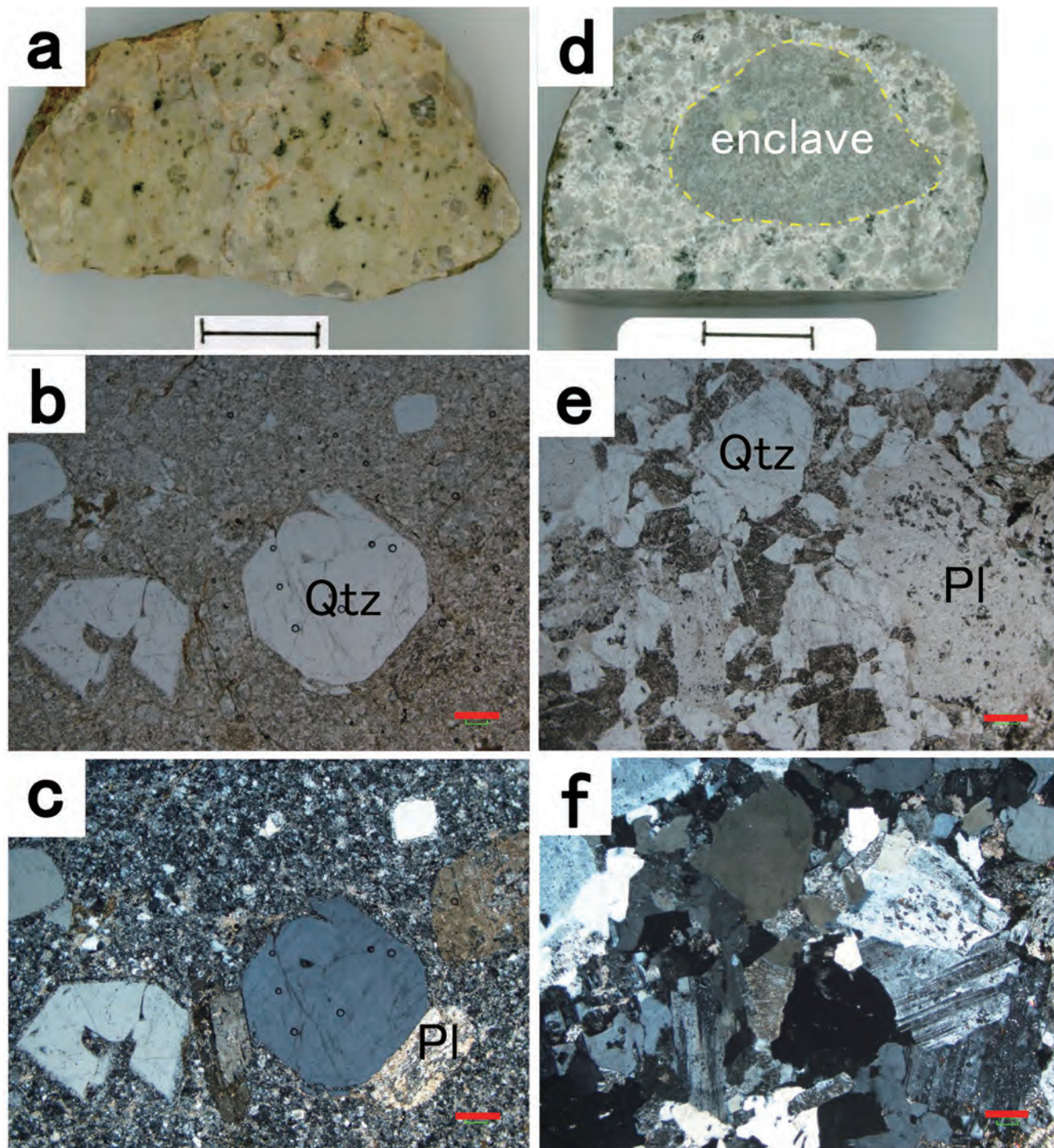


FIGURE 9. Photographs of studied igneous-rock clasts. **a–c**, A rhyolite clast from the Yunoki Formation (sample Yulg-1). **a**, A hand specimen (Scale bar = 1.0 cm); **b**, A photomicrograph (Open nicol; Scale bar = 0.2 mm); **c**, A photomicrograph (Crossed nicols; Scale bar = 0.2 mm.). **d–f**, A granodiorite clast from the Hibihara Formation (Hilg-1). **d**, A hand specimen (Scale bar = 1.0 cm); **e**, A photomicrograph (Open nicol; Scale bar = 0.2 mm); **f**, A photomicrograph (Crossed nicols; Scale bar = 0.2 mm). Qtz: quartz, Pl: plagioclase.

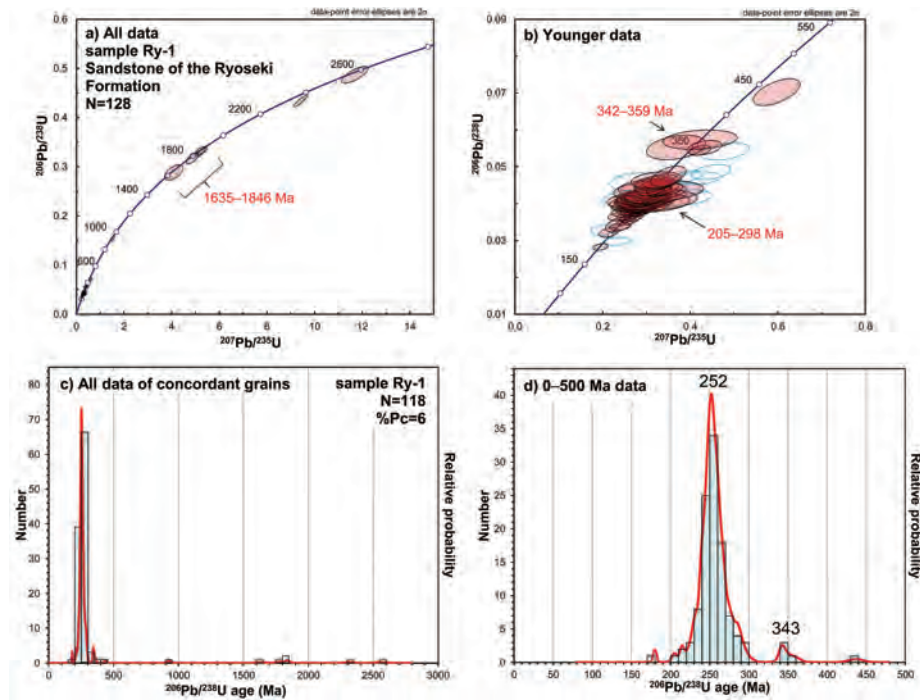


FIGURE 10. Analytical data of detrital zircons from sandstone of the Ryoseki Formation (sample Ry-1). **a**, Concordia diagram for all data; **b**, Concordia diagram for a younger data set; **c**, Probability density plot with a histogram for all data of concordant grains; **d**, Probability density plot with a histogram for the 0–500 Ma data set. Open (light blue) circles in the concordia diagrams from Fig. 10 to Fig. 26 show the analytical data for discordant grains. N: total number, %Pc: percentage of Precambrian zircons.

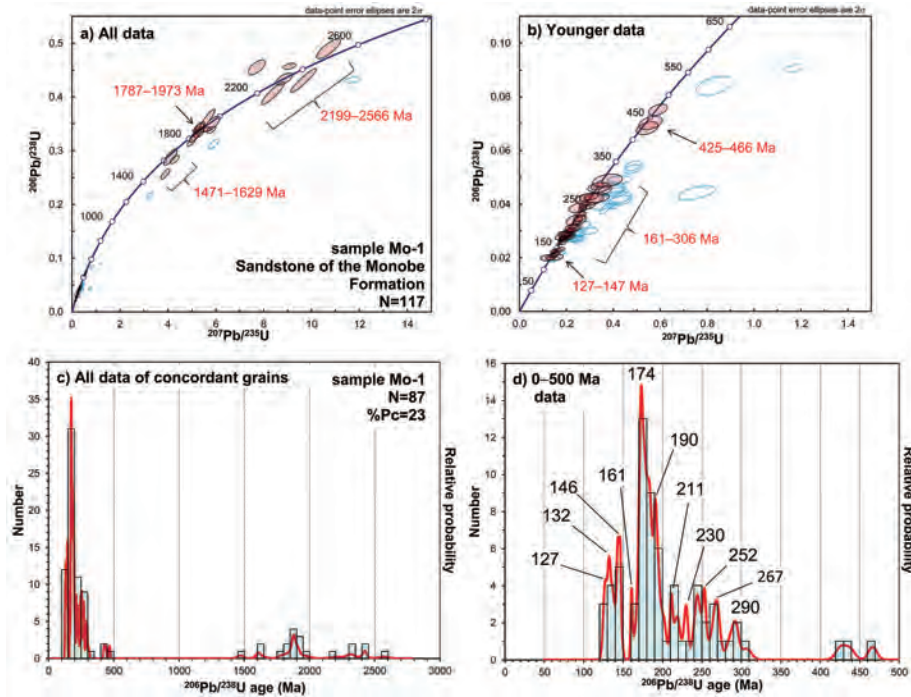


FIGURE 11. Analytical data of detrital zircons from sandstone of the Monobe Formation (sample Mo-1). **a**, Concordia diagram for all data; **b**, Concordia diagram for a younger data set; **c**, Probability density plot with a histogram for all data of concordant grains; **d**, Probability density plot with a histogram for the 0–500 Ma data set. N: total number, %Pc: percentage of Precambrian zircons.

Sandstone of the Shirakidani Group (Sample 16091701; 33° 37' 16.18" N, 133° 35' 47.18" E)

The Shirakidani Group is a geologic unit of the Permian AC of the Northern Chichibu Belt in the Ryoseki area (Fig. 3). The Shirakidani Group consists mainly of sandy mudstone, sandstone, and mudstone, with blocks (olistoliths; Suyari et al., 1983) of chert, limestone, and basaltic tuff and lava. Sample 16091701 of the Shirakidani Group was collected from an exposure on the northern side of Kochi Prefectural Road 269 along the Kasanokawa River (Fig. 3). The sample was of gray, moderately- to ill-sorted, sub-angular to rounded, medium- to coarse-grained lithic arenite, consisting of quartz (18%), feldspar (24.4%), rock fragments (51.2%), and matrix (6.4%). The rock fragments were mostly of volcanic rocks. Among the zircon grains we collected, 50% were euhedral, and 50% were abraded. They were mostly colorless, 2% were purple, and 5% were brown. The euhedral zircons had the aspect ratio of 1.4–4.3 (2.2 in average). Most of the collected zircons showed oscillatory zoning in CL images.

ANALYTICAL METHOD

The zircon samples for analyses were prepared following the procedures described in Kawagoe et al. (2012). The measurement was carried out on laser ablation inductively coupled plasma mass spectrometers (LA-ICPMS) equipped in the Graduate School of Environmental Studies, Nagoya University. The ICPMS instrument was an Agilent 7700x quadrupole-based ICPMS connected with a New Wave Research NWR-213-type LA system, which used the frequency quintupled Nd-YAG 213-nm wavelength. The measurement conditions, optimized to reduce matrix effects, were as follows: energy density of 11.7 J/cm², pulse repetition rate of 10 Hz, pre-ablation time of 8 s, ablation time of 10 s, and the ablation pit size of 25 μ m (Kouchi et al., 2015). The analyses were carried out in a peak-jumping mode, and the peaks of ²⁰²Hg, ²⁰⁴(Hg+Pb), ²⁰⁶Pb, ²⁰⁷Pb, ²³²Th, and ²³⁸U were monitored. Data were acquired in sequences of 28 analyses, consisting of 5 analyses of gas blank, 4 NIST (National Institute of Standards and Technology, U.S.A.) SRM 610 glass standard, one standard zircon (91500 zircon with the ²⁰⁶Pb/²³⁸U age of 1062.4 \pm 0.4 Ma; Wiedenbeck et al., 2004), nine unknown, 4 SRM 610 standard, and five gas blank.

RESULTS

We sampled an outer part (rim or mantle) of collected zircon grains with the laser ablation technique and analyzed with the ICPMS. After the analyses, we plotted all the data on a concordia diagram. Then we chose concordant grains with the %conc value ($100 \cdot (^{206}\text{Pb}/^{238}\text{U age}) / (^{207}\text{Pb}/^{235}\text{U age})$) between 90 and 110 and drew a probability density plot and a histogram with the data interval of 50 Myr (²⁰⁶Pb/²³⁸U age). Among the peaks in the probability density plot that consist of two or more zircon data, the youngest one will be designated as the youngest peak (YP) in this paper. The data processing was carried out using the Isoplot 4.15 software (Ludwig, 2012). Here follow the results of our analyses.

Monobegawa Group

Sandstone of the Ryoseki Formation (Sample Ry-1)

We obtained 128 analyses from 128 zircon grains collected from sandstone sample Ry-1 of the Ryoseki Formation. 118 grains out of 128 gave concordant results (Fig. 10). We detected three age groups and five single plots of concordant detrital zircons on the concordia diagram: 205–298 Ma (105 grains; 89% of 118 concordant grains), 342–359 Ma (3%), 1635–1846 Ma (3%), 180 Ma (1%), 437 Ma (1%), 929 Ma (1%), 2318 Ma (1%), and 2552 Ma (1%) (Each age denotes the ²⁰⁶Pb/²³⁸U age at the centers of the youngest and oldest age plots of each cluster or at the center of each single plot.) (Fig. 10a, b). The percentage of Precambrian zircons (%Pc) was 6, and the 206Pb/238U age of the youngest zircon (YZ) was 179.8 \pm 4.8 Ma. The probability density plot for the 0–500 Ma data set showed a single peak at 252 Ma (Fig. 10d).

Sandstone of the Monobe Formation (Sample Mo-1)

We obtained 117 analyses from 117 zircon grains collected from sandstone sample Mo-1 of the Monobe Formation. 87 grains out of 117 gave concordant results (Fig. 11). We detected six age groups of concordant zircons: 161–306 Ma (60%), 127–147 Ma (14%), 1787–1973 Ma (13%), 2199–2566 Ma (7%), 425–466 Ma (3%), and 1471–1629 Ma (3%), with %Pc of 23 and the YZ of 126.8 \pm 4.2 Ma (Fig. 11a–c). The probability density plot for the 0–500 Ma data set showed the largest peak at 174 Ma, second largest peaks at 146 Ma and 190 Ma, and small peaks at 127 Ma, 132 Ma, 161 Ma, 211 Ma, 230 Ma, 244 Ma, 252 Ma, 267 Ma, and 290 Ma (Fig. 11d). The youngest peak (YP) was at 127 Ma, and the concordant age of the three grains that constitute the 127 Ma peak was 127.4 \pm 2.9 Ma (MSWD = 0.14, Probability = 0.71).

Sandstone of the lower part of the Yunoki Formation (Sample Yu-1)

We obtained 131 analyses from 131 zircon grains collected from sandstone sample Yu-1 of the lower part of the Yunoki Formation. 92 grains out of 131 gave concordant results (Fig. 12). We detected three age groups and two single plots of concordant detrital zircons: 116–237 Ma (74%), 1580–2036 Ma (16%), 254–301 Ma (8%), around 2209 Ma (1%), and around 2961 Ma (1%), with %Pc of 19 and the YZ of 115.5 \pm 2.7 Ma (Fig. 12a–c). The probability density plot for the 0–500 Ma data set showed the largest peaks at 173 Ma, 181 Ma, and 189 Ma, a second largest peak at 131 Ma, and small peaks at 124 Ma, 221 Ma, 235 Ma, and 259 Ma (Fig. 12d). The YP was at 124 Ma, and the concordant age of the two grains that constitute the 124 Ma peak was 124.3 \pm 2.4 Ma (MSWD = 0.67, Probability = 0.41).

Sandstone of the middle part of the Yunoki Formation (Sample Yu-2)

We obtained 125 analyses from 125 zircon grains collected from sandstone sample Yu-2 of the middle part of the Yunoki Formation. 91 grains out of 125 gave concordant results (Fig. 13). We detected four age groups and one single plot of concordant detrital zircons: 107–318 Ma (65%), 379–466 Ma (20%), 1638–1852 Ma (12%), 2067–2198 Ma (2%), and around 2407 Ma (1%), with %Pc of 15 and the YZ of 107.3 \pm 3.1 Ma (Fig. 13a–c). The probability density plot for the 0–500 Ma data set showed

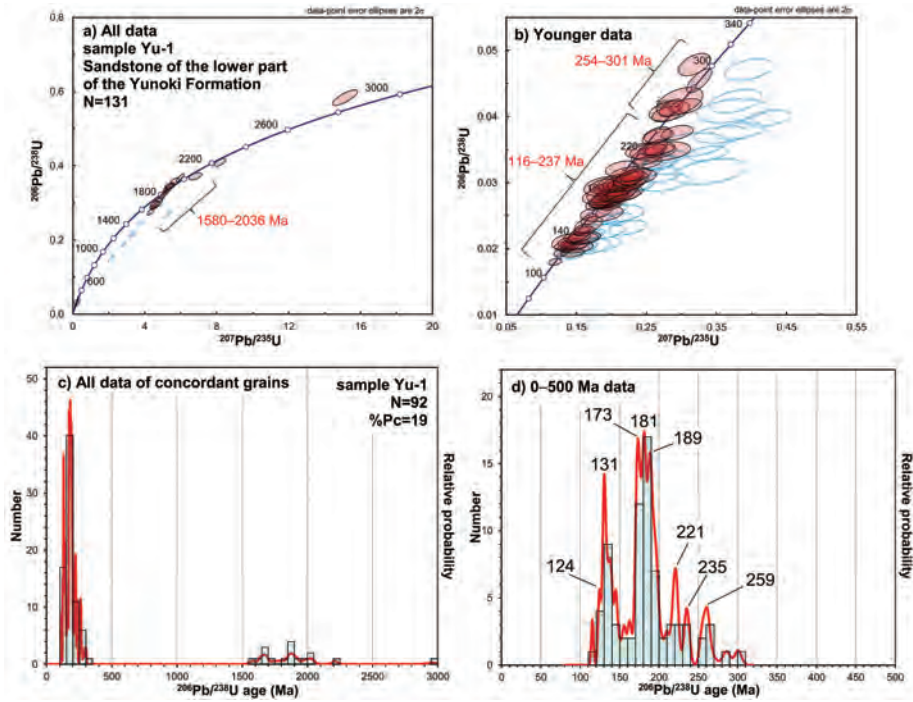


FIGURE 12. Analytical data of detrital zircons from sandstone of the lower part of the Yunoki Formation (sample Yu-1). **a**, Concordia diagram for all data; **b**, Concordia diagram for a younger data set; **c**, Probability density plot with histogram for all data of concordant grains; **d**, Probability density plot with a histogram for the 0–500 Ma data set. N: total number, %Pc: percentage of Precambrian zircons.

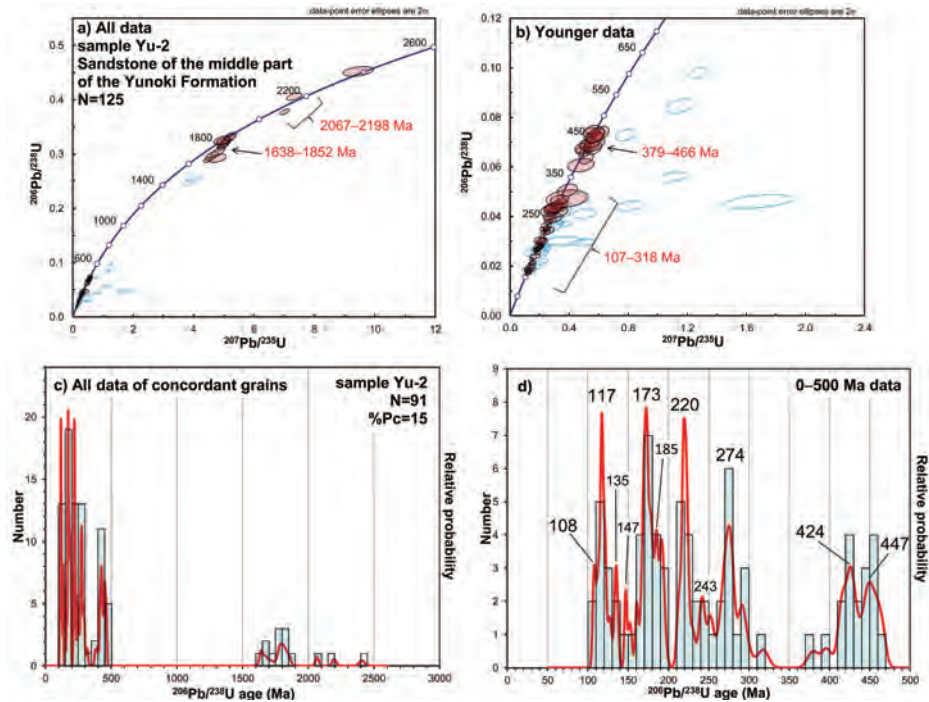


FIGURE 13. Analytical data of detrital zircons from sandstone of the middle part of the Yunoki Formation (sample Yu-2). **a**, Concordia diagram for all data; **b**, Concordia diagram for a younger data set; **c**, Probability density plot with histogram for all data of concordant grains; **d**, Probability density plot with a histogram for the 0–500 Ma data set. N: total number, %Pc: percentage of Precambrian zircons.

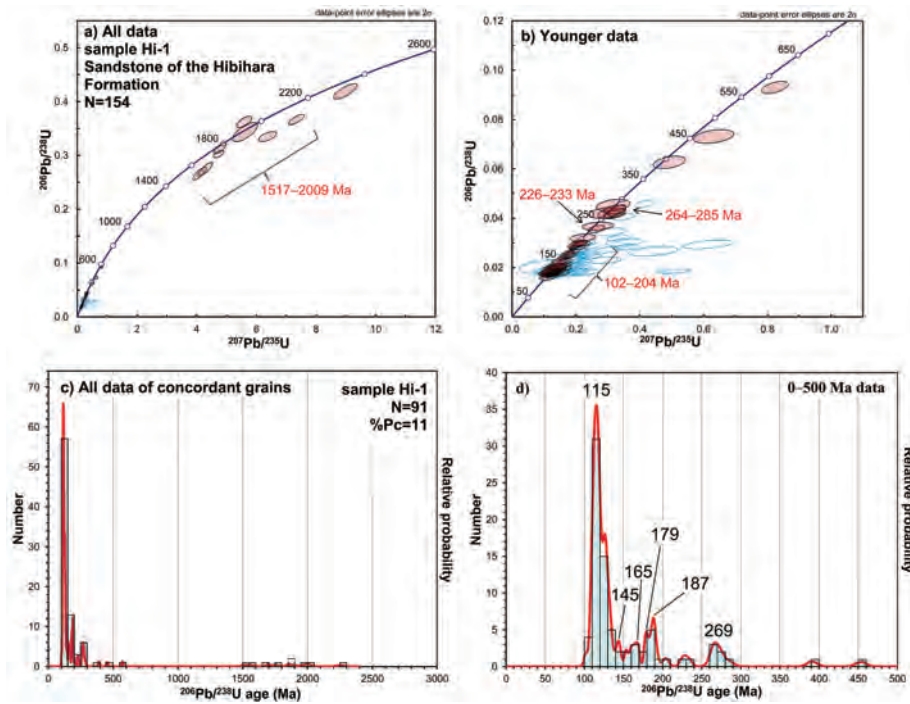


FIGURE 14. Analytical data of detrital zircons from sandstone of the Hibihara Formation (sample Hi-1). **a**, Concordia diagram for all data; **b**, Concordia diagram for a younger data set; **c**, Probability density plot with a histogram for all data of concordant grains; **d**, Probability density plot with a histogram for the 0–500 Ma data set. N: total number, %Pc: percentage of Precambrian zircons.

the largest peaks at 117 Ma, 173 Ma, and 220 Ma, second largest peaks at 274 Ma and 185 Ma, and small peaks at 108 Ma, 135 Ma, 147 Ma, 191 Ma, 243 Ma, 274 Ma, 424 Ma, and 447 Ma (Fig. 13d). The YP was at 108 Ma, and the concordant age of the two grains that constitute the 108 Ma peak was 108.2 ± 2.4 Ma (MSWD = 3.7, Probability = 0.053).

Sandstone of the Hibihara Formation (Sample Hi-1)

We obtained 154 analyses from 154 zircon grains collected from sandstone sample Hi-1 of the Hibihara Formation. 91 grains out of 154 gave concordant results (Fig. 14). We detected four age groups and four single plots of concordant detrital zircons: 102–204 Ma (78%), 1517–2009 Ma (9%), 264–285 Ma (7%), 226–233 Ma (2%), 391 Ma (1%), 454 Ma (1%), 572 Ma (1%), and 2251 Ma (1%), with %Pc of 11 and the YZ of 102.0 ± 4.8 Ma (Fig. 14a–c). The probability density plot for the 0–500 Ma data set showed the largest and youngest peak at 115 Ma, a second largest peak at 187 Ma, and small peaks at 145 Ma, 165 Ma, 179 Ma, and 269 Ma (Fig. 14d). The YP was at 115 Ma, and the concordant age of the thirty grains that constitute the 115 Ma peak was 114.9 ± 0.8 Ma (MSWD = 5.9, Probability = 0.015).

Nankai Group

Sandstone of the lower part of the Birafu Formation (Sample Bi-1)

We obtained 128 analyses from 128 zircon grains collected from sandstone sample Bi-1 of the lower part of the Birafu

Formation. 82 grains out of 128 gave concordant results (Fig. 15). We detected six age groups of concordant detrital zircons: 1489–2181 Ma (44%), 150–221 Ma (35%), 241–270 Ma (11%), 292–320 Ma (4%), 2413–2625 Ma (4%), and 397–420 Ma (3%), with %Pc of 48 and the YZ of 149.9 ± 3.6 Ma (Fig. 15a–c). The probability density plot for the 0–500 Ma data set showed the largest peak at 179 Ma, second largest peaks at 188 Ma and 197 Ma, and small peaks at 169 Ma (YP), 214 Ma, 221 Ma, 241 Ma, and 267 Ma (Fig. 15d).

Sandstone of the middle part of the Birafu Formation (Sample Bi-2)

We obtained 126 analyses from 126 zircon grains collected from sandstone sample Bi-2 of the middle part of the Birafu Formation. 104 grains out of 126 gave concordant results (Fig. 16). We detected six age groups of concordant detrital zircons: 128–255 Ma (66%), 1509–1980 Ma (23%), 290–317 Ma (3%), 2110–2205 Ma (3%), 2535–2605 Ma (3%), and 2390–2409 Ma (2%), with %Pc of 31 and the YZ of 128.1 ± 4.7 Ma (Fig. 16a–c). The probability density plot for the 0–500 Ma data set showed the largest peak at 172 Ma, the second largest and youngest peak at 136 Ma, and small peaks at 151 Ma, 221 Ma, and 242 Ma (Fig. 16d). The eight grains that constitute the YP gave the concordant age of 136.5 ± 2.5 Ma (MSWD = 0.65, Probability = 0.42).

Sandstone of the Funadani Formation (Sample Fu-1)

We obtained 123 analyses from 123 zircon grains collected from sandstone sample Fu-1 of the Funadani Formation. 98 grains out of 123 gave concordant results (Fig. 17). We detected four

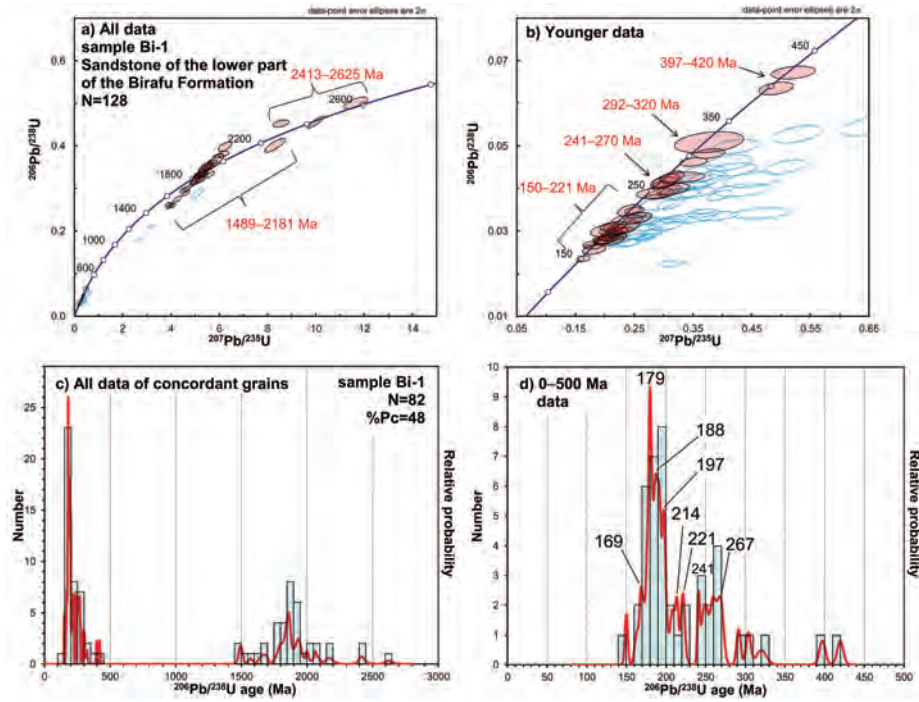


FIGURE 15. Analytical data of detrital zircons from sandstone of the lower part of the Birafu Formation (sample Bi-1). **a**, Concordia diagram for all data; **b**, Concordia diagram for a younger data set; **c**, Probability density plot with a histogram for all data of concordant grains; **d**, Probability density plot with a histogram for the 0–500 Ma data set. N: total number, %Pc: percentage of Precambrian zircons.

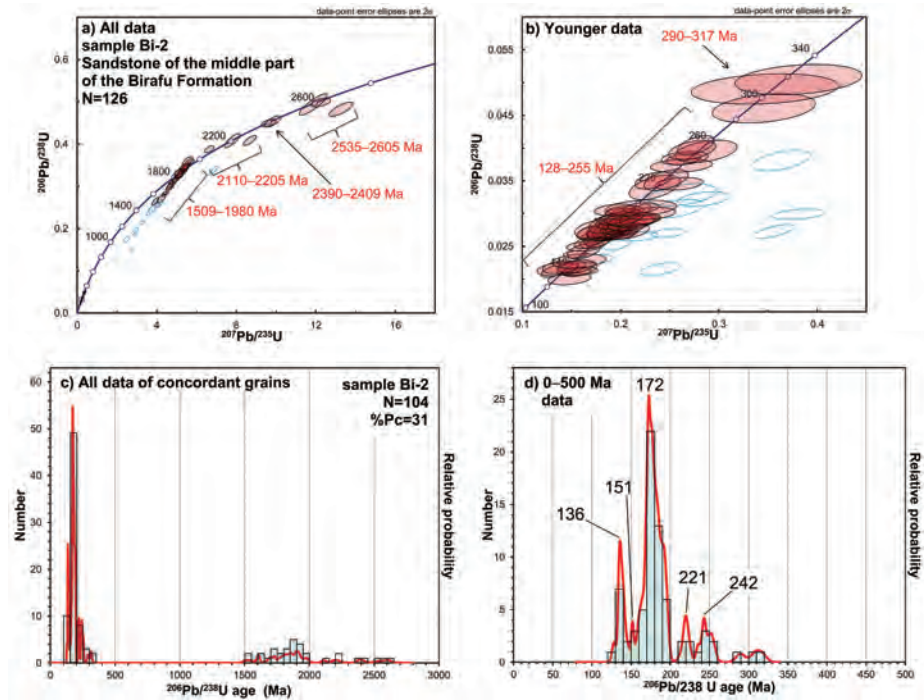


FIGURE 16. Analytical data of detrital zircons from sandstone of the middle part of the Birafu Formation (sample Bi-2). **a**, Concordia diagram for all data; **b**, Concordia diagram for a younger data set; **c**, Probability density plot with a histogram for all data of concordant grains; **d**, Probability density plot with a histogram for the 0–500 Ma data set. N: total number, %Pc: percentage of Precambrian zircons.

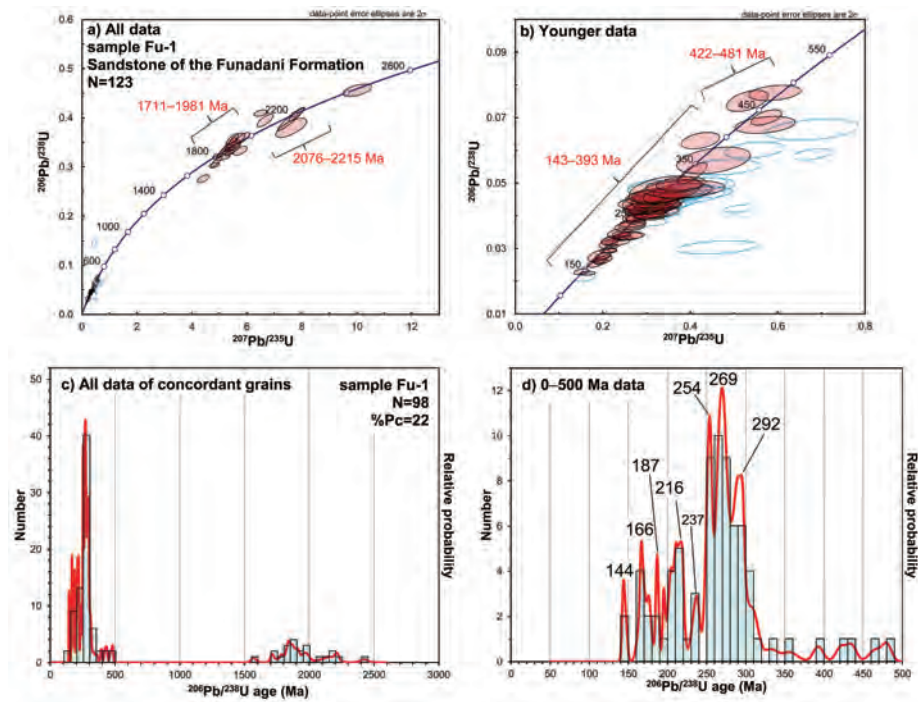


FIGURE 17. Analytical data of detrital zircons from sandstone of the Funadani Formation (sample Fu-1). **a**, Concordia diagram for all data; **b**, Concordia diagram for a younger data set; **c**, Probability density plot with a histogram for all data of concordant grains; **d**, Probability density plot with a histogram for the 0–500 Ma data set. N: total number, %Pc: percentage of Precambrian zircons.

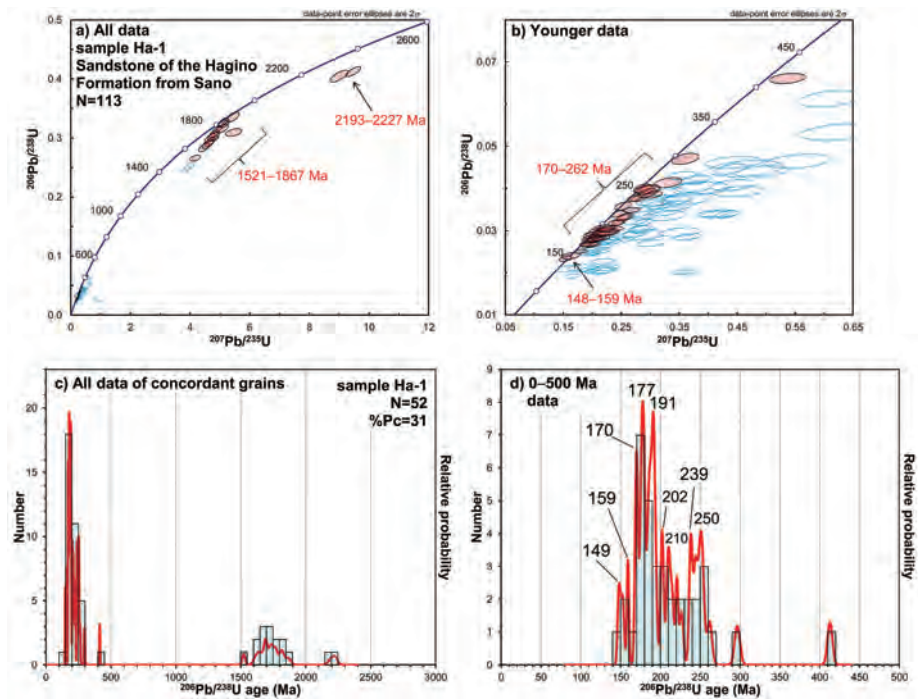


FIGURE 18. Analytical data of detrital zircons from sandstone of the Hagino Formation from Sano (sample Ha-1). **a**, Concordia diagram for all data; **b**, Concordia diagram for a younger data set; **c**, Probability density plot with a histogram for all data of concordant grains; **d**, Probability density plot with a histogram for the 0–500 Ma data set. N: total number, %Pc: percentage of Precambrian zircons.

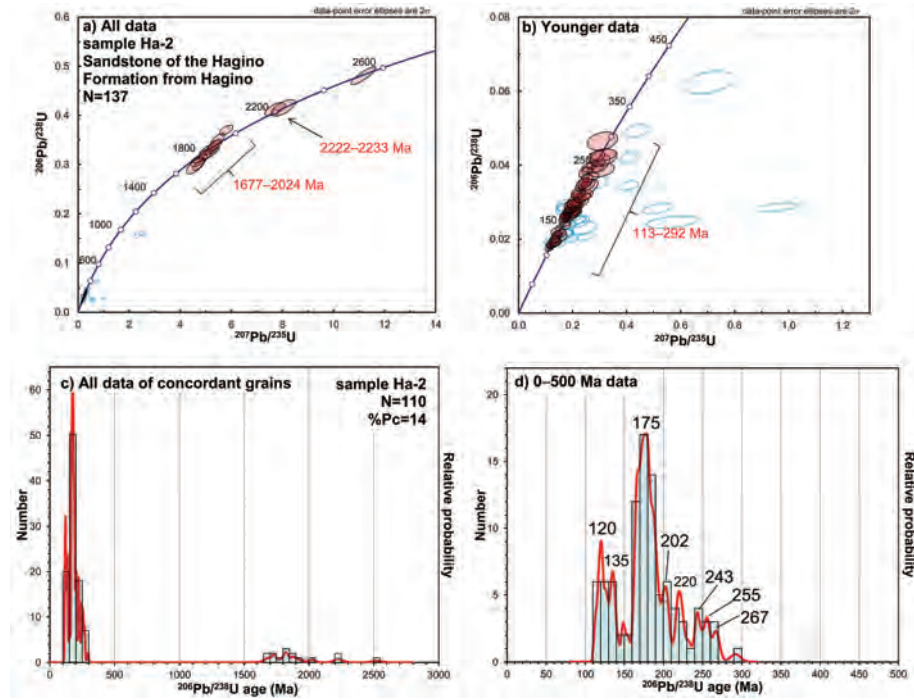


FIGURE 19. Analytical data of detrital zircons from sandstone of the Hagino Formation from Hagino (sample Ha-2). **a**, Concordia diagram for all data; **b**, Concordia diagram for a younger data set; **c**, Probability density plot with a histogram for all data of concordant grains; **d**, Probability density plot with a histogram for the 0–500 Ma data set. N: total number, %Pc: percentage of Precambrian zircons.

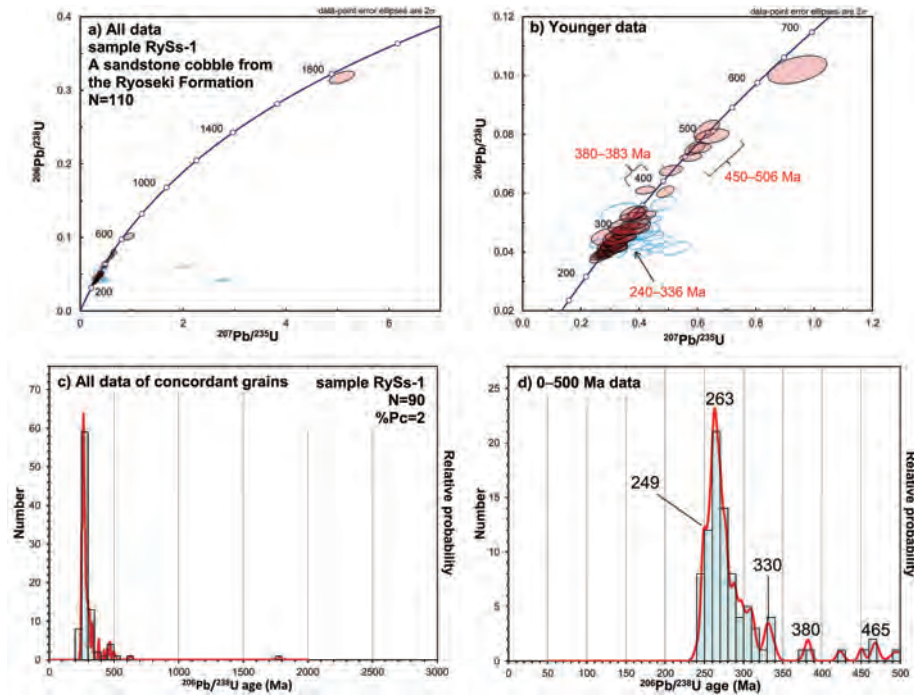


FIGURE 20. Analytical data of detrital zircons from a sandstone cobble from the Ryoseki Formation (sample RySs-1). **a**, Concordia diagram for all data; **b**, Concordia diagram for a younger data set; **c**, Probability density plot with a histogram for all data of concordant grains; **d**, Probability density plot with a histogram for the 0–500 Ma data set. N: total number, %Pc: percentage of Precambrian zircons.

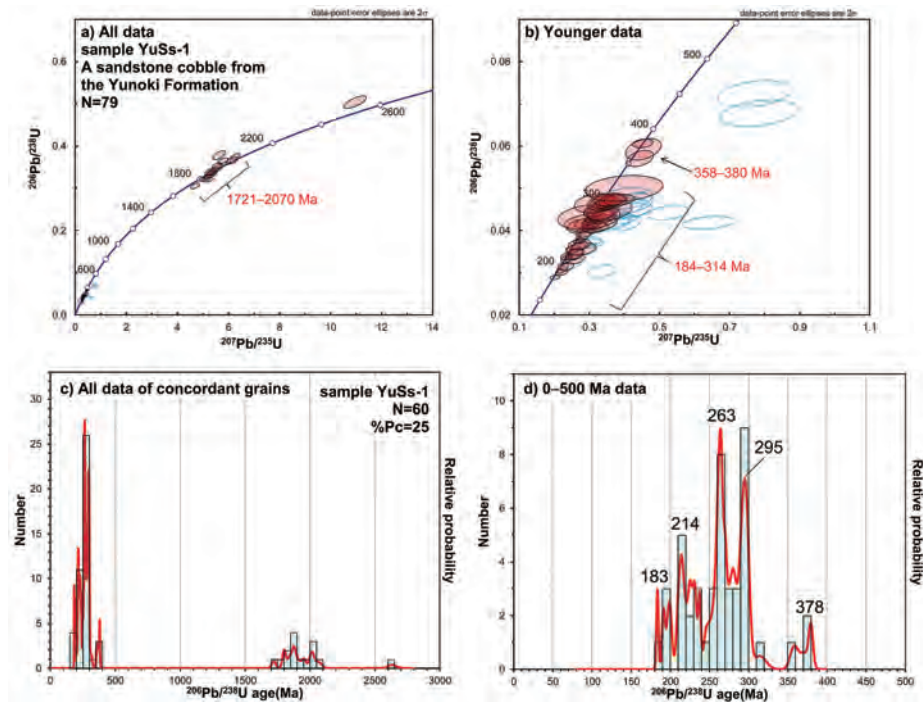


FIGURE 21. Analytical data of detrital zircons from a sandstone cobble of the Yunoki Formation (sample YuSs-1). **a**, Concordia diagram for all data; **b**, Concordia diagram for a younger data set; **c**, Probability density plot with a histogram for all data of concordant grains; **d**, Probability density plot with a histogram for the 0–500 Ma data set. N: total number, %Pc: percentage of Precambrian zircons.

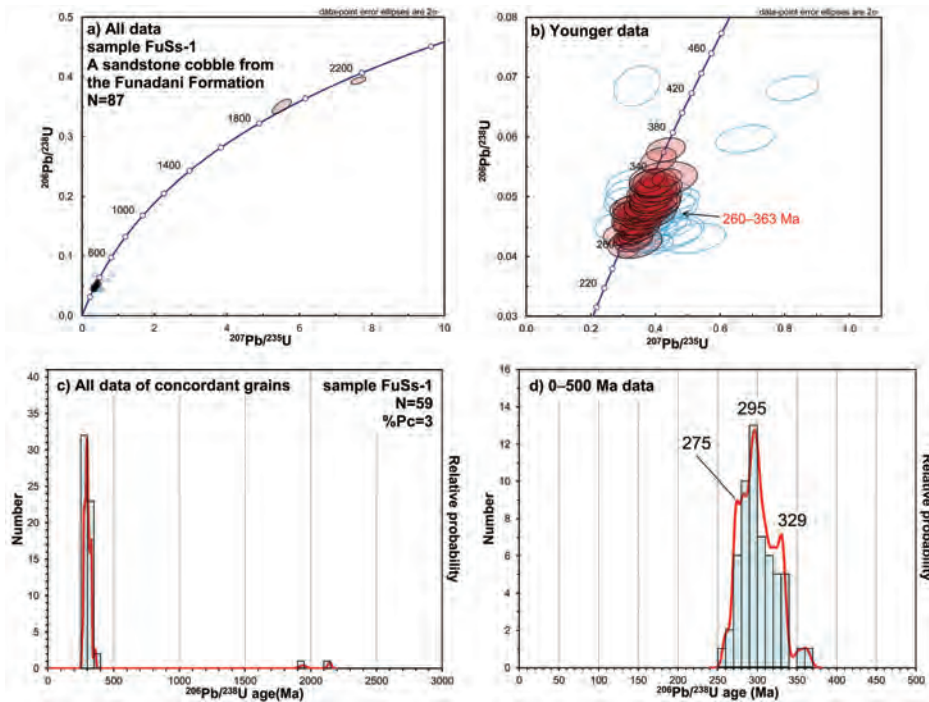


FIGURE 22. Analytical data of detrital zircons from a sandstone cobble of the Funadani Formation (sample FuSs-1). **a**, Concordia diagram for all data; **b**, Concordia diagram for a younger data set; **c**, Probability density plot with a histogram for all data of concordant grains; **d**, Probability density plot with a histogram for the 0–500 Ma data set. N: total number, %Pc: percentage of Precambrian zircons.

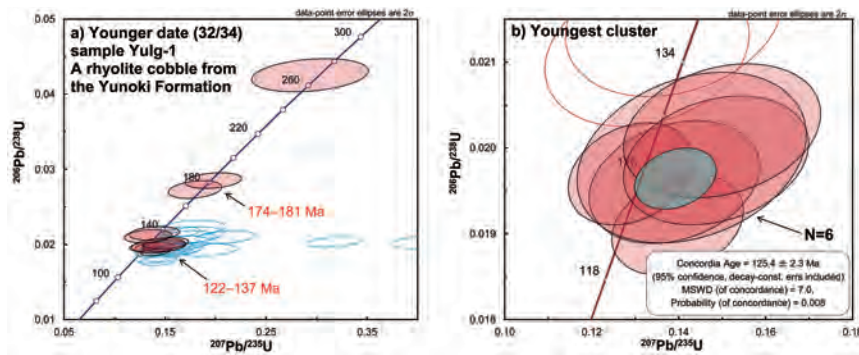


FIGURE 23. Analytical data of zircons from a rhyolite cobble of the Yunoki Formation (sample YuIg-1). **a**, Concordia diagram for a younger data set; **b**, Concordia diagram for the data set forming the youngest cluster (the light blue filled ellipse denotes the concordant age). N: total number.

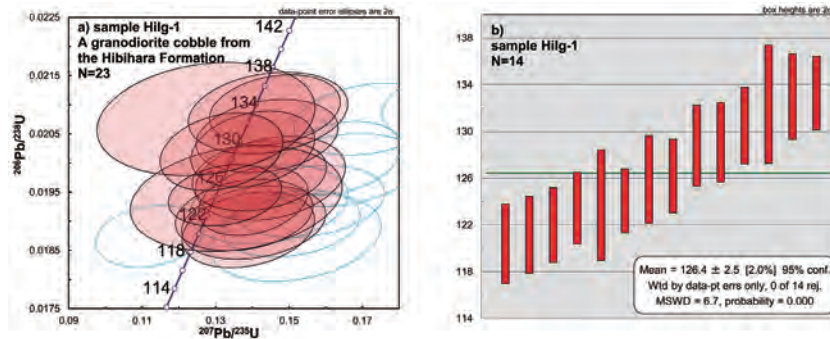


FIGURE 24. Analytical data of zircons from a granodiorite cobble of the Hibihara Formation (sample HiIg-1). **a**, Concordia diagram for all data (except for no.15 zircon of Table 1); **b**, $^{206}\text{Pb}/^{238}\text{U}$ ages for the 14 concordant zircons with the calculated weighted mean age. N: total number.

age groups and two single plots of concordant detrital zircons: 143–393 Ma (73%), 1711–1981 Ma (15%), 2076–2215 Ma (5%), 422–481 Ma (4%), around 1570 Ma (1%), and around 2424 Ma (1%), with %Pc of 22 and the YZ of 143.4 ± 3.2 Ma (Fig. 17a–c). The probability density plot for the 0–500 Ma data set showed the largest peak at 269 Ma, second largest peaks at 254 Ma and 292 Ma, and small peaks at 144 Ma (YP), 166 Ma, 187 Ma, 216 Ma, and 237 Ma (Fig. 17d).

Sandstone of the Hagino Formation from Sano (Sample Ha-1)

We obtained 113 analyses from 113 zircon grains collected from sandstone sample Ha-1 of the Hagino Formation. 52 grains out of 113 gave concordant results (Fig. 18). We detected four age groups and two single plots of concordant detrital zircons: 170–262 Ma (60%), 1521–1867 Ma (26%), 148–159 Ma (6%), 2193–2227 Ma (4%), 297 Ma (2%), and 413 Ma (2%), with %Pc of 31 and the YZ of 148.1 ± 3.5 Ma (Fig. 18a–c). The probability density plot for the 0–500 Ma data set showed the largest peaks at 177 Ma and 191 Ma, a second largest peak at 170 Ma, and small peaks at 149 Ma (YP), 159 Ma, 202 Ma, 210 Ma, 239 Ma, and 250 Ma (Fig. 18d).

Sandstone of the Hagino Formation from Hagino (Sample Ha-2)

We obtained 137 analyses from 137 zircon grains collected from sandstone sample Hs-2 of the Hibihara Formation. 110 grains out of 137 gave concordant results (Fig. 19). We detected three age groups and one single plot of concordant detrital zircons: 113–292 Ma (86%), 1677–2024 Ma (11%), 2222–2233 Ma (2%), and around 2525 Ma (1%), with %Pc of 14 and the YZ of 112.9 ± 3.9 Ma (Fig. 19a–c). The probability density plot for the 0–500 Ma data set showed the largest peak at 175 Ma, the second largest and youngest peak at 120 Ma, and small peaks at 135 Ma, 150 Ma, 202 Ma, 220 Ma, 243 Ma, 255 Ma, and 267 Ma (Fig. 19d). The ten grains that constitute the YP gave the concordant age of 119.3 ± 1.8 Ma (MSWD = 0.051, Probability = 0.82).

Cobbles from conglomerate

A sandstone cobble from the Ryoseki Formation, Monobegawa Group (Sample RySs-1)

We obtained 110 analyses from 110 zircon grains collected from sandstone cobble sample RySs-1 of the Ryoseki Formation. 90 grains out of 110 gave concordant results (Fig. 20). We detected three age groups and three single plots of concordant detrital zircons: 240–336 Ma (89%), 450–506 Ma (6%), 380–383

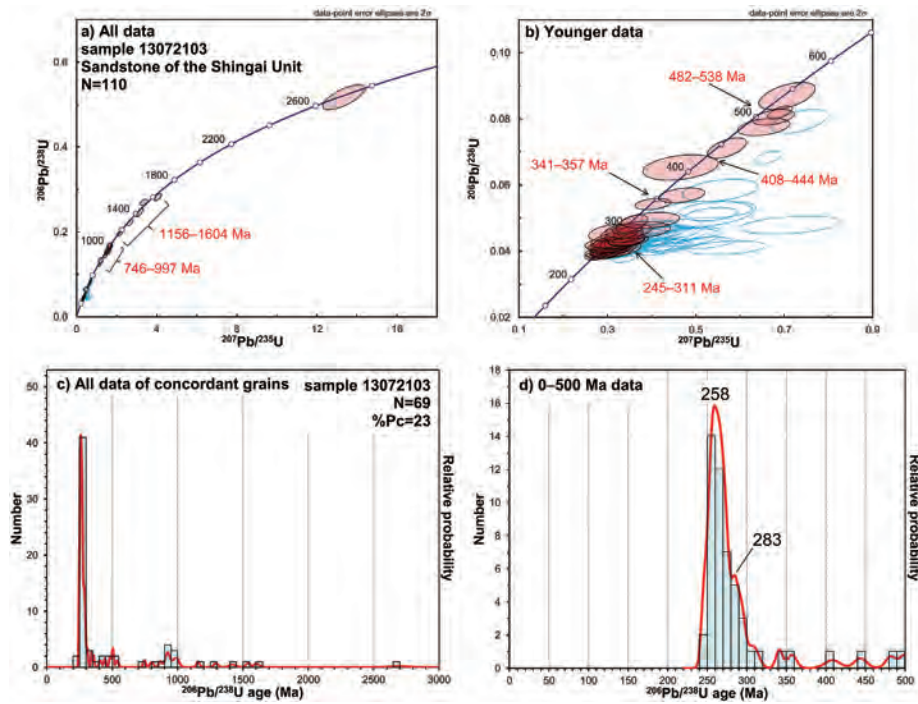


FIGURE 25. Analytical data of detrital zircons from sandstone of the Shingai Unit (sample 13072103). **a**, Concordia diagram for all data; **b**, Concordia diagram for a younger data set; **c**, Probability density plot with a histogram for all data of concordant grains; **d**, Probability density plot with a histogram for the 0–500 Ma data set. N: total number, %Pc: percentage of Precambrian zircons.

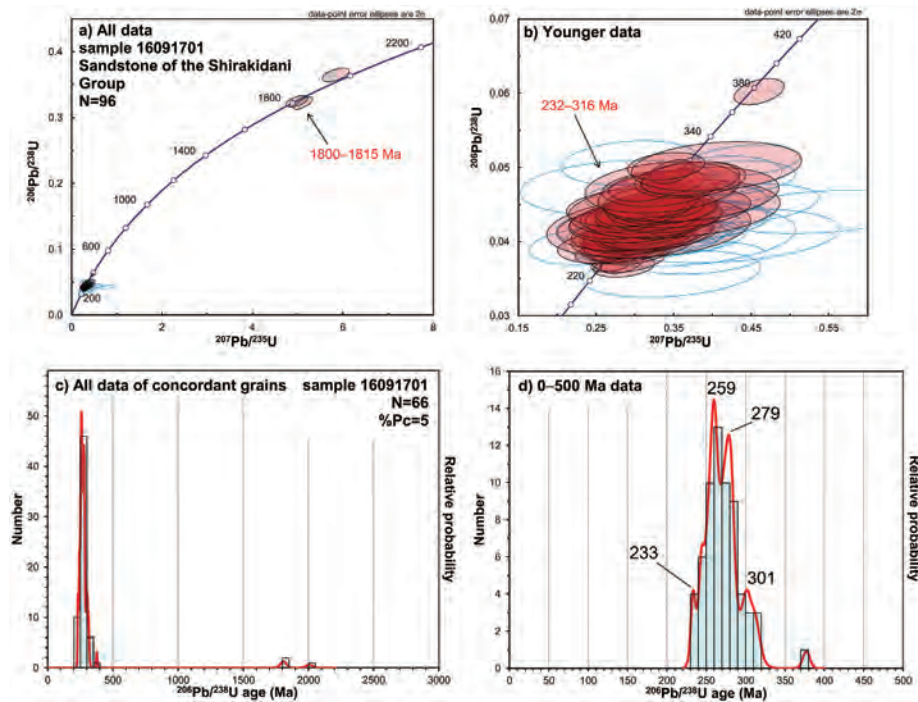


FIGURE 26. Analytical data of detrital zircons from sandstone of the Shirakidani Group (sample 16091701). **a**, Concordia diagram for all data; **b**, Concordia diagram for a younger data set; **c**, Probability density plot with a histogram for all data of concordant grains; **d**, Probability density plot with a histogram for the 0–500 Ma data set. N: total number, %Pc: percentage of Precambrian zircons.

Ma (2%), 423 Ma (1%), 626 Ma (1%), and 1779 Ma (1%), with %Pc of 2 and the YZ of 240.2 ± 7.7 Ma (Fig. 20a–c). The probability density plot for the 0–500 Ma data set showed the largest peak at 263 Ma and small peaks at 330 Ma, 380 Ma, and 465 Ma (Fig. 20d).

A sandstone cobble from the Yunoki Formation, Monobegawa Group (Sample YuSs-1)

We obtained 79 analyses from 79 zircon grains collected from sandstone cobble sample YuSs-1 of the middle part of the Yunoki Formation. 60 grains out of 79 gave concordant results (Fig. 21). We detected three age groups and one single plot of concordant detrital zircons: 184–314 Ma (70%), 1721–2070 Ma (23%), 358–380 Ma (5%), and 2633 Ma (2%), with %Pc of 25 and the YZ of 183.6 ± 2.6 Ma (Fig. 21a–c). The probability density plot for the 0–500 Ma data set showed the largest peak at 263 Ma, a second largest peak at 295 Ma, and small peaks at 183 Ma (YP), 199 Ma, 214 Ma, 230 Ma, 281 Ma, and 378 Ma (Fig. 21d).

A sandstone cobble from the Funadani Formation, Nankai Group (Sample FuSs-1)

We obtained 87 analyses from 87 zircon grains collected from sandstone cobble sample FuSs-1 of the Funadani Formation. 59 grains out of 87 gave concordant results (Fig. 22). We detected one age group and two single plots of concordant detrital zircons: 260–363 Ma (97%), 1940 Ma (2%), and 2143 Ma (2%) with %Pc of 3 and the YZ of 259.7 ± 7.2 Ma (Fig. 22a–c). The probability density plot for the 0–500 Ma data set showed the largest peak at 295 Ma and second largest peaks at 275 Ma (YP) and 329 Ma (Fig. 22d).

A rhyolite cobble from the Yunoki Formation, Monobegawa Group (Sample YuIg-1)

We obtained 34 analyses from 34 zircon grains collected from rhyolite cobble sample YuIg-1 of the middle part of the Yunoki Formation. 12 grains out of 34 gave concordant results (Fig. 23). We detected two age groups and two single plots of concordant zircons: 122–137 Ma (8 grains), 174–181 Ma (2 grains), 269 Ma (1 grain), and 2334 Ma (1 grain) (Fig. 23a). The concordia age of the youngest 6 grains was 125.4 ± 2.3 Ma (MSWD = 7.0, Probability = 0.008), which we interpreted as the formation age of the rhyolite (Fig. 23b).

A granodiorite cobble from the Hibihara Formation, Monobegawa Group (Sample HiIg-1)

We obtained 24 analyses from 24 zircon grains collected from granodiorite cobble sample HiIg-1 of the Hibihara Formation. 14 grains out of 24 gave concordant results, which form a single age group at 120–133 Ma (Fig. 24a). The weighted mean of the $^{206}\text{Pb}/^{238}\text{U}$ ages of 14 grains was 126.4 ± 2.5 Ma (MSWD = 6.7, Probability = 0.0), which we interpreted as the formation age of the granodiorite (Fig. 24b).

Pre-Cretaceous sandstone of the Northern Chichibu Belt

Sandstone of the Shingai Unit (Sample 13072103)

We obtained 110 analyses from 110 zircon grains collected from sandstone sample 13072103 of the Shingai Unit. 69 grains out of 110 gave concordant results (Fig. 25). We detected six age

groups and one single plot of concordant detrital zircons: 245–311 Ma (65%), 746–997 Ma (15%), 1156–1604 Ma (7%), 482–538 Ma (6%), 341–357 Ma (3%), 408–444 Ma (3%), and 2690 Ma (1%), with %Pc of 23 and the YZ of 245.2 ± 7.0 Ma (Fig. 25a–c). The probability density plot for the 0–500 Ma data set showed a single peak at 258 Ma (Fig. 25d).

Sandstone of the Shirakidani Group (Sample 16091701)

We obtained 96 analyses from 96 zircon grains collected from sandstone sample 16091701 of the Shirakidani Group. 66 grains out of 96 gave concordant results (Fig. 26). We detected two age groups and two single plots of concordant detrital zircons: 232–316 Ma (94%), 1800–1815 Ma (3%), 377 Ma (2%), and 2007 Ma (2%), with %Pc of 5 and the YZ of 232.2 ± 7.5 Ma (Fig. 26a–c). The probability density plot for the 0–500 Ma data set showed the largest peak at 259 Ma, second largest peak at 279 Ma, and small peaks 233 Ma (YP) and 301 Ma (Fig. 26d).

DISCUSSION

Age of deposition of the Lower Cretaceous formations in the study area

The mineral zircon is crystallized from acidic to intermediate magma (e.g., Hoskin and Schaltegger, 2003) and memorizes the age of formation of the felsic to intermediate-igneous-rock body from the magma. Due to the erosion of the igneous-rock body, the zircon grains in the rock body are transported to a sedimentary basin, together with reworked older zircons from sedimentary and/or metamorphic rock bodies. Okawa et al. (2013) concluded, from their study of detrital zircon ages from 14 sandstone samples of the South Kitakami Belt, that the YP of a sandstone sample on the probability density plot is a good measure for the upper age limit of the deposition of the sample. Following Okawa et al. (2013), we assume that the YP age or the concordia age of the YP-forming zircons (if calculated) of a sample is the upper limit of the age of deposition. In this study, we found that the upper age limit of the Yunoki and Birafo formations inferred from detrital zircon ages is significantly younger than the age of deposition inferred from fossils. In the following discussion, we will revise the age of deposition of the two formations.

Yunoki Formation

The Yunoki Formation has been correlated with the upper Barremian from a Neocomian type ammonite, *Paracrioceras* (?) sp. from the upper part of the formation (Tanaka et al., 1984; Fig. 4). The overlying Hibihara Formation, on the other hand, was correlated with the Aptian–Albian from ammonites. The lower Middle Member of the Hibihara Formation yields *Chelonicerias* (C.) sp. and is correlated with the lower Aptian; the upper Middle Member yields *Eodouvilleicerias* sp. and *Nolanicerias* (?) sp. and is correlated with the upper Aptian; and the Uppermost Member yields *Hysterocheras* aff. *H. carinatum*, *Engonoceras* aff. *E. stolleyi*, *Tetragonites* cf. *T. timotheanus*, *Idiohamites* sp., and *Pseudohelioceras* sp. and is correlated with the Albian (Tanaka et al., 1984; Fig. 4). In this study, we found that the concordia age of the two zircon grains forming the YP of sample Yu-1

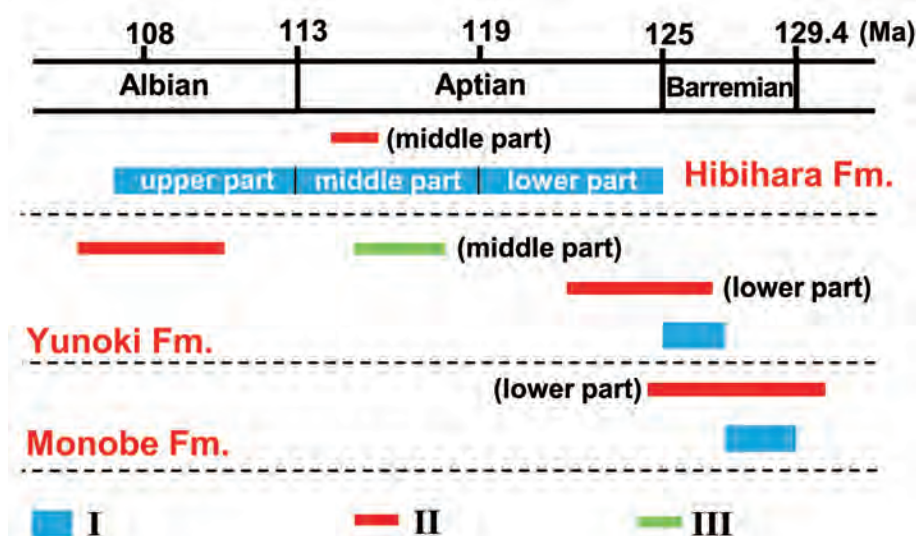


FIGURE 27. A diagram comparing the age constraints from fossils and zircons of the Monobegawa Group. Keys I: The age-range of index fossils, II: The age-range of zircons (with 2σ errors) forming the YP of each sample of the Monobegawa Group, III: The age-range of zircons (with 2σ errors) forming the second YP in sample Yu-2, Fm.: Formation, YP: youngest peak in the probability density plot.

from the lower part of the Yunoki Formation was 124.3 ± 2.4 Ma. For sample Yu-2 from the middle part, the concordia age of the two zircon grains forming the YP was 108.2 ± 2.4 Ma, and the concordia age of the five zircon grains forming the second youngest peak was 116.4 ± 1.5 Ma (MSWD = 0.7, Probability = 0.4). Moreover, the age of the rhyolite cobble from the middle part of the Yunoki Formation (sample YuIg-1) was 125.4 ± 2.3 Ma. According to International Commission for Stratigraphy (ICS) (2016), these age data strongly suggest that the Yunoki Formation is correlated with the Aptian (–Albian) (Fig. 27). The reason for the discrepancy between the fossil and zircon ages is still unknown. We have to wait for the definition of the base Aptian GSSP and its numerical age assignment, and the reexamination of the first appearance and last appearance biohorizons of the ammonite fossils from the Yunoki and Hibihara formations.

Birafu Formation

There were two interpretations on the correlation of the Birafu Formation, which was subdivided into A1–3, B1–2, and C members, in ascending order (Kozai et al., 2004, 2006). Morino et al. (1989) found radiolarian fossils from two locations including the B members along the Nishinokawa River and correlated the formation with the upper Valanginian–Barremian. Kozai et al. (2004, 2006), on the other hand, studied the radiolarian and bivalve fossils from the formation and correlated it with the Oxfordian–lower Valanginian, suggesting that the Jurassic–Cretaceous boundary lies between the A3 and B1 members. We found that sample Bi-1 from the A2 Member had the YZ and YP of 149.9 ± 3.6 Ma and 169 Ma, respectively, and did not contain Early Cretaceous zircons. Since a tuff layer just above Bi-1 yields Oxfordian radiolarians such as *Kilinora spiralis* (Kozai et al., 2006), we propose that sample Bi-1 is Oxfordian or younger in age, and our data do not contradict with the interpretation of

Kozai et al. (2004, 2006) that the A members are correlated with the Upper Jurassic. We also found that sample Bi-2 from the B members had the YZ and YP of 128.1 ± 4.7 Ma and 136 Ma, respectively, and 9 zircon grains out of 104 were of the Early Cretaceous. Since the concordia age of the 8 grains forming the YP was 136.5 ± 2.5 Ma, the age of deposition of sample Bi-2 must have been 139 Ma (Early Valanginian; ICS, 2016) or younger. Considering the fact that the C Member of the Birafu Formation, overlying the B members, consists of more than 200 m thick fine-grained rocks such as mudstone and interbedded fine sandstone and mudstone, we suppose that the age of the Birafu Formation ranges from the Oxfordian (Fig. 20) to the Late Valanginian or even the Hauterivian.

Provenance change of the Monobegawa and Nankai groups

Monobegawa Group

The detrital-zircon-age spectra of the Monobegawa Group are summarized as follows. The detrital zircons of the Ryoseki Formation (sample Ry-1) consisted mostly of Permian (51%) and Triassic (38%) zircons (Table. 1; Figs. 28 and 29), and the probability density plot showed a prominent peak at 252 Ma. On the other hand, the Monobe and Yunoki formations (samples Mo-1 and Yu-1) contained abundant Mesozoic zircons: i.e., Triassic, Jurassic, and Early Cretaceous zircons, whereas the uppermost Hibihara Formation (sample Hi-1) contained 60% of Early Cretaceous zircons (Figs. 28 and 29). Previous petrographical study of clastic rocks of the Monobegawa Group indicated that the clastic grains of the Ryoseki Formation were mainly derived from older sedimentary rocks, whereas the contribution of felsic to intermediate (the former in particular) igneous-rock fragments gradually increased upwards from the Monobe to Hibihara

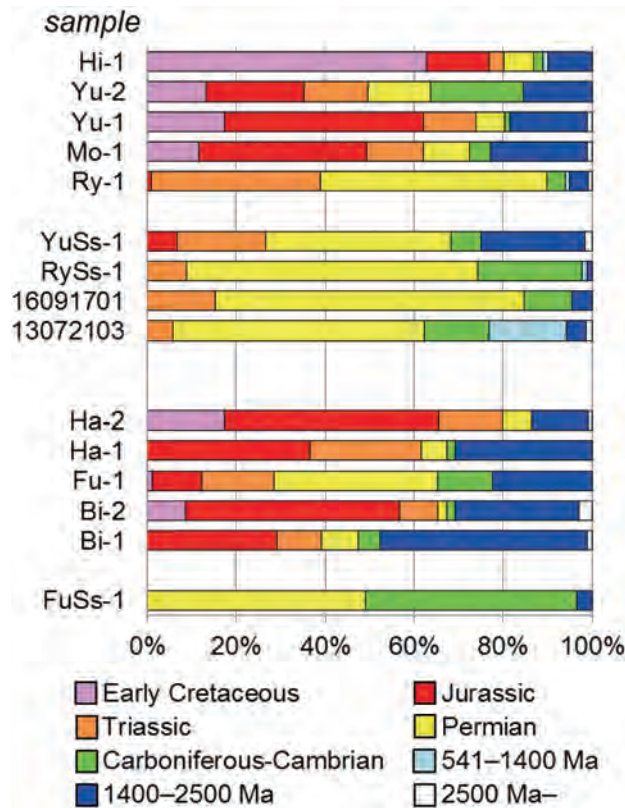


FIGURE 28. Bar graphs showing the age composition of detrital zircons from sandstone samples including the samples of sandstone cobbles.

formations (Miyamoto and Nakai, 1974; Miyamoto, 1980). We will discuss the provenance of detrital zircons in the Monobegawa Group from these data and previous studies.

The predominant Permian and Triassic zircons in the Ryoseki Formation strongly indicate the rework of detrital zircons from the pre-Cretaceous AC of the Northern Chichibu Belt, for four reasons. (1) Previous studies suggested that the clastic grains of the Ryoseki Formation were mainly supplied from the pre-Cretaceous sedimentary rocks of the Northern Chichibu Belt (Miyamoto and Nakai, 1974; Miyamoto, 1980). (2) The sandstone cobbles in the Ryoseki and Yunoki Formations (samples RySs-1 and YuSs-1) contain many Permian and Triassic zircons. (3) In particular, the detrital-zircon-age spectra of the sandstone cobble (sample RySs-1) and sandstone (sample Ry-1) of the Ryoseki Formation are very similar. (4) The detrital-zircon-age spectra of the sandstone of the Shingai Unit (sample 13072103), the Shirakidani Group (sample 16091701) and the Ryoseki Formation (sample Ry-1) are also very similar (Figs. 28 and 29).

On the other hand, our data and previous studies imply that igneous activity gradually became active in the hinterland during the deposition of the Monobe, Yunoki, and Hibihara formations. The reasons are as follows. (1) The proportion of Early Cretaceous zircons, which were absent in the Ryoseki Formation, gradually increases upwards (Fig. 28). (2) The proportion of feldspar and

rock fragments in sandstone and of felsic-igneous-rock clasts in conglomerate gradually increases upwards (Figs. 5–7). (3) The age of igneous rock cobbles in the Monobegawa Group (samples YuIg-1 and HiIg-1) is approximately 125 Ma.

Thus the provenance of the Monobegawa Group in the Ryoseki–Monobe area changed from the pre-Cretaceous rocks of the Northern Chichibu Belt (Ryoseki period) to an Early Cretaceous igneous province and pre-Cretaceous rocks of the Northern Chichibu Belt (Monobe–Hibihara period). A similar provenance change has been proposed in the Lower Cretaceous Sanchu Group in the Kanto Mountains from the petrography of clastic rocks (Takei, 1980) and the temporal change of the detrital-zircon-age spectra (Nakahata et al., 2016).

Nankai Group

The detrital-zircon-age spectra of the Nankai Group are summarized as follows. The Funadani Formation (sample Fu-1) was characterized by the abundance of Permian (37%) zircons, whereas the Birafo and Hagino formations (samples Bi-1, Bi-2, Ha-1, and Ha-2) were characterized by the abundance of Jurassic (28–48%) zircons (Figs. 28 and 29). Among them, the Permian zircons in the Funadani Formation were likely derived from older sedimentary rocks from the following reasons. (1) The conglomerate of the Funadani Formation mostly contains sedimentary-rock clasts, and (2) the sandstone cobble of the Funadani Formation (sample FuSs-1) was rich in Permian zircons (Figs. 28 and 29).

Origin of Triassic and Jurassic zircons

It is a little hard to judge if the Triassic and Jurassic zircons in the two groups have been derived from older sedimentary rocks or older igneous rocks. However, we propose that Jurassic igneous rocks were widespread in the hinterland of the Birafo Formation, because the sandstone of the Birafo Formation (samples Bi-1 and Bi-2), containing many Jurassic zircons, is feldspathic arenite derived from felsic plutonic rocks. Further, the Aptian Kurohara Formation (Kozai and Ishida, 2006) in the Sakawa area, some 50 km to the west of the study area, contains a 227 Ma granite cobble (Ikeda et al., 2016), suggesting that Triassic igneous rocks were also exposed in the hinterland of the Lower Cretaceous beds of the study area.

Paleogeography of the Lower Cretaceous formations of the Ryoseki–Monobe area

Sediment supply from South China

We inferred that Early Cretaceous igneous rocks were exposed in the hinterland of most of the Lower Cretaceous formations in the study area from the detrital-zircon-age spectra. Along the present continental margin of East Asia, Early Cretaceous rock bodies that can supply enough detrital zircons occur most widely along the eastern margin of South China (145–90 Ma; e.g., Li et al., 2014; Wang et al., 2013). Smaller Early Cretaceous igneous rock bodies also occur in the Kitakami (130–110 Ma; Tsuchiya et al., 2015) and Abukuma (120–85 Ma; e.g., Kawano and Ueda, 1965; Shibata and Uchiumi, 1983; Ishihara and Orihashi, 2015; Kon et al., 2015) belts of Northeast Japan, in the Higo Belt of

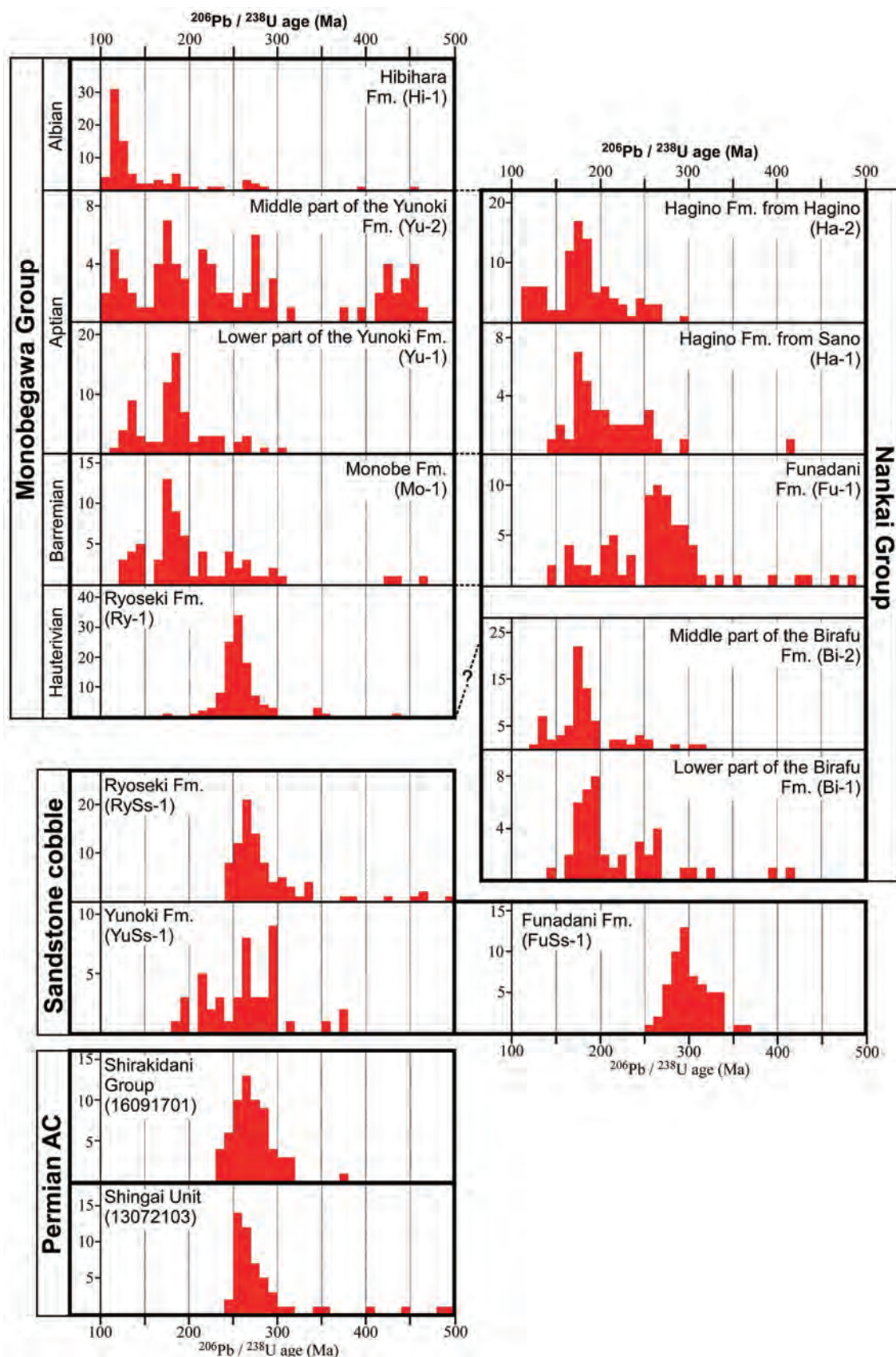


FIGURE 29. Histograms showing the detrital-zircon-age distribution of sandstone samples including the samples of sandstone cobbles. Fm: Formation.

Kyushu, Southwest Japan (120–110 Ma; e.g., Sakashima et al., 2003), and around the Bohai and West Korea bays, Northeast China (135–110 Ma; e.g., Kiminami and Imaoka, 2013; Wang et al., 2012; Wu et al., 2007). Among these areas, we propose that the Early Cretaceous zircons in the Lower Cretaceous formations of the study area were supplied from the Zhejiang–Fujian coast of South China, for three reasons.

(1) The detrital-zircon-age spectra of the Monobegawa and Nankai groups do not show the influence of the magmatic hiatus in Korea, which is supposed to have been 158–110 Ma (Sagong et al., 2005). The distribution of 145–100 Ma felsic-igneous rocks is limited along the eastern margin of South China among the above areas.

(2) Possible provenances of the 125 Ma felsic-igneous-rock clast (cobble) are along the east coast of South China, Kitakami Belt, and around the Bohai and West Korea bays, where felsic-igneous-rocks of approximately 125 Ma are widely exposed (Fig. 30). Considering the size and abundance of igneous rock clasts, it is hard to imagine that they were transported from rock bodies far from the coast. In this sense we exclude the 125 Ma felsic-igneous-rock-bodies around the Bohai and West Korea bays from the candidates of the provenance.

(3) The Ryoseki Formation of the Monobegawa Group yields many elements of the Ryoseki-type flora, which occurs in South China (Zhejiang Province and to the south), Indochina, and the Malay Peninsula in continental Asia (Kimura, 1987). The distribution of the flora is concordant with our idea that the Monobegawa Group was deposited along the eastern coast of South China.

The Monobegawa and Nankai groups also contain many Triassic and Jurassic zircons, and at least parts of them are igneous origin as discussed above. However, the Triassic–Jurassic zircons were not enough useful to detect the provenance, because Triassic–Jurassic (> 158 Ma) igneous rocks widely occur in East Asia. Nevertheless, the presence of Triassic–Jurassic zircons does not contradict with our idea; Triassic–Jurassic igneous rocks, including those formed during the magmatic hiatus of Korea, are widely distributed in the eastern part of the Zhejiang–Fujian provinces of South China.

Sandstone from the middle part of the Yunoki Formation (sample Yu-2) of the Monobegawa Group (Northern Chichibu Belt) contains a certain amount of 460–400 Ma zircons (18%). In Japan, 460–400 Ma felsic-igneous-rock bodies occur in (1) the South Kitakami Belt, Northeast Japan (e.g., Shimojo et al., 2010), (2) the Yakuno Complex, Inner Zone of Southwest Japan, and (3) the Kurosegawa Belt, Outer Zone of Southwest Japan (Mitaki igneous rocks; e.g., Hada et al., 2000), but the present areas of their distribution are very narrow. Although we cannot completely deny the possibility that the 460–400 Ma zircons in sample Yu-2 were supplied from the 460–400 Ma rock bodies in present-day Japan, the age composition of igneous rocks in South China (Fig. 30) and the presence of the Ryoseki-type flora in the Monobegawa Group strongly indicates that the 460–400 Ma Kwangsi Granite in South China (e.g., Wang et al., 2013) was most likely the provenance of the 460–400 Ma zircons.

Evaluation of sinistral strike-slip models

In the previous section, we concluded that the provenance of Early Cretaceous zircons in the Monobegawa and Nankai groups and 460–400 Ma zircons in the Yunoki Formation was Early Cretaceous and 460–400 Ma igneous rock bodies in the Zhejiang–Fujian province of South China. The distance from the Ryoseki–Monobe area and the Zhejiang–Fujian province is roughly 1,500 km. It is also possible that the basement of the Yellow Sea Basin consists partly of Early Cretaceous igneous rocks that cropped out on the land surface in the Early Cretaceous and supplied Early Cretaceous zircons to the Monobegawa Group and/or Nankai Group. Even in this case, the distance between the Ryoseki–Monobe area and the mouth of the Yellow Sea is about 500 km. Hence we interpret that the Monobegawa and Nankai groups have moved at least 500–1,500 km northeastward (Fig. 30). We further interpret that the sinistral strike-slip motion along the Median Tectonic Line (Miyata and Iwamoto, 1994; Yamakita and Otoh, 2000a, b) was responsible for at least a part of the above displacement.

It is still hard to verify, only with our zircon data, the strike-slip model of Tashiro (1985), which described that the arc-subparallel sinistral strike-slip motion between the Monobegawa and Nankai groups had carried the Nankai Group relatively northward by the Albian. There are significant differences in the detrital-zircon-age spectra between the coeval samples of the Monobegawa and Nankai groups, but we cannot so precisely specify the site of deposition of each sample as to evaluate the strike-slip model of Tashiro (1985). For example, samples Ry-1 (Ryoseki Formation, Monobegawa Group) and Bi-2 (middle part of the Birafu Formation, Nankai Group) can be contemporaneous, but the differences in the positions of the largest peak (Ry-1 at 252 Ma and Bi-2 at 172 Ma; Figs. 10d and 16d) and in %Pc value (6 for Ry-1 and 31 for Bi-2; Figs. 10c and 16c) suggest different provenances. Sample Fu-1 (Funadani Formation, Nankai Group) can also be coeval with sample Ry-1, but the position of the largest peak (269 Ma; Fig. 17d) and %Pc value (22; Fig. 17c) differ from those of sample Ry-1. Sample Mo-1 (Monobe Formation, Monobegawa Group) in turn can be coeval with sample Fu-1, but the position of the largest peak (174 Ma; Fig. 11d) differs from that of sample Fu-1. Moreover, the following differences in sandstone and conglomerate petrography also indicate the different provenances between the Monobegawa and Nankai groups. (1) The sandstone of the Monobegawa Group is primarily ill-sorted wacke, whereas that of the Nankai Group is mainly well-sorted arenite (Tashiro, 1985). (2) The conglomerate of the Shobu Formation of the Nankai Group in the Katsuura area characteristically contains felsic-igneous-rock clasts, whereas the coeval conglomerate of the Tatsukawa Formation of the Monobegawa Group is characterized by sedimentary-rock clasts (Matsukawa and Eto, 1987). In contrast, the detrital-zircon-age spectra of the following two Aptian samples are similar with each other: sample Yu-1 from the lower part of the Yunoki Formation and sample Ha-2 from the Hagino Formation from Hagino (Fig. 31). The similarity indicates the common provenance of the Monobegawa and Nankai groups in the Aptian. Even if the strike-

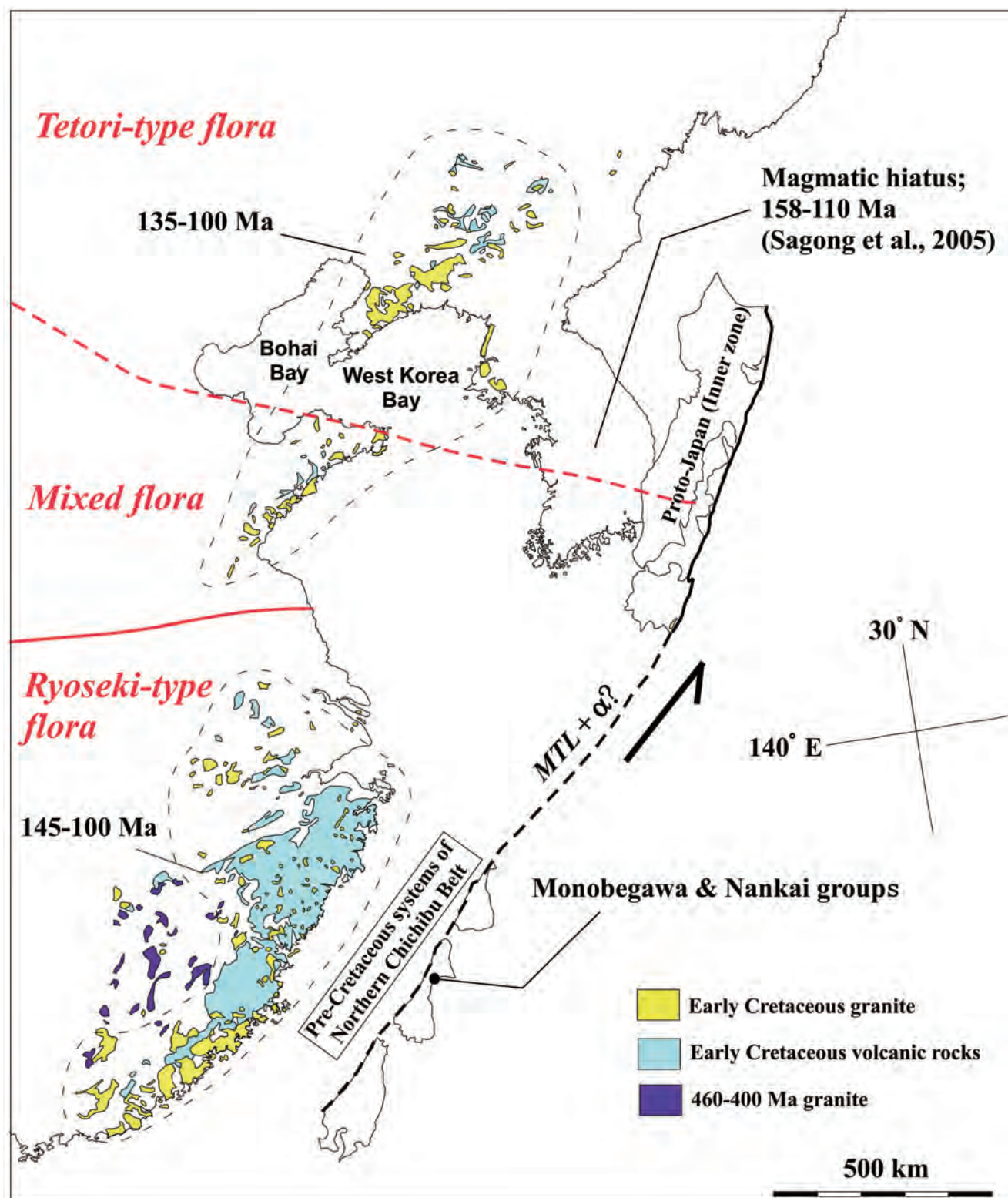


FIGURE 30. A paleogeographic map showing the possible reconstruction model for the sedimentary basins of the Lower Cretaceous formations in the Ryoseki–Monobe area, Outer Zone of Southwest Japan.

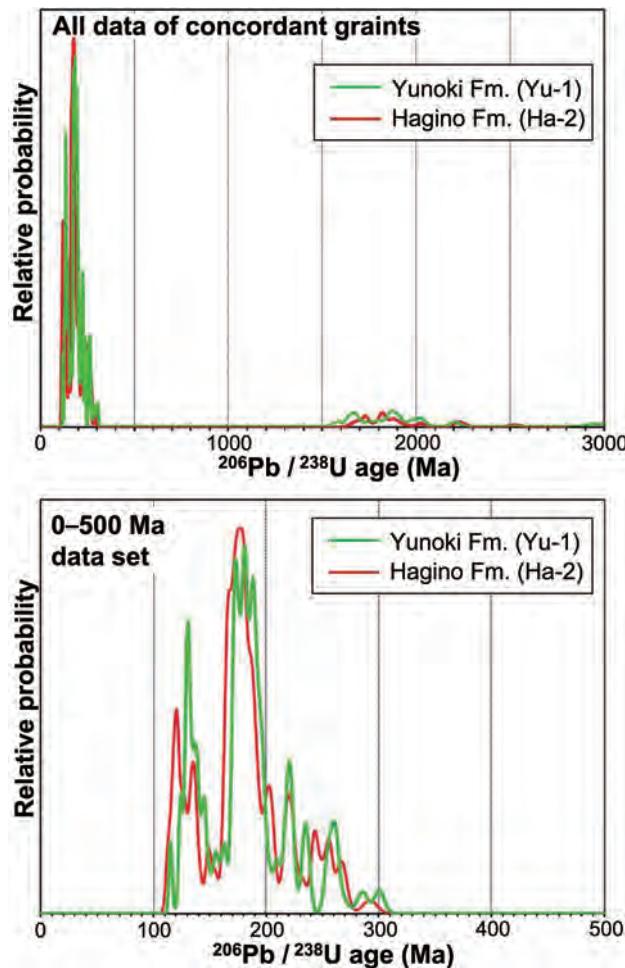


FIGURE 31. Probability density plots showing the similarity of detrital-zircon-age distribution between sample Yu-1 (lower part of the Yunoki Formation) and Ha-2 (Hagino Formation from Hagino).

slip model of Tashiro (1985) is close to the reality, the movement may have ceased by the end of Aptian.

Evaluation of the Paleo-Ryoke model

Many previous studies implied that a geologic entity called the Paleo-Ryoke Belt, consisting of Permian and Early Cretaceous granite and metamorphic rocks, was once exposed between the Ryoke and Sambagawa belts but have mostly been eroded away (Ichikawa, 1964; Takagi and Shibata, 2000; Miyamoto et al., 2000). Miyamoto (1980) attributed the origin of igneous-rock clasts in the Monobegawa Group of the study area to the missing geologic entity along the southern margin of the Ryoke Belt. As we discussed above, however, we concluded that the igneous-rock clasts in the Monobegawa Group were supplied from igneous-rock bodies in the Zhejiang–Fujian provinces of South China from the botanical paleogeography (Kimura, 1987) and the sinistral strike-slip motion along the Median Tectonic Line separating the Ryoke and Sambagawa belts (e.g., Miyata and Iwamoto, 1994; Yamakita and Otoh, 2000a, b). Moreover, (1) the presence of Permian

igneous and metamorphic rocks along the southern margin of the Jurassic AC of the Ryoke Belt and (2) the short distance between the Lower Cretaceous AC (i.e., Early Cretaceous subduction zone) of the Shimanto Belt and the Ryoke Belt (ca. 60 km) have not been explained in the Paleo-Ryoke model in a plate-tectonic framework.

Aoki et al. (2014) proposed that there was a topographic barrier that obstructed the southward transport of continent-derived sediments in the Early Cretaceous, because the Ryoseki Formation of the Hauterivian forearc basin contained very few continent-derived Proterozoic zircons that dominated in the brackish to shallow-marine Toyonishi Group (Inner Zone of Southwest Japan) of the latest Jurassic to earliest Cretaceous back-arc basin. Aoki et al. (2014) concluded that the barrier was the Early Cretaceous igneous arc developed in the older orogen and was thrust southward for more than 200 km along the Median Tectonic Line during the opening of the Sea of Japan in the Middle Miocene. However, we detected more than 20% Proterozoic zircons from the Monobe (Barremian; 22%), lower Birafo (latest Jurassic; 46%), middle Birafo (early Early Cretaceous; 28%), and Funadani (Hauterivian–Barremian; 22%) formations. Moreover, the Monobegawa and Nankai groups contained many Triassic to Jurassic zircons, in spite of the fact that there are virtually no Triassic to Jurassic igneous rocks to the south of the distribution of the Toyonishi Group. Thus, our data are not concordant with the barrier model of Aoki et al. (2014). We tentatively think that the amount of Proterozoic detrital zircons depends on the area of exposure of Proterozoic igneous rocks in the hinterland and the distance between the Proterozoic igneous rock bodies and the sedimentary basin. In addition, we doubt the Miocene southward thrust model, because the distance between the Paleogene volcanic front (the southern boundary of the San-in granite belt) and trench (Southern Shimanto Belt) was 300 km, close to the arc-trench gap in the present-day Northeast Japan, and we expect no arc-orthogonal shortening in the Miocene.

Importance of reworked zircons in the study of detrital-zircon-age spectra

Nakahata et al. (2016) conducted a similar study with ours of the Sanchu Cretaceous in the Kanto Mountains, north of Tokyo. They concluded that Permo–Triassic igneous rock bodies were widely exposed in the hinterland of the Hauterivian Shiroy Formation, because Permo–Triassic zircons occupied 76% of the detrital zircons in the formation. They further suggested that clastic materials from Permo–Triassic igneous rock bodies were widely supplied to the Hauterivian forearc of Kanto and Shikoku, because the detrital-zircon-age spectra of the Shiroy and Ryoseki formations are very similar, and the Ryoseki Formation contains many 300–200 Ma zircons (Aoki et al., 2012). However, the distribution of Permian igneous rocks near Japan is limited to Northeast China and Indochina, although there are few Permian igneous rock bodies in the Maizuru Belt in Southwest Japan (e.g., Herzig et al., 1997). This study implied that the detrital zircons of the Ryoseki Formation were mainly derived from the Permian clastic rocks of the Northern Chichibu Belt. The sandstone of the Sanchu Cretaceous is lithic with many sedimentary-rock fragments

in the lower part and felspathic in the upper part, suggesting the change from a sedimentary-rock-rich hinterland to a granite-rich hinterland (Takei, 1980). Moreover the conglomerate of the Hauterivian Tatsukawa Formation of the Monobegawa Group in the Katsuura area consists mostly of older-sedimentary-rock clasts (Ishida and Hashimoto, 1997; Matsukawa and Eto, 1987; Ogawa, 1971). Hence we propose that the Hauterivian formations of the Outer Zone of Southwest Japan from Kanto to Shikoku had a hinterland widely occupied by older sedimentary rock bodies and received detrital zircons from them. We further propose that it is misleading to think that the detrital zircons were all derived from igneous-rock bodies in the hinterland. To make a proper provenance analysis using detrital zircons, we have to make a comprehensive study including (1) the modal composition of the sandstone for detrital zircon study and (2) the detrital-zircon-age spectra of the basement sedimentary rocks and sandstone clasts in the conglomerate. Although the proportion of abraded zircons might be a criterion for the recognition of reworked zircons, the criterion cannot be applied to our present study. The proportion of abraded zircons in the sandstone of the Ryoseki Formation (Ry-1), the sandstone clast in the Ryoseki Formation (RySs-1), and the 300–230 Ma zircons in the sandstone of the Shirakidani Group (16091701) were 57, 54, and 50%, respectively, and did not show a significant difference. The result may reflect a short distance of transportation of the reworked zircons.

CONCLUSIONS

We studied detrital-U-Pb-zircon-age spectra of the sandstone sample from every formation of the Lower Cretaceous Monobegawa and Nankai groups (part of the Nankai Group is Upper Jurassic) of the Chichibu Composite Belt in the Ryoseki–Monobe area, Southwest Japan. In addition, we measured the U-Pb zircon age of (1) igneous rock cobbles in these formations and detrital-zircon-age spectra of (2) the sandstone cobbles from these formations and (3) the basement Permian sandstone of the Northern Chichibu Belt. The major results are summarized as follows.

1. The detrital-zircon-age spectra of the sandstone and sandstone cobble of the Ryoseki Formation and the Permian sandstone of the Northern Chichibu Belt are very similar. Combining the data with previous studies, we conclude that the clastic materials of the Ryoseki Formation were supplied from the pre-Cretaceous sedimentary rocks of the Northern Chichibu Belt.
2. Early Cretaceous zircons were absent in the Ryoseki Formation, but suddenly increased in the Monobe–Hibihara formations. Moreover, the U-Pb zircon age of the igneous rock cobbles from the Yunoki and Hibihara formations was approximately 125 Ma. Combining with the previous petrographical studies of sandstone and conglomerate, we conclude that an acidic to intermediate igneous activity took place in the hinterland concurrently with the deposition of the Monobegawa Group.
3. The petrography of clastic rocks implies that felsic-igneous-

rock-bodies were exposed in the hinterland of the Nankai Group. The detrital-zircon-age spectra of the group indicate that the igneous rock bodies contained Early Cretaceous ones.

4. The hinterland of the two groups must have been the Zhejiang–Fujian provinces of South China, because (1) the study of botanical paleogeography of Kimura (1987) indicated that the Ryoseki Formation and South China commonly yield the Ryoseki-type flora, (2) detrital zircons formed during the magmatic hiatus in Korea were included in both the Monobegawa and Nankai groups, and (3) 460–400 Ma detrital zircons from the middle part of the Yunoki Formation were most likely from the Kwangsi Granite of South China.
5. The Monobegawa and Nankai groups likely had different hinterland by the Aptian. The previous petrographical studies and the similarity of detrital-zircon-age spectra of the lower part of the Yunoki Formation (Monobegawa Group) and the Hagino Formation (Nankai Formation) indicate that the two groups had common hinterland in the Aptian.
6. The two groups were deposited with the Zhejiang–Fujian provinces as the hinterland. The two groups must have shifted relatively northward by 500–1,500 km along the Median Tectonic Line sinistral fault system.
7. Detrital zircons were not all supplied from igneous rock bodies in the hinterland, but can be provided from older sedimentary and metamorphic rocks as reworked zircons. To make a proper provenance analysis using detrital zircons, we have to make a comprehensive study including (1) the modal composition of the sandstone for detrital zircon study and (2) the detrital-zircon-age spectra of the basement sedimentary rocks and sandstone clasts in the conglomerate.

ACKNOWLEDGMENTS

We would like to express our sincere gratitude to Dr. Shin-ichi Sano of the Fukui Prefectural Dinosaur Museum for his encouragement to submit our work to this volume; and to Professor Masaaki Shimizu and Associate Professor Yasuo Ishizaki of the University of Toyama for various discussions and instructions during the course of this study. Critical reviews of the submitted manuscript by Professor Haruyoshi Maeda of Kyushu University, Professor Makoto Takeuchi of Nagoya University, and Dr. Soichiro Kawabe of the Fukui Prefectural Dinosaur Museum are greatly appreciated. This study was supported by JSPS KAKENHI Grant Number 25400484.

REFERENCES

- Aoki, K., Y. Isozaki, D. Kofukuda, T. Sato, A. Yamamoto, K. Maki, S. Sakata and T. Hirata. 2014. Provenance diversification within an arc-trench system induced by batholith development: The Cretaceous Japan case. *Terra Nova* 28: 139–149.
- Aoki, K., Y. Isozaki, S. Yamamoto, K. Maki, T. Yokoyama and T. Hirata. 2012. Tectonic erosion in a Pacific-type orogen: Detrital

- zircon response to Cretaceous tectonics in Japan. *Geology* 40: 1087–1090.
- Hada, S., M. Tashiro and T. Ikuma. 1982. Geological structure of the Upper Cretaceous strata in Monobe area, Shikoku; pp. 9–13 in T. Matsumoto and M. Tashiro (eds.), *Multidisciplinary Research in the Upper Cretaceous of the Monobe Area, Shikoku*. Palaeontological Society of Japan, Special Papers, no. 25.
- Hada, S., S. Yoshikura and J. E. Gabites. 2000. U-Pb zircon ages for the Mitaki igneous rocks, Siluro-Devonian tuff, and granitic boulders in the Kurosegawa Terrane, Southwest Japan. *Memoirs of the Geological Society of Japan* 56: 183–198.
- Herzig, C. T., D. L. Kimbrough and Y. Hayasaka. 1997. Early Permian zircon uranium-lead ages for plagiogranites in the Yakuno ophiolite, Asago district, Southwest Japan. *Island Arc* 6: 396–403.
- Hoskin, P. W. O., and U. Schaltegger. 2003. The composition of zircon and igneous and metamorphic petrogenesis; pp. 27–62 in J. M. Hancher and P. W. O. Hoskin (eds.), *Zircon, Reviews in Mineralogy and Geochemistry* 53. Mineralogical Society of America, Washington, DC.
- Ichikawa, K. 1964. Tectonic status of the Honshu major belt in Southwest Japan during the early Mesozoic. *Journal of Geosciences Osaka City University* 8: 71–107.
- Ikeda, T., T. Harada, Y. Kouchi, K. Yamamoto and S. Otoh. 2016. U-Pb geochronology of igneous-rock clasts from the Lower Cretaceous formations of the Chichibu Composite belt, SW Japan. Abstracts, the 123rd Annual Meeting of the Geological Society of Japan: R5-P-34. **
- Ikuma, T. 1980. Deformation of the Cretaceous strata of the Chichibu Belt in the Ryoseki-Monobegawa area, Kochi Prefecture, Shikoku. *Journal of the Geological Society of Japan* 86: 389–407. *
- International Commission on Stratigraphy. 2016. International chronostratigraphic chart, v2016/04. <http://www.stratigraphy.org/ICSChart/ChronostratChart2016-04.pdf>.
- Ishida, K., and H. Hashimoto. 1997. Mesozoic and Paleozoic radiolarians from the chert pebbles and fine clastics of the Ryoseki and Monobegawa Groups in East Shikoku. *News of Osaka Micropaleontologists, Special Volume* 10: 217–235. *
- Ishihara, S., and Y. Orihashi. 2015. Cretaceous granitoids and their zircon U-Pb ages across the south-central part of the Abukuma Highland, Japan. *Island Arc* 24: 159–168.
- Kawagoe, Y., S. Sano, Y. Orihashi, H. Obara, Y. Kouchi and S. Otoh. 2012. New detrital zircon age data from the Tetori Group in the Mana and Itoshiro areas of Fukui Prefecture, Central Japan. *Memoir of the Fukui Prefectural Dinosaur Museum* 11: 1–18.
- Kawano, Y., and Y. Ueda. 1965. K-A dating on the igneous rocks in Japan (3) — Granitic rocks in Abukuma massif —. *Journal of the Japanese Association of Mineralogists, Petrologists and Economic Geologists* 54: 162–172. *
- Kiminami, K., and T. Imaoka. 2013. Spatiotemporal variations of Jurassic–Cretaceous magmatism in eastern Asia (Tan-Lu Fault to SW Japan): evidence for flat-slab subduction and slab rollback. *Terra Nova* 25: 414–422.
- Kimura, T. 1987. Geographical distribution of Palaeozoic and Mesozoic plants in East and Southeast Asia; pp. 135–200 in A. Taira and M. Tashiro (eds.), *Historical Biogeography and Plate Tectonic Evolution of Japan and Eastern Asia*, TERRAPUB, Tokyo.
- Kon, Y., T. Ejima, S. Morita and T. Takagi. 2015. Spatial U-Pb age distribution of plutonic rocks in the central Abukuma Plateau, northeastern Japan Arc. *Journal of Mineralogical and Petrological Sciences* 110: 145–149.
- Kouchi, Y., Y. Orihashi, H. Obara, T. Fujimoto, Y. Haruta and K. Yamamoto. 2015. Zircon U-Pb dating by 213 nm Nd: YAG laser ablation inductively coupled plasma mass spectrometry: optimization of the analytical condition to use NIST SRM 610 for Pb/U fractionation correction. *Chikyukagaku (Geochemistry)* 49: 19–35. *
- Kozai, T. 2008. Faunal change of Early Cretaceous bivalves in the eastern margin of Asian Continent. Doctoral Thesis at Graduate School of Science and Engineering of Waseda University, 151 pp. *
- Kozai, T., and K. Ishida. 2000. Stratigraphy of the Nankai Group in the Tosayamada area, Central Kochi, and correlation with the Monobegawa Group. *Research Bulletin of Naruto University of Education, Natural Science* 15: 13–25. *
- Kozai, T., and K. Ishida. 2003. “Tethyan” - “Northern Tethyan” transitional bivalve-fauna from the Kurosegawa Belt of Central Shikoku. *Research Bulletin of Naruto University of Education, Natural Science* 18: 19–28. *
- Kozai, T., and K. Ishida. 2006. Lower Cretaceous litho- and bivalve-stratigraphy of the Sakawa-Ochi area, Kochi Prefecture, SW Japan. *Research Bulletin of Naruto University of Education, Natural Science* 21: 283–293. *
- Kozai, T., K. Ishida and Y. Kondo. 2004. Radiolarian ages and bivalve fauna of the Birafo Formation, Central Shikoku. *News of Osaka Micropaleontologists, Special Volume* 13: 149–165. *
- Kozai, T., K. Ishida and Y. Kondo. 2006. Jurassic–Cretaceous boundary and Cretaceous formations in the Tosayamada–Birafo area, Kochi Prefecture. *Journal of the Geological Society of Japan* 112: 89–99. **
- Kozai, T., T. Nishikawa and K. Ishida. 2007. “Tethyan” and “Northern Tethyan” faunas from the Lower Hanoura Formation of the Monobegawa Group. Abstracts with Programs, 2007 Annual Meeting, the Palaeontological Society of Japan: 44. **
- Li, J. H., Y. Q. Zhang, S. W. Dong and S. T. Johnston. 2014. Cretaceous tectonic evolution of South China: a preliminary synthesis. *Earth-Science Reviews* 134: 98–136.
- Ludwig, K. R. 2012. User’s manual for Isoplot 3.75: a geochronological toolkit for Microsoft Excel. Berkeley Geochronology Center Special Publication 5, 75 pp.
- Matsukawa, M., and F. Eto. 1987. Stratigraphy and sedimentary environment of the Lower Cretaceous system in the Katsuragawa Basin, Southwest Japan—Comparison of the two Cretaceous subbelts in the Chichibu Belt—. *Journal of the Geological Society of Japan* 93: 491–511. *
- Matsuoka, A., S. Yamakita, M. Sakakibara and K. Hisada. 1998.

- Unit division for the Chichibu Composite Belt from a view point of accretionary tectonics and geology of western Shikoku, Japan. *Journal of the Geological Society of Japan* 104: 634–653.*
- Miyamoto, T. 1980. Stratigraphical and sedimentological studies of the Cretaceous System in the Chichibu Terrain of the Outer Zone of Southwest Japan. *Geological Report of the Hiroshima University* 23: 1–138.*
- Miyamoto, T., and I. Nakai. 1973. Petrography of the Cretaceous sandstones in the Monobegawa Valley, Shikoku. *Journal of Science of the Hiroshima University, Series C*, 7: 69–100.
- Miyamoto, T., I. Hara and M. Yamane. 2000. Reconstruction of tectonic framework of the Kurosegawa–Paleo-Ryoke–Southern Kitakami continent. *Memoirs of the Geological Society of Japan* 56: 13–22.*
- Miyata, T., and M. Iwamoto. 1994. Growth mechanism of Cretaceous Izumi sedimentary basin. *Structural Geology* 40: 139–144.*
- Morino, Y. 1993. Depositional environments of the Lower Cretaceous Torinosu type limestone in the Monobe area, Kochi Prefecture. *Journal of the Geological Society of Japan* 99: 173–183.*
- Morino, Y., T. Kozai, T. Wada and M. Tashiro. 1989. On the Lower Cretaceous Birafo Formation including the Torinosu type limestone in the Monobe area, Kochi Prefecture. *Research Reports of Kochi University, Natural Science* 38: 73–83.*
- Nakahata, H., Y. Isozaki, Y. Tsutsumi and N. Iwamoto. 2016. Age spectra of detrital zircons from shallow marine Cretaceous in southern Kanto, SW Japan: Change in composition of fore-arc sandstones in response to the rejuvenation of provenance crust. *Journal of Geography* 125: 353–380.*
- Ogawa, Y. 1971. Geology of Katsuuragawa district, Tokushima Prefecture, its stratigraphy and structure. *Journal of the Geological Society of Japan* 77: 617–634.*
- Okada, H. 1971. Again on classification and nomenclature of sandstone. *Journal of the Geological Society of Japan* 77: 395–396.**
- Okawa, H., M. Shimojo, Y. Orihashi, K. Yamamoto, T. Hirata, S. Sano, Y. Ishizaki, Y. Kouchi, S. Yanai and S. Otoh. 2013. Detrital zircon geochronology of the Silurian–Lower Cretaceous continuous succession of the South Kitakami Belt, Northeast Japan. *Memoir of the Fukui Prefectural Dinosaur Museum* 12: 35–78.
- Otoh, S., and S. Yanai. 1996. Mesozoic inverse wrench tectonics in far east Asia: examples from Korea and Japan; pp. 401–419 in A. Yin and M. Harrison (eds.), *The Tectonic Evolution of Asia*. Cambridge University Press, Stanford.
- Sagong, H., S. T. Kwon and J. H. Ree. 2005. Mesozoic episodic magmatism in South Korea and its tectonic implication. *Tectonics* 24: TC5002 (doi: 10.1029/2004TC001720)
- Sakashima, T., K. Terada, T. Takeshita and Y. Sano. 2003. Large-scale displacement along the Median Tectonic Line, Japan: evidence from SHRIMP zircon U–Pb dating of granites and gneisses from the South Kitakami and paleo-Ryoke belts. *Journal of Asian Earth Sciences* 21: 1019–1039.
- Shibata, K., and S. Uchiumi. 1983. K–Ar ages on hornblendes from granitic rocks in the southern Abukuma Plateau. *Journal of the Japanese Association of Mineralogists, Petrologists and Economic Geologists* 78: 405–410.*
- Shimojo, M., S. Otoh, S. Yanai, T. Hirata and S. Maruyama. 2010. LA-ICP-MS U–Pb age of some older rocks of the South Kitakami belt, Northeast Japan. *Journal of Geography* 119: 257–269.*
- Suyari, K., Y. Kuwano and K. Ishida. 1983. Biostratigraphic study of the North Subbelt of the Chichibu Belt in Central Shikoku. *Journal of Science College of General Education, University of Tokushima* 16: 143–167.*
- Taira, A., and M. Tashiro. 1987. Late Paleozoic and Mesozoic accretion tectonics in Japan and eastern Asia; pp. 1–43 in A. Taira and M. Tashiro (eds.), *Historical Biogeography and Plate Tectonic Evolution of Japan and Eastern Asia*. TERRAPUB, Tokyo.
- Takagi, H., and K. Shibata. 2000. Constituents of the Paleo-Ryoke Belt and restoration of the Paleo-Ryoke and Kurosegawa Terranes. *Memoirs of the Geological Society of Japan* 56: 1–12.*
- Takei, K. 1980. Petrography, provenance and deposition of the Cretaceous sandstones of the Sanchu Graben, Kanto Mountains, Japan. *Journal of the Geological Society of Japan* 86: 755–769.*
- Tanaka, H., T. Kozai and M. Tashiro. 1984. Lower Cretaceous stratigraphy in the Monobe area, Shikoku. *Research Reports of Kochi University, Natural Science* 32: 215–223.*
- Tashiro, M. 1985. The Cretaceous System of the Chichibu Belt in Shikoku — on the Early Cretaceous lateral fault in the Chichibu Belt —. *Fossils* 38: 23–35.*
- Tashiro, M. 1986. Paleobiogeography and paleoecology of the Cretaceous System of Southwest Japan. *Fossils* 41: 1–16.*
- Tashiro, M. 1993. Bivalve faunas from Cretaceous of Japan, Part 1: On the bivalve faunas from the Chichibu and “Ryoke” Belts in Southwest Japan. *Research Reports of Kochi University, Natural Science* 42: 105–155.*
- Tashiro, M. 1994. Cretaceous tectonic evolution of southwest Japan from the bivalve faunal view-points. *Research Reports of Kochi University, Natural Science* 43: 43–54.*
- Tashiro, M., and M. Ikeda. 1987. Cretaceous System of the Yatsushiro Mountains. *Research Reports of Kochi University, Natural Science* 36: 71–91.*
- Tashiro, M., and T. Kozai. 1984. Bivalve fossils from the type Monobegawa Group (Part 1). *Research Reports of Kochi University, Natural Science* 32: 259–293.
- Terabe, K., and A. Matsuoka. 2009. Barremian bivalves of Tethyan fauna from the Sebayashi Formation of the Sanchu Cretaceous System in the Chichibu Composite Belt, Kanto Mountains. *Journal of the Geological Society of Japan* 115: 130–140.*
- Tsuchiya, N., T. Takeda, T. Adachi, N. Nakano, Y. Osanai and Y. Adachi. 2015. Early Cretaceous adakitic magmatism and tectonics in the Kitakami Mountains, Japan. *Japanese Magazine of Mineralogical and Petrological Sciences* 44: 69–90.*

- Wakamatsu, H., K. Sugiyama and H. Furutani. 1990. Silurian and Devonian radiolarians from the Kurosegawa Tectonic Zone, Southwest Japan. *Journal of Earth Sciences, Nagoya University* 37: 157–192.
- Wakita, K., K. Miyazaki, S. Toshimitsu, S. Yokoyama and M. Nakagawa. 2007. *Geology of the Ino district. Quadrangle Series, 1:50,000, Geological Survey of Japan, AIST, Tsukuba, 140 pp.**
- Wang, T., L. Guo, Y. Zheng, T. Donskaya, D. Gladkochub, L. Zeng, J. Li, Y. Wang and A. Mazukabzov. 2012. Timing and processes of late Mesozoic mid-lower-crustal extension in continental NE Asia and implications for the tectonic setting of the destruction of the North China Craton: Mainly constrained by zircon U-Pb ages from metamorphic core complexes. *Lithos* 154: 313–345.
- Wang, Y. J., W. M. Fan, G. W. Zhang and Y. H. Zhang. 2013. Phanerozoic tectonics of the South China Block: Key observations and controversies. *Gondwana Research* 23: 1273–1305.
- Wiedenbeck, M., J. M. Hanchar, W. H. Peck, P. Sylvester, J. Valley, M. Whitehouse, A. Kronz, Y. Morishita, L. Nasdala, J. Fiebig, I. Franchi, J.-P. Girard, R. C. Greenwood, R. Hinton, N. Kita, P. R. D. Mason, M. Norman, M. Ogasawara, P. M. Piccoli, D. Rhede, H. Satoh, B. Schulz-Dobrick, O. Skar, M. J. Spicuzza, K. Terada, A. Tindle, S. Togashi, T. Vennemann, Q. Xie and T.-F. Zheng. 2004. Further characterisation of the 91500 zircon crystal. *Geostandards and Geoanalytical Research* 28: 9–39.
- Wu, F. Y., R. H. Han, J. H. Yang, S. A. Wilde, M. G. Zhai and S. C. Park. 2007. Initial constraints on the timing of granitic magmatism in North Korea using U-Pb zircon geochronology. *Chemical Geology* 238: 232–248.
- Yabe, A., K. Terada and S. Sekido. 2003. The Tetori-type flora, revisited: a review. *Memoir of the Fukui Prefectural Dinosaur Museum* 2: 23–42.
- Yamakita, S. 1998. What belongs to the Northern Chichibu Belt? —Tectonic division between the Northern Chichibu Belt and the Kurosegawa Belt—. *Journal of the Geological Society of Japan* 104: 623–633.*
- Yamakita, S., and S. Otoh. 2000a. Estimation of the amount of Late Cretaceous left-lateral strike-slip displacement along the Median Tectonic Line and its implications in the juxtaposition of some geologic belts of Southwest Japan. *Association for the Geological Collaboration in Japan, Monograph* 49: 93–104.*
- Yamakita, S., and S. Otoh. 2000b. Cretaceous rearrangement processes of pre-Cretaceous geologic units of the Japanese Islands by MTL–Kurosegawa left-lateral strike-slip fault system. *Memoirs of the Geological Society of Japan* 56: 23–38.*
- * : in Japanese with English abstract
** : in Japanese

＜ 地名・地層名 ＞

Abukuma Belt 阿武隈帯
Birafo 美良布
Birafo Formation 美良布層
Chichibu Composite Belt ... 秩父累帯
Funadani Formation 船谷層
Hagino 萩野
Hagino Formation 萩野層
Haginogawa River 萩野川
Hibihara Formation 日比原層
Hibiharagawa River 日比原川
Higo Belt 肥後帯
Igenoki Formation 神母ノ木層
Kagamiimai 鏡今井
Kajisakogawa River 椿佐古川
Kasanokawagawa River 笠ノ川川
Katsuura area 勝浦地域
Kitakami Belt 北上帯
Kochi City 高知市
Kochi Prefecture 高知県
Kubogawa River 久保川
Kurohara Formation 黒原層

Kurosegawa Belt 黒瀬川帯
Kyushu 九州
Kanto Mountains 関東山地
Meoto Pond 女夫池
Mitaki igneous rocks ... 三滝火成岩類
Monobe Formation 物部層
Monobegawa Group 物部川層群
Monobegawa River 物部川
Yokokurayama Group 横倉山層群
Nankai Group 南海層群
Nishinokawa River 西の川
Northeast Japan 東北日本
Northern Chichibu Belt ... 北部秩父帯
Odochi 大栃
Pre-Sotoizumi Group ... 先外和泉層群
Ryoke Belt 領家帯
Ryoseki Formation 領石層
Ryoseki-Monobe area 領石-物部地域
Sakawa area 佐川地域
Sanbagawa Belt 三波川帯

Sano 佐野
Sasagawa River 笹川
Shikoku 四国
Shimanto Belt 四万十帯
Shingai Unit 新改ユニット
Shirakidani Group 白木谷層群
Shobu Formation 菖蒲層
Sotoizumi Group 外和泉層群
Southern Chichibu Belt ... 南部秩父帯
Southwest Japan 西南日本
Suita Group 杉田層群
Tachibana 立花
Tatsukawa Formation 立川層
Tokushima Prefecture 徳島県
Torinosu Group 鳥巢層群
Torinosu-type Limestone 鳥巢式石灰岩
Tosayamada 土佐山田
Yakuno Complex ... 夜久野複合岩類
Yukigamine Formation 雪ヶ峰層
Yunoki Formation 柚ノ木層

TABLE 1. U-Pb isotopic data for zircons analyzed in this study. All errors are 2σ . % conc = $100 \times (207\text{Pb}/235\text{U age}) / (206\text{Pb}/238\text{U age})$ is a measure of concordance between $206\text{Pb}/238\text{U}$ and $207\text{Pb}/235\text{U}$ ages. Analyses shown in italics are discordant and are not included in the probability density plots and histograms.

Grain	$^{206}\text{Pb}/^{238}\text{U}$	$^{207}\text{Pb}/^{235}\text{U}$	$^{206}\text{Pb}/^{238}\text{U}$ age (Ma)	$^{207}\text{Pb}/^{235}\text{U}$ age (Ma)	%conc	Th/U	$^{206}\text{Pb}/^{238}\text{U}$	$^{207}\text{Pb}/^{235}\text{U}$	$^{206}\text{Pb}/^{238}\text{U}$ age (Ma)	$^{207}\text{Pb}/^{235}\text{U}$ age (Ma)	%conc	Th/U
Sandstone of the Ryosaki Formation (Ry-1; 33° 37' N, 133° 36' 39.87" E)												
Ry-1-1	0.0454 ± 0.0012	0.329 ± 0.029	286.1 ± 7.3	289 ± 25	99.0	0.34	0.0413 ± 0.0014	0.311 ± 0.028	260.7 ± 8.8	275 ± 25	94.8	0.84
Ry-1-2	0.0378 ± 0.0012	0.258 ± 0.031	239.5 ± 7.4	233 ± 28	102.7	0.22	0.0378 ± 0.0012	0.269 ± 0.016	239.3 ± 7.3	242 ± 15	98.9	0.48
Ry-1-3	0.0392 ± 0.0009	0.248 ± 0.022	248.1 ± 6.0	235 ± 19	105.5	0.68	0.0435 ± 0.0023	0.327 ± 0.084	274.6 ± 14.5	287 ± 74	95.5	0.34
Ry-1-4	0.0410 ± 0.0008	0.285 ± 0.016	259.0 ± 5.3	255 ± 14	101.6	0.35	0.0393 ± 0.0012	0.275 ± 0.020	248.5 ± 7.9	247 ± 18	100.7	0.83
Ry-1-5	0.0400 ± 0.0009	0.295 ± 0.022	252.9 ± 5.9	263 ± 19	96.3	0.51	0.1550 ± 0.0046	1.530 ± 0.068	929.0 ± 0.68	942 ± 42	98.6	0.15
Ry-1-6	0.0404 ± 0.0013	0.296 ± 0.036	255.0 ± 8.1	263 ± 32	96.8	0.47	0.4856 ± 0.0143	11.668 ± 0.455	2551.7 ± 27.5	2578 ± 101	99.0	0.34
Ry-1-7	0.0379 ± 0.0008	0.267 ± 0.016	240.1 ± 5.1	240 ± 15	99.8	0.70	<i>0.0542 ± 0.0019</i>	<i>0.479 ± 0.046</i>	<i>340.0 ± 12.0</i>	<i>397 ± 38</i>	<i>83.5</i>	<i>1.03</i>
Ry-1-8	0.0399 ± 0.0008	0.271 ± 0.016	252.3 ± 5.4	244 ± 15	103.5	0.39	0.0402 ± 0.0013	0.320 ± 0.024	261.1 ± 8.4	282 ± 21	92.7	0.57
Ry-1-9	0.0418 ± 0.0014	0.292 ± 0.041	264.1 ± 9.0	260 ± 37	101.5	0.44	0.0393 ± 0.0012	0.288 ± 0.017	248.7 ± 7.7	253 ± 14	98.3	0.27
Ry-1-10	0.0366 ± 0.0010	0.244 ± 0.027	231.8 ± 6.5	222 ± 24	104.4	0.81	<i>0.0485 ± 0.0017</i>	<i>0.448 ± 0.036</i>	<i>305.5 ± 10.5</i>	<i>376 ± 30</i>	<i>81.3</i>	<i>0.40</i>
<i>Ry-1-11</i>	<i>0.0297 ± 0.0009</i>	<i>0.233 ± 0.027</i>	<i>189.0 ± 5.8</i>	<i>213 ± 25</i>	<i>88.9</i>	<i>0.50</i>	0.0403 ± 0.0014	0.278 ± 0.027	254.7 ± 9.0	249 ± 24	102.2	0.42
Ry-1-12	0.0393 ± 0.0012	0.272 ± 0.034	248.3 ± 7.7	244 ± 30	101.6	0.69	0.0401 ± 0.0013	0.295 ± 0.023	253.3 ± 8.4	263 ± 20	96.4	0.95
Ry-1-13	0.0395 ± 0.0009	0.283 ± 0.019	249.8 ± 5.6	253 ± 17	98.7	0.38	<i>Ry-1-61</i>	<i>0.0459 ± 0.0019</i>	<i>289.5 ± 12.2</i>	<i>245 ± 41</i>	<i>118.2</i>	<i>0.60</i>
<i>Ry-1-14</i>	<i>0.0438 ± 0.0015</i>	<i>0.369 ± 0.050</i>	<i>276.2 ± 9.7</i>	<i>319 ± 43</i>	<i>86.6</i>	<i>0.60</i>	0.0405 ± 0.0013	0.295 ± 0.017	256.1 ± 8.1	262 ± 15	97.6	0.43
Ry-1-15	0.0338 ± 0.0008	0.240 ± 0.020	214.5 ± 5.2	218 ± 18	98.3	0.80	0.0415 ± 0.0014	0.294 ± 0.021	262.2 ± 8.5	262 ± 19	100.2	0.49
Ry-1-16	0.0381 ± 0.0009	0.257 ± 0.021	241.1 ± 5.8	232 ± 19	103.7	0.56	0.0410 ± 0.0015	0.320 ± 0.032	258.9 ± 9.4	282 ± 29	91.9	0.58
Ry-1-17	0.0317 ± 0.0062	0.259 ± 0.187	184.6 ± 34.4	1862 ± 66	99.2	0.16	0.0463 ± 0.0018	0.322 ± 0.047	292.1 ± 11.5	284 ± 41	102.9	0.44
Ry-1-18	0.0344 ± 0.0017	0.237 ± 0.025	217.8 ± 10.6	216 ± 23	100.8	0.59	0.0421 ± 0.0012	0.294 ± 0.017	265.9 ± 7.7	262 ± 15	101.5	0.45
Ry-1-19	0.0425 ± 0.0020	0.323 ± 0.028	268.3 ± 12.6	284 ± 24	94.4	1.15	0.0406 ± 0.0011	0.285 ± 0.014	255.7 ± 7.2	255 ± 13	100.7	0.62
Ry-1-20	0.0474 ± 0.0023	0.350 ± 0.032	298.4 ± 14.2	305 ± 28	97.9	0.43	0.0405 ± 0.0017	0.297 ± 0.051	266.4 ± 45	264 ± 45	96.7	0.77
Ry-1-21	0.0401 ± 0.0018	0.294 ± 0.019	253.2 ± 11.5	262 ± 17	96.7	0.33	0.0461 ± 0.0016	0.332 ± 0.033	290.6 ± 9.8	291 ± 29	99.9	0.52
Ry-1-22	0.0363 ± 0.0016	0.270 ± 0.018	229.6 ± 10.4	242 ± 16	94.8	0.40	0.0386 ± 0.0011	0.288 ± 0.018	244.3 ± 7.2	257 ± 16	95.2	0.52
Ry-1-23	0.0398 ± 0.0019	0.306 ± 0.028	251.4 ± 12.0	271 ± 25	92.8	0.45	0.0380 ± 0.0013	0.276 ± 0.028	240.5 ± 8.2	247 ± 25	97.3	0.55
Ry-1-24	0.0399 ± 0.0019	0.290 ± 0.024	252.0 ± 11.8	258 ± 22	97.6	0.42	0.0402 ± 0.0014	0.276 ± 0.029	254.2 ± 8.6	248 ± 26	102.7	0.59
Ry-1-25	0.0392 ± 0.0013	0.277 ± 0.028	247.6 ± 8.4	248 ± 25	99.8	0.39	0.0438 ± 0.0016	0.332 ± 0.041	276.5 ± 10.3	291 ± 36	95.0	0.86
Ry-1-26	0.0415 ± 0.0014	0.282 ± 0.027	262.3 ± 8.8	252 ± 24	103.9	0.37	0.0386 ± 0.0018	0.403 ± 0.317	1634.6 ± 72.6	1653 ± 128	98.9	1.20
Ry-1-27	0.0402 ± 0.0021	0.308 ± 0.075	254.1 ± 13.5	272 ± 66	93.3	0.38	0.0702 ± 0.0030	0.597 ± 0.044	437.2 ± 18.6	475 ± 35	92.0	0.36
Ry-1-28	0.0410 ± 0.0023	0.314 ± 0.084	259.2 ± 14.6	277 ± 74	93.6	0.57	0.0393 ± 0.0019	0.283 ± 0.021	248.5 ± 10.5	253 ± 19	98.3	0.86
Ry-1-29	0.0443 ± 0.0019	0.296 ± 0.049	279.3 ± 11.7	263 ± 44	106.2	0.46	0.0446 ± 0.0019	0.328 ± 0.022	281.4 ± 11.7	288 ± 19	97.8	0.71
Ry-1-30	0.0391 ± 0.0012	0.288 ± 0.017	247.1 ± 7.3	257 ± 15	96.2	0.96	0.0407 ± 0.0018	0.302 ± 0.031	257.4 ± 11.6	268 ± 28	96.2	0.60
Ry-1-31	0.0418 ± 0.0015	0.290 ± 0.033	264.2 ± 9.4	259 ± 29	102.1	0.68	0.0402 ± 0.0019	0.298 ± 0.038	254.0 ± 12.1	265 ± 33	95.8	0.67
Ry-1-32	0.0396 ± 0.0012	0.298 ± 0.022	250.6 ± 7.9	264 ± 20	94.8	0.36	0.0386 ± 0.0016	0.290 ± 0.022	244.4 ± 10.4	258 ± 20	94.6	0.64
Ry-1-33	0.0366 ± 0.0011	0.275 ± 0.017	231.6 ± 6.9	246 ± 15	94.0	0.37	0.0552 ± 0.0027	0.368 ± 0.055	346.2 ± 17.1	318 ± 48	108.8	0.41
Ry-1-34	0.0388 ± 0.0011	0.277 ± 0.019	245.3 ± 6.9	248 ± 17	99.0	0.39	0.0423 ± 0.0008	0.322 ± 0.015	267.1 ± 5.1	284 ± 14	94.2	1.27
Ry-1-35	0.0413 ± 0.0013	0.277 ± 0.026	260.9 ± 8.0	249 ± 23	105.0	0.74	0.0386 ± 0.0007	0.279 ± 0.013	243.9 ± 4.6	250 ± 12	97.7	0.48
Ry-1-36	0.0414 ± 0.0013	0.307 ± 0.028	261.6 ± 8.1	272 ± 25	96.2	0.59	0.0390 ± 0.0008	0.277 ± 0.018	246.7 ± 5.3	248 ± 16	99.3	0.53
Ry-1-37	0.0451 ± 0.0016	0.432 ± 0.033	345.8 ± 10.1	365 ± 28	94.8	0.58	0.0399 ± 0.0008	0.291 ± 0.015	252.0 ± 4.9	259 ± 13	97.2	0.32
Ry-1-38	0.0405 ± 0.0017	0.287 ± 0.048	255.7 ± 10.5	256 ± 43	99.7	0.54	0.0373 ± 0.0021	0.422 ± 0.069	359.1 ± 13.4	358 ± 59	100.4	0.51
Ry-1-39	0.0455 ± 0.0016	0.320 ± 0.039	286.9 ± 9.9	282 ± 34	101.9	0.64	0.0418 ± 0.0014	0.304 ± 0.043	263.9 ± 8.7	270 ± 38	97.8	0.34
Ry-1-40	0.0413 ± 0.0014	0.286 ± 0.036	260.6 ± 9.1	256 ± 32	102.0	0.76	0.0376 ± 0.0007	0.276 ± 0.010	238.1 ± 4.4	248 ± 9	96.1	0.75
Ry-1-41	0.0385 ± 0.0010	0.286 ± 0.017	243.4 ± 6.6	255 ± 15	95.4	0.55	0.0435 ± 0.0010	0.328 ± 0.023	274.8 ± 6.3	288 ± 20	95.5	0.55
<i>Ry-1-42</i>	<i>0.0413 ± 0.0018</i>	<i>0.260 ± 0.049</i>	<i>261.1 ± 11.1</i>	<i>234 ± 44</i>	<i>111.4</i>	<i>0.53</i>	0.0368 ± 0.0011	0.250 ± 0.015	232.9 ± 6.7	227 ± 13	102.6	0.49
Ry-1-43	0.0441 ± 0.0017	0.323 ± 0.041	278.0 ± 10.8	284 ± 36	97.9	0.50	<i>0.0328 ± 0.0012</i>	<i>0.204 ± 0.025</i>	<i>208.3 ± 7.5</i>	<i>188 ± 23</i>	<i>110.6</i>	<i>0.41</i>
Ry-1-44	0.0390 ± 0.0013	0.284 ± 0.027	246.8 ± 8.5	254 ± 24	97.3	0.60	0.0404 ± 0.0012	0.291 ± 0.018	255.5 ± 11.7	259 ± 16	98.5	1.11
Ry-1-45	0.0410 ± 0.0015	0.294 ± 0.032	259.3 ± 9.4	262 ± 29	99.0	0.69	0.0403 ± 0.0015	0.285 ± 0.036	254.8 ± 9.5	255 ± 32	100.0	0.62
<i>Ry-1-46</i>	<i>0.0416 ± 0.0018</i>	<i>0.385 ± 0.052</i>	<i>262.6 ± 11.1</i>	<i>331 ± 45</i>	<i>79.4</i>	<i>0.44</i>	0.0408 ± 0.0013	0.287 ± 0.026	258.0 ± 8.3	256 ± 23	100.7	0.58
Ry-1-47	0.0433 ± 0.0018	0.330 ± 0.050	273.4 ± 11.6	289 ± 43	94.5	0.24	0.0395 ± 0.0014	0.312 ± 0.034	249.5 ± 9.9	275 ± 30	90.6	0.73
Ry-1-48	0.0399 ± 0.0013	0.266 ± 0.021	252.2 ± 8.2	239 ± 19	105.4	0.50	0.0371 ± 0.0010	0.275 ± 0.012	234.8 ± 6.4	247 ± 11	95.2	0.12
Ry-1-49	0.0395 ± 0.0012	0.271 ± 0.017	249.5 ± 7.7	243 ± 15	102.6	0.60	0.0396 ± 0.0012	0.307 ± 0.021	250.6 ± 7.5	272 ± 19	92.2	0.65
Ry-1-50	0.3164 ± 0.0094	4.885 ± 0.212	1771.9 ± 52.9	1800 ± 78	98.5	0.40	0.0397 ± 0.0012	0.387 ± 0.019	250.8 ± 7.4	256 ± 17	98.0	0.48

TABLE 1. (Continued)

Grain	$^{206}\text{Pb}/^{238}\text{U}$	$^{207}\text{Pb}/^{235}\text{U}$	$^{206}\text{Pb}/^{238}\text{U}$ age (Ma)	$^{207}\text{Pb}/^{235}\text{U}$ age (Ma)	$^{207}\text{Pb}/^{235}\text{U}$ age (Ma)	Grain	$^{206}\text{Pb}/^{238}\text{U}$	$^{207}\text{Pb}/^{235}\text{U}$	$^{206}\text{Pb}/^{238}\text{U}$ age (Ma)	$^{207}\text{Pb}/^{235}\text{U}$ age (Ma)	$^{207}\text{Pb}/^{235}\text{U}$ age (Ma)	Grain	$^{206}\text{Pb}/^{238}\text{U}$	$^{207}\text{Pb}/^{235}\text{U}$	$^{206}\text{Pb}/^{238}\text{U}$ age (Ma)	$^{207}\text{Pb}/^{235}\text{U}$ age (Ma)	$^{207}\text{Pb}/^{235}\text{U}$ age (Ma)	Th/U	%conc	Th/U
Ry-1-102	0.0435 \pm 0.0014	0.330 \pm 0.023	274.7 \pm 9.0	289 \pm 20	95.0	Mo-1-23	0.0444 \pm 0.0013	0.406 \pm 0.045	280.3 \pm 8.3	346 \pm 38	81.0	Mo-1-23	0.0444 \pm 0.0013	0.406 \pm 0.045	280.3 \pm 8.3	346 \pm 38	81.0	0.47		
Ry-1-103	0.0403 \pm 0.0014	0.276 \pm 0.026	255.0 \pm 9.0	248 \pm 24	102.9	Mo-1-24	0.0290 \pm 0.0008	0.250 \pm 0.026	184.0 \pm 5.2	226 \pm 24	81.3	Mo-1-24	0.0290 \pm 0.0008	0.250 \pm 0.026	184.0 \pm 5.2	226 \pm 24	81.3	0.57		
Ry-1-104	0.0323 \pm 0.0011	0.214 \pm 0.018	204.8 \pm 6.9	197 \pm 16	104.0	Mo-1-25	0.0400 \pm 0.0013	0.278 \pm 0.018	253.1 \pm 8.3	249 \pm 16	101.5	Mo-1-25	0.0400 \pm 0.0013	0.278 \pm 0.018	253.1 \pm 8.3	249 \pm 16	101.5	0.38		
Ry-1-105	0.0414 \pm 0.0019	0.306 \pm 0.052	261.6 \pm 11.9	271 \pm 46	96.5	Mo-1-26	0.0458 \pm 0.0019	0.380 \pm 0.057	288.5 \pm 11.9	327 \pm 49	88.1	Mo-1-26	0.0458 \pm 0.0019	0.380 \pm 0.057	288.5 \pm 11.9	327 \pm 49	88.1	0.38		
Ry-1-106	0.0383 \pm 0.0013	0.280 \pm 0.024	242.3 \pm 8.4	251 \pm 22	96.7	Mo-1-27	0.0269 \pm 0.0009	0.193 \pm 0.016	171.4 \pm 5.9	179 \pm 15	95.8	Mo-1-27	0.0269 \pm 0.0009	0.193 \pm 0.016	171.4 \pm 5.9	179 \pm 15	95.8	0.21		
Ry-1-107	0.0449 \pm 0.0016	0.310 \pm 0.032	282.9 \pm 10.2	275 \pm 28	103.0	Mo-1-28	0.0214 \pm 0.0008	0.153 \pm 0.016	136.8 \pm 5.0	145 \pm 16	94.4	Mo-1-28	0.0214 \pm 0.0008	0.153 \pm 0.016	136.8 \pm 5.0	145 \pm 16	94.4	0.31		
Ry-1-108	0.0411 \pm 0.0017	0.279 \pm 0.041	259.9 \pm 10.9	250 \pm 37	104.0	Mo-1-29	0.0289 \pm 0.0010	0.202 \pm 0.016	183.6 \pm 6.2	187 \pm 15	98.4	Mo-1-29	0.0289 \pm 0.0010	0.202 \pm 0.016	183.6 \pm 6.2	187 \pm 15	98.4	0.31		
Ry-1-109	0.0354 \pm 0.0011	0.247 \pm 0.012	224.1 \pm 6.9	224 \pm 11	99.8	Mo-1-30	0.0385 \pm 0.0014	0.249 \pm 0.030	243.4 \pm 9.0	226 \pm 27	107.7	Mo-1-30	0.0385 \pm 0.0014	0.249 \pm 0.030	243.4 \pm 9.0	226 \pm 27	107.7	0.84		
Ry-1-110	0.0417 \pm 0.0019	0.291 \pm 0.048	263.2 \pm 11.7	259 \pm 43	101.5	Mo-1-31	0.0272 \pm 0.0009	0.185 \pm 0.014	172.9 \pm 5.8	172 \pm 13	100.4	Mo-1-31	0.0272 \pm 0.0009	0.185 \pm 0.014	172.9 \pm 5.8	172 \pm 13	100.4	0.39		
Ry-1-111	0.0395 \pm 0.0012	0.292 \pm 0.029	249.9 \pm 7.6	260 \pm 26	96.2	Mo-1-32	0.0278 \pm 0.0009	0.189 \pm 0.012	176.7 \pm 5.7	176 \pm 11	100.3	Mo-1-32	0.0278 \pm 0.0009	0.189 \pm 0.012	176.7 \pm 5.7	176 \pm 11	100.3	0.20		
Ry-1-112	0.0283 \pm 0.0008	0.195 \pm 0.014	179.8 \pm 4.8	181 \pm 13	99.6	Mo-1-33	0.0262 \pm 0.0008	0.173 \pm 0.015	147.0 \pm 4.5	161 \pm 64	91.0	Mo-1-33	0.0262 \pm 0.0008	0.173 \pm 0.015	147.0 \pm 4.5	161 \pm 64	91.0	0.42		
Ry-1-113	0.0361 \pm 0.0009	0.260 \pm 0.015	228.7 \pm 8.8	234 \pm 14	97.6	Mo-1-34	0.0270 \pm 0.0010	0.238 \pm 0.022	171.6 \pm 6.3	217 \pm 20	79.2	Mo-1-34	0.0270 \pm 0.0010	0.238 \pm 0.022	171.6 \pm 6.3	217 \pm 20	79.2	0.59		
Ry-1-114	0.0408 \pm 0.0015	0.282 \pm 0.040	257.8 \pm 9.5	252 \pm 36	102.2	Mo-1-35	0.0488 \pm 0.0151	0.488 \pm 0.0151	256.6 \pm 79.4	2499 \pm 95	102.7	Mo-1-35	0.0488 \pm 0.0151	0.488 \pm 0.0151	256.6 \pm 79.4	2499 \pm 95	102.7	1.04		
Ry-1-115	0.0391 \pm 0.0010	0.269 \pm 0.020	247.1 \pm 8.6	242 \pm 18	102.0	Mo-1-36	0.0841 \pm 0.0029	0.830 \pm 0.062	520.3 \pm 18.1	614 \pm 46	84.8	Mo-1-36	0.0841 \pm 0.0029	0.830 \pm 0.062	520.3 \pm 18.1	614 \pm 46	84.8	0.62		
Ry-1-116	0.0380 \pm 0.0009	0.274 \pm 0.014	240.7 \pm 8.9	246 \pm 13	97.8	Mo-1-37	0.0452 \pm 0.0015	0.366 \pm 0.023	284.9 \pm 9.4	316 \pm 20	90.0	Mo-1-37	0.0452 \pm 0.0015	0.366 \pm 0.023	284.9 \pm 9.4	316 \pm 20	90.0	0.59		
Ry-1-117	0.04326 \pm 0.00098	0.409 \pm 0.023	2317.6 \pm 52.4	2379 \pm 59	97.4	Mo-1-38	0.0273 \pm 0.0012	0.242 \pm 0.023	173.9 \pm 6.7	220 \pm 23	79.1	Mo-1-38	0.0273 \pm 0.0012	0.242 \pm 0.023	173.9 \pm 6.7	220 \pm 23	79.1	0.55		
Ry-1-118	0.03283 \pm 0.0075	5.245 \pm 0.144	1830.3 \pm 41.9	1860 \pm 51	98.4	Mo-1-39	0.0322 \pm 0.0012	0.273 \pm 0.025	204.1 \pm 7.4	245 \pm 22	83.2	Mo-1-39	0.0322 \pm 0.0012	0.273 \pm 0.025	204.1 \pm 7.4	245 \pm 22	83.2	0.59		
Ry-1-119	0.0474 \pm 0.0013	0.394 \pm 0.026	298.8 \pm 7.9	338 \pm 22	88.5	Mo-1-40	0.0750 \pm 0.0017	0.591 \pm 0.033	466.4 \pm 10.8	471 \pm 26	98.9	Mo-1-40	0.0750 \pm 0.0017	0.591 \pm 0.033	466.4 \pm 10.8	471 \pm 26	98.9	0.89		
Ry-1-120	0.0544 \pm 0.0011	0.422 \pm 0.021	341.7 \pm 6.7	357 \pm 17	95.7	Mo-1-41	0.0219 \pm 0.0007	0.174 \pm 0.018	139.5 \pm 4.3	163 \pm 17	85.5	Mo-1-41	0.0219 \pm 0.0007	0.174 \pm 0.018	139.5 \pm 4.3	163 \pm 17	85.5	0.92		
Ry-1-121	0.0468 \pm 0.0014	0.416 \pm 0.046	295.1 \pm 8.9	353 \pm 39	83.6	Mo-1-42	0.0361 \pm 0.0009	0.261 \pm 0.020	228.9 \pm 5.9	236 \pm 18	97.1	Mo-1-42	0.0361 \pm 0.0009	0.261 \pm 0.020	228.9 \pm 5.9	236 \pm 18	97.1	0.80		
Ry-1-122	0.0426 \pm 0.0010	0.294 \pm 0.026	268.9 \pm 6.6	261 \pm 23	102.8	Mo-1-43	0.0278 \pm 0.0008	0.175 \pm 0.020	176.8 \pm 5.3	164 \pm 18	107.9	Mo-1-43	0.0278 \pm 0.0008	0.175 \pm 0.020	176.8 \pm 5.3	164 \pm 18	107.9	0.45		
Ry-1-123	0.0378 \pm 0.0008	0.262 \pm 0.015	239.4 \pm 5.0	236 \pm 14	101.5	Mo-1-44	0.0465 \pm 0.0011	0.333 \pm 0.022	293.2 \pm 7.1	292 \pm 19	100.4	Mo-1-44	0.0465 \pm 0.0011	0.333 \pm 0.022	293.2 \pm 7.1	292 \pm 19	100.4	0.20		
Ry-1-124	0.0403 \pm 0.0013	0.312 \pm 0.039	254.6 \pm 8.1	276 \pm 35	92.3	Mo-1-45	0.0340 \pm 0.0073	0.353 \pm 0.171	1906.1 \pm 40.6	1877 \pm 60	101.5	Mo-1-45	0.0340 \pm 0.0073	0.353 \pm 0.171	1906.1 \pm 40.6	1877 \pm 60	101.5	0.25		
Ry-1-125	0.0422 \pm 0.0017	0.319 \pm 0.058	266.3 \pm 10.8	281 \pm 51	94.7	Mo-1-46	0.0302 \pm 0.0010	0.150 \pm 0.031	128.7 \pm 6.1	142 \pm 29	90.5	Mo-1-46	0.0302 \pm 0.0010	0.150 \pm 0.031	128.7 \pm 6.1	142 \pm 29	90.5	0.57		
Ry-1-126	0.0392 \pm 0.0010	0.250 \pm 0.024	248.0 \pm 6.4	226 \pm 22	109.6	Mo-1-47	0.0276 \pm 0.0009	0.196 \pm 0.020	175.5 \pm 5.5	181 \pm 18	96.7	Mo-1-47	0.0276 \pm 0.0009	0.196 \pm 0.020	175.5 \pm 5.5	181 \pm 18	96.7	0.64		
Ry-1-127	0.0401 \pm 0.0009	0.270 \pm 0.020	253.4 \pm 5.8	243 \pm 18	104.3	Mo-1-48	0.0424 \pm 0.0012	0.285 \pm 0.021	267.8 \pm 7.5	255 \pm 19	105.2	Mo-1-48	0.0424 \pm 0.0012	0.285 \pm 0.021	267.8 \pm 7.5	255 \pm 19	105.2	0.73		
Ry-1-128	0.0427 \pm 0.0011	0.306 \pm 0.027	269.7 \pm 6.7	271 \pm 24	99.5	Mo-1-49	0.0450 \pm 0.0017	0.383 \pm 0.052	283.8 \pm 10.9	329 \pm 45	86.2	Mo-1-49	0.0450 \pm 0.0017	0.383 \pm 0.052	283.8 \pm 10.9	329 \pm 45	86.2	0.46		
Mo-1-1	0.0319 \pm 0.0009	0.230 \pm 0.014	202.3 \pm 5.5	210 \pm 13	96.4	Mo-1-50	0.0208 \pm 0.0006	0.140 \pm 0.010	132.5 \pm 3.7	133 \pm 10	99.6	Mo-1-50	0.0208 \pm 0.0006	0.140 \pm 0.010	132.5 \pm 3.7	133 \pm 10	99.6	0.49		
Mo-1-2	0.0287 \pm 0.0008	0.186 \pm 0.013	182.5 \pm 5.1	173 \pm 12	105.5	Mo-1-51	0.0347 \pm 0.0010	0.258 \pm 0.019	219.7 \pm 6.2	233 \pm 17	94.3	Mo-1-51	0.0347 \pm 0.0010	0.258 \pm 0.019	219.7 \pm 6.2	233 \pm 17	94.3	0.84		
Mo-1-3	0.0289 \pm 0.0008	0.211 \pm 0.017	183.5 \pm 5.4	194 \pm 15	94.4	Mo-1-52	0.0200 \pm 0.0009	0.124 \pm 0.027	127.5 \pm 5.9	119 \pm 25	107.6	Mo-1-52	0.0200 \pm 0.0009	0.124 \pm 0.027	127.5 \pm 5.9	119 \pm 25	107.6	0.97		
Mo-1-4	0.0286 \pm 0.0008	0.211 \pm 0.014	181.6 \pm 5.0	194 \pm 13	93.5	Mo-1-53	0.0454 \pm 0.0115	0.454 \pm 0.0115	2414.8 \pm 60.9	2199 \pm 84	109.8	Mo-1-53	0.0454 \pm 0.0115	0.454 \pm 0.0115	2414.8 \pm 60.9	2199 \pm 84	109.8	0.54		
Mo-1-5	0.3127 \pm 0.0078	5.917 \pm 0.187	1753.9 \pm 43.5	1964 \pm 62	89.3	Mo-1-54	0.0425 \pm 0.0018	0.410 \pm 0.056	268.1 \pm 11.7	349 \pm 47	76.8	Mo-1-54	0.0425 \pm 0.0018	0.410 \pm 0.056	268.1 \pm 11.7	349 \pm 47	76.8	0.48		
Mo-1-6	0.0543 \pm 0.0015	0.485 \pm 0.030	340.7 \pm 9.4	402 \pm 24	84.8	Mo-1-55	0.0195 \pm 0.0008	0.148 \pm 0.020	124.5 \pm 5.1	140 \pm 19	88.8	Mo-1-55	0.0195 \pm 0.0008	0.148 \pm 0.020	124.5 \pm 5.1	140 \pm 19	88.8	0.91		
Mo-1-7	0.0413 \pm 0.0014	0.429 \pm 0.040	261.1 \pm 8.8	362 \pm 34	72.1	Mo-1-56	0.0274 \pm 0.0100	0.277 \pm 0.0009	1825.6 \pm 55.8	1846 \pm 72	98.9	Mo-1-56	0.0274 \pm 0.0100	0.277 \pm 0.0009	1825.6 \pm					

TABLE 1. (Continued)

Grain	$^{206}\text{Pb}/^{238}\text{U}$	$^{207}\text{Pb}/^{235}\text{U}$	$^{206}\text{Pb}/^{238}\text{U}$ age (Ma)	$^{207}\text{Pb}/^{235}\text{U}$ age (Ma)	%conc	Th/U	Grain	$^{206}\text{Pb}/^{238}\text{U}$	$^{207}\text{Pb}/^{235}\text{U}$	$^{206}\text{Pb}/^{238}\text{U}$ age (Ma)	$^{207}\text{Pb}/^{235}\text{U}$ age (Ma)	%conc	Th/U
Mo-1-74	0.0401 \pm 0.0006	0.286 \pm 0.015	253.2 \pm 3.7	255 \pm 14	99.2	0.48	Yu-1-6	0.0294 \pm 0.0012	0.187 \pm 0.021	187.0 \pm 7.4	174 \pm 20	107.2	0.57
Mo-1-75	0.4317 \pm 0.0046	11.732 \pm 0.274	2313.3 \pm 24.5	2583 \pm 60	89.6	0.65	Yu-1-7	0.0273 \pm 0.0010	0.193 \pm 0.019	173.9 \pm 6.7	179 \pm 18	97.1	0.55
Mo-1-76	0.3360 \pm 0.0042	5.314 \pm 0.171	1867.6 \pm 23.2	1871 \pm 60	99.8	0.65	Yu-1-8	0.0275 \pm 0.0010	0.188 \pm 0.015	174.6 \pm 6.3	175 \pm 14	99.9	0.67
Mo-1-77	0.0418 \pm 0.0018	0.299 \pm 0.049	263.7 \pm 11.2	265 \pm 44	99.4	0.63	Yu-1-9	0.0271 \pm 0.0010	0.200 \pm 0.016	172.1 \pm 6.3	185 \pm 15	92.9	0.35
Mo-1-78	0.301 \pm 0.0009	0.216 \pm 0.014	191.3 \pm 6.5	198 \pm 13	96.5	0.54	Yu-1-10	0.2456 \pm 0.0043	3.773 \pm 0.088	1415.6 \pm 25.0	1587 \pm 37	89.2	0.19
Mo-1-79	0.0230 \pm 0.0007	0.173 \pm 0.016	146.7 \pm 4.7	162 \pm 15	90.3	0.68	Yu-1-11	0.0340 \pm 0.0007	0.285 \pm 0.018	215.2 \pm 4.7	255 \pm 16	84.4	0.32
Mo-1-80	0.0381 \pm 0.0010	0.269 \pm 0.014	240.8 \pm 6.5	242 \pm 12	99.6	0.57	Yu-1-12	0.0351 \pm 0.0008	0.265 \pm 0.020	222.1 \pm 5.3	239 \pm 18	93.1	0.32
Mo-1-81	0.0199 \pm 0.0007	0.136 \pm 0.014	126.8 \pm 4.2	129 \pm 13	98.2	0.63	Yu-1-13	0.0277 \pm 0.0007	0.204 \pm 0.013	176.3 \pm 4.1	188 \pm 14	93.5	0.39
Mo-1-82	0.0270 \pm 0.0007	0.181 \pm 0.010	171.5 \pm 4.8	169 \pm 10	101.3	0.36	Yu-1-14	0.0286 \pm 0.0006	0.211 \pm 0.011	181.7 \pm 3.7	194 \pm 10	93.6	0.55
Mo-1-83	0.0310 \pm 0.0011	0.226 \pm 0.025	196.9 \pm 6.9	207 \pm 23	95.2	0.60	Yu-1-15	0.0373 \pm 0.0010	0.358 \pm 0.033	236.0 \pm 6.6	310 \pm 28	76.0	0.83
Mo-1-84	0.0214 \pm 0.0007	0.154 \pm 0.012	136.6 \pm 4.2	145 \pm 12	94.1	0.61	Yu-1-16	0.3368 \pm 0.0061	5.212 \pm 0.138	1871.1 \pm 34.1	1855 \pm 49	100.9	0.29
Mo-1-85	0.0682 \pm 0.0020	0.545 \pm 0.038	425.3 \pm 12.2	442 \pm 31	96.3	0.66	Yu-1-17	0.0243 \pm 0.0006	0.191 \pm 0.014	154.8 \pm 3.6	177 \pm 13	87.4	0.43
Mo-1-86	0.2160 \pm 0.0054	3.243 \pm 0.106	1260.6 \pm 31.6	1468 \pm 48	85.9	0.28	Yu-1-18	0.0297 \pm 0.0008	0.219 \pm 0.021	188.6 \pm 5.0	201 \pm 19	93.7	0.54
Mo-1-87	0.0299 \pm 0.0010	0.300 \pm 0.027	189.9 \pm 6.2	266 \pm 24	71.3	1.10	Yu-1-19	0.4087 \pm 0.0085	8.189 \pm 0.255	2209.1 \pm 45.9	2252 \pm 70	98.1	0.47
Mo-1-88	0.0395 \pm 0.0011	0.303 \pm 0.017	249.6 \pm 6.8	269 \pm 15	92.8	0.13	Yu-1-20	0.0397 \pm 0.0010	0.423 \pm 0.026	251.1 \pm 6.3	358 \pm 22	70.1	0.44
Mo-1-89	0.0207 \pm 0.0006	0.150 \pm 0.012	132.2 \pm 3.9	142 \pm 11	93.1	0.81	Yu-1-21	0.0313 \pm 0.0009	0.227 \pm 0.024	198.7 \pm 6.0	208 \pm 22	95.6	0.50
Mo-1-90	0.0292 \pm 0.0006	0.198 \pm 0.016	185.5 \pm 5.5	184 \pm 15	100.9	0.34	Yu-1-22	0.0379 \pm 0.0010	0.381 \pm 0.030	239.6 \pm 6.6	328 \pm 26	73.0	0.71
Mo-1-91	0.0702 \pm 0.0020	0.559 \pm 0.041	437.1 \pm 12.7	451 \pm 33	96.9	0.99	Yu-1-23	0.0223 \pm 0.0005	0.179 \pm 0.010	142.5 \pm 3.4	167 \pm 10	85.3	0.47
Mo-1-92	0.0273 \pm 0.0008	0.213 \pm 0.015	173.4 \pm 5.0	196 \pm 14	88.3	0.21	Yu-1-24	0.0402 \pm 0.0009	0.279 \pm 0.017	254.4 \pm 6.0	250 \pm 15	101.9	0.75
Mo-1-93	0.0225 \pm 0.0007	0.150 \pm 0.012	143.2 \pm 4.2	142 \pm 12	101.0	0.32	Yu-1-25	0.0297 \pm 0.0007	0.211 \pm 0.013	188.8 \pm 4.5	194 \pm 12	97.3	0.35
Mo-1-94	0.0339 \pm 0.0016	0.234 \pm 0.027	214.9 \pm 10.2	214 \pm 25	100.5	0.75	Yu-1-26	0.0181 \pm 0.0004	0.120 \pm 0.008	115.5 \pm 2.7	115 \pm 7	100.6	1.06
Mo-1-95	0.4299 \pm 0.0182	9.672 \pm 0.437	2305.4 \pm 97.6	2404 \pm 109	95.9	0.24	Yu-1-27	0.0200 \pm 0.0007	0.150 \pm 0.021	127.6 \pm 4.7	142 \pm 20	89.7	0.58
Mo-1-96	0.0442 \pm 0.0021	0.756 \pm 0.064	278.8 \pm 13.3	372 \pm 49	48.7	1.02	Yu-1-28	0.0204 \pm 0.0006	0.140 \pm 0.009	130.4 \pm 3.8	133 \pm 8	98.2	0.50
Mo-1-97	0.3580 \pm 0.0152	5.656 \pm 0.263	1972.6 \pm 83.8	1925 \pm 90	102.5	0.19	Yu-1-29	0.0273 \pm 0.0008	0.193 \pm 0.012	173.6 \pm 5.1	179 \pm 11	97.1	0.49
Mo-1-98	0.0384 \pm 0.0017	0.367 \pm 0.020	242.7 \pm 10.5	317 \pm 18	76.5	0.56	Yu-1-30	0.3119 \pm 0.0086	4.865 \pm 0.182	1750.0 \pm 48.4	1796 \pm 67	97.4	0.24
Mo-1-99	0.2874 \pm 0.0125	4.125 \pm 0.230	1628.5 \pm 70.7	1659 \pm 92	98.2	0.63	Yu-1-31	0.0357 \pm 0.0015	0.269 \pm 0.020	209.7 \pm 6.5	242 \pm 18	86.6	0.77
Mo-1-100	0.0339 \pm 0.0016	0.258 \pm 0.024	215.1 \pm 9.9	233 \pm 22	92.4	0.74	Yu-1-32	0.0299 \pm 0.0010	0.224 \pm 0.019	189.9 \pm 6.1	206 \pm 18	92.4	0.43
Mo-1-101	0.4064 \pm 0.0173	8.405 \pm 0.397	2198.5 \pm 93.7	2276 \pm 107	96.6	0.92	Yu-1-33	0.0290 \pm 0.0009	0.210 \pm 0.019	184.6 \pm 6.0	193 \pm 17	95.5	0.37
Mo-1-102	0.0395 \pm 0.0015	0.356 \pm 0.040	250.0 \pm 8.3	310 \pm 34	80.8	0.45	Yu-1-34	0.0357 \pm 0.0015	0.210 \pm 0.019	226.2 \pm 9.3	276 \pm 38	81.8	0.62
Mo-1-103	0.0461 \pm 0.0015	0.340 \pm 0.039	290.8 \pm 9.3	297 \pm 34	97.8	0.60	Yu-1-35	0.0304 \pm 0.0010	0.228 \pm 0.021	193.0 \pm 6.4	208 \pm 19	92.6	0.53
Mo-1-104	0.0281 \pm 0.0007	0.195 \pm 0.012	178.9 \pm 4.3	181 \pm 11	98.9	0.81	Yu-1-36	0.0477 \pm 0.0014	0.318 \pm 0.019	300.5 \pm 8.7	280 \pm 16	107.2	0.27
Mo-1-105	0.0277 \pm 0.0008	0.210 \pm 0.021	176.1 \pm 5.3	194 \pm 20	90.8	0.69	Yu-1-37	0.0370 \pm 0.0008	0.267 \pm 0.017	234.2 \pm 5.3	240 \pm 15	97.5	0.35
Mo-1-106	0.2830 \pm 0.0062	4.305 \pm 0.151	1606.3 \pm 35.1	1694 \pm 59	94.8	0.37	Yu-1-38	0.0194 \pm 0.0005	0.145 \pm 0.013	124.1 \pm 3.4	137 \pm 13	90.4	1.25
Mo-1-107	0.0271 \pm 0.0006	0.192 \pm 0.012	172.5 \pm 4.1	178 \pm 11	96.7	0.39	Yu-1-39	0.0282 \pm 0.0009	0.209 \pm 0.026	179.2 \pm 5.9	193 \pm 24	93.1	0.87
Mo-1-108	0.0277 \pm 0.0007	0.193 \pm 0.014	175.9 \pm 4.4	179 \pm 13	98.2	0.37	Yu-1-40	0.0261 \pm 0.0007	0.202 \pm 0.016	165.8 \pm 4.3	187 \pm 15	88.8	0.69
Mo-1-109	0.0428 \pm 0.0011	0.307 \pm 0.024	270.2 \pm 7.0	272 \pm 21	99.5	0.49	Yu-1-41	0.0270 \pm 0.0006	0.189 \pm 0.014	171.7 \pm 4.1	176 \pm 13	97.6	0.62
Mo-1-110	0.0271 \pm 0.0006	0.185 \pm 0.012	172.7 \pm 4.1	172 \pm 11	100.1	0.40	Yu-1-42	0.2895 \pm 0.0058	4.492 \pm 0.147	1639.0 \pm 32.6	1730 \pm 57	94.8	0.42
Mo-1-111	0.4326 \pm 0.0091	8.868 \pm 0.288	2317.4 \pm 48.8	2324 \pm 76	99.7	0.39	Yu-1-43	0.0330 \pm 0.0008	0.252 \pm 0.017	209.5 \pm 4.9	228 \pm 15	91.8	0.50
Mo-1-112	0.0298 \pm 0.0008	0.244 \pm 0.022	189.3 \pm 5.4	221 \pm 20	85.5	0.74	Yu-1-44	0.0415 \pm 0.0009	0.306 \pm 0.018	261.9 \pm 5.9	271 \pm 16	96.6	0.44
Mo-1-113	0.0423 \pm 0.0014	0.332 \pm 0.042	267.0 \pm 9.1	291 \pm 37	91.8	0.61	Yu-1-45	0.0347 \pm 0.0009	0.269 \pm 0.019	219.6 \pm 5.5	242 \pm 17	90.8	0.71
Mo-1-114	0.0394 \pm 0.0009	0.402 \pm 0.023	248.8 \pm 5.9	343 \pm 19	72.6	0.33	Yu-1-46	0.3451 \pm 0.0075	5.411 \pm 0.228	1911.0 \pm 41.5	1887 \pm 80	101.3	0.19
Mo-1-115	0.0530 \pm 0.0013	0.480 \pm 0.029	333.2 \pm 8.0	398 \pm 24	83.7	0.53	Yu-1-47	0.0312 \pm 0.0009	0.270 \pm 0.024	198.1 \pm 5.6	243 \pm 21	81.5	0.57
Mo-1-116	0.3330 \pm 0.0069	5.318 \pm 0.172	1848.2 \pm 38.6	1872 \pm 60	98.7	0.19	Yu-1-48	0.0311 \pm 0.0007	0.229 \pm 0.014	197.4 \pm 4.7	210 \pm 13	94.2	0.37
Mo-1-117	0.0267 \pm 0.0006	0.180 \pm 0.011	169.6 \pm 3.9	168 \pm 10	100.8	0.53	Yu-1-49	0.0217 \pm 0.0006	0.167 \pm 0.014	138.3 \pm 3.8	157 \pm 13	88.3	0.47
Sandstone of the lower part of the Yunoki Formation (Yu-1: 33° 42' 31.17" N, 133° 50' 01.71" E)													
Yu-1-1	0.0453 \pm 0.0015	0.325 \pm 0.015	285.6 \pm 9.4	286 \pm 13	100.0	0.70	Yu-1-50	0.3713 \pm 0.0082	6.817 \pm 0.294	2035.7 \pm 44.8	2088 \pm 90	97.5	0.21
Yu-1-2	0.0232 \pm 0.0009	0.223 \pm 0.022	147.9 \pm 5.9	204 \pm 20	72.4	0.59	Yu-1-51	0.2975 \pm 0.0066	4.587 \pm 0.201	1679.1 \pm 37.0	1747 \pm 77	96.1	0.26
Yu-1-3	0.0283 \pm 0.0010	0.216 \pm 0.015	180.1 \pm 6.3	198 \pm 14	90.8	0.45	Yu-1-52	0.0208 \pm 0.0007	0.148 \pm 0.017	132.6 \pm 4.2	140 \pm 16	94.6	0.74
Yu-1-4	0.0286 \pm 0.0010	0.216 \pm 0.018	182.0 \pm 6.6	198 \pm 16	91.8	0.37	Yu-1-53	0.0215 \pm 0.0007	0.158 \pm 0.019	137.4 \pm 4.5	149 \pm 18	92.3	0.68
Yu-1-5	0.0302 \pm 0.0011	0.221 \pm 0.015	192.0 \pm 6.7	203 \pm 14	94.6	0.52	Yu-1-54	0.0195 \pm 0.0006	0.129 \pm 0.009	124.6 \pm 3.6	123 \pm 8	101.5	0.82
			</										

TABLE 1. (Continued)

Grain	$^{206}\text{Pb}/^{238}\text{U}$	$^{207}\text{Pb}/^{235}\text{U}$	$^{206}\text{Pb}/^{238}\text{U}$ age (Ma)	$^{207}\text{Pb}/^{235}\text{U}$ age (Ma)	%conc	Th/U
Yu-1-57	0.0353 ± 0.0010	0.264 ± 0.013	223.5 ± 6.1	238 ± 12	94.0	0.36
Yu-1-58	0.0407 ± 0.0012	0.283 ± 0.023	257.4 ± 7.9	253 ± 21	101.8	0.55
Yu-1-59	0.2956 ± 0.0078	4.636 ± 0.162	1669.5 ± 43.9	1756 ± 61	95.1	0.46
Yu-1-60	0.0412 ± 0.0011	0.286 ± 0.014	260.2 ± 7.0	255 ± 12	102.0	0.31
Yu-1-61	0.0253 ± 0.0010	0.186 ± 0.025	161.1 ± 6.2	173 ± 23	92.9	0.59
Yu-1-62	0.0211 ± 0.0009	0.133 ± 0.015	134.8 ± 6.0	127 ± 15	106.0	0.63
Yu-1-63	0.0237 ± 0.0010	0.167 ± 0.016	150.8 ± 6.4	157 ± 15	96.1	1.00
Yu-1-64	0.0204 ± 0.0009	0.175 ± 0.019	130.1 ± 5.8	164 ± 18	79.5	0.77
Yu-1-65	0.0222 ± 0.0009	0.154 ± 0.020	141.7 ± 5.8	146 ± 12	97.4	0.61
Yu-1-66	0.0285 ± 0.0012	0.189 ± 0.020	180.9 ± 7.8	176 ± 18	102.8	0.64
Yu-1-67	0.2971 ± 0.0118	4.646 ± 0.279	1676.8 ± 66.4	1758 ± 106	95.4	0.70
Yu-1-68	0.0317 ± 0.0013	0.342 ± 0.043	201.2 ± 9.8	298 ± 38	67.4	0.71
Yu-1-69	0.0207 ± 0.0009	0.190 ± 0.018	131.8 ± 5.7	176 ± 17	74.8	0.71
Yu-1-70	0.0422 ± 0.0018	0.297 ± 0.027	266.2 ± 11.2	264 ± 24	100.8	0.44
Yu-1-71	0.0257 ± 0.0007	0.189 ± 0.010	163.3 ± 5.8	176 ± 9	92.7	0.45
Yu-1-72	0.0245 ± 0.0008	0.211 ± 0.015	155.8 ± 4.9	195 ± 14	80.0	1.45
Yu-1-73	0.0192 ± 0.0006	0.146 ± 0.012	122.5 ± 4.0	138 ± 12	88.6	1.00
Yu-1-74	0.2778 ± 0.0078	4.350 ± 0.165	1580.4 ± 44.6	1703 ± 64	92.8	0.33
Yu-1-75	0.0306 ± 0.0009	0.231 ± 0.014	194.6 ± 5.8	211 ± 13	92.4	0.44
Yu-1-76	0.0254 ± 0.0011	0.209 ± 0.030	161.4 ± 6.7	193 ± 28	83.8	0.76
Yu-1-77	0.0279 ± 0.0011	0.192 ± 0.027	177.6 ± 7.0	178 ± 25	99.7	0.39
Yu-1-78	0.0204 ± 0.0007	0.158 ± 0.018	130.0 ± 4.7	149 ± 17	87.5	0.62
Yu-1-79	0.0370 ± 0.0011	0.264 ± 0.017	234.4 ± 7.1	238 ± 15	98.4	0.91
Yu-1-80	0.0339 ± 0.0011	0.251 ± 0.019	215.2 ± 7.1	228 ± 17	94.6	0.30
Yu-1-81	0.3409 ± 0.0102	5.287 ± 0.202	1890.8 ± 56.3	1867 ± 71	101.3	0.28
Yu-1-82	0.0333 ± 0.0011	0.265 ± 0.016	211.4 ± 6.7	238 ± 15	88.7	0.72
Yu-1-83	0.0299 ± 0.0011	0.207 ± 0.021	189.8 ± 6.8	191 ± 20	99.3	0.56
Yu-1-84	0.5831 ± 0.0174	15.116 ± 0.570	2961.4 ± 88.4	2822 ± 106	104.9	0.44
Yu-1-85	0.0203 ± 0.0007	0.140 ± 0.010	129.8 ± 4.2	133 ± 10	97.3	1.15
Yu-1-86	0.3407 ± 0.0101	5.380 ± 0.204	1889.9 ± 56.2	1882 ± 71	100.4	0.38
Yu-1-87	0.0423 ± 0.0014	0.377 ± 0.030	267.3 ± 9.1	325 ± 26	82.3	1.03
Yu-1-88	0.2161 ± 0.0065	3.375 ± 0.138	1261.1 ± 38.0	1498 ± 61	84.2	0.87
Yu-1-89	0.3324 ± 0.0069	5.229 ± 0.149	1850.2 ± 38.2	1857 ± 53	99.6	0.71
Yu-1-90	0.0204 ± 0.0005	0.152 ± 0.010	130.1 ± 3.2	143 ± 10	90.8	0.67
Yu-1-91	0.0294 ± 0.0007	0.209 ± 0.015	186.6 ± 4.7	192 ± 14	97.0	0.55
Yu-1-92	0.0274 ± 0.0007	0.202 ± 0.015	174.1 ± 4.4	187 ± 14	93.1	0.47
Yu-1-93	0.0347 ± 0.0010	0.249 ± 0.024	220.2 ± 6.2	226 ± 21	97.6	0.32
Yu-1-94	0.0375 ± 0.0009	0.294 ± 0.018	237.2 ± 5.7	261 ± 16	90.7	0.57
Yu-1-95	0.2136 ± 0.0043	3.223 ± 0.078	1248.2 ± 25.4	1463 ± 36	83.3	0.39
Yu-1-96	0.0344 ± 0.0009	0.338 ± 0.023	218.2 ± 5.7	295 ± 20	73.9	0.41
Yu-1-97	0.0284 ± 0.0007	0.200 ± 0.009	180.5 ± 4.6	185 ± 9	97.7	0.39
Yu-1-98	0.0217 ± 0.0008	0.161 ± 0.020	138.5 ± 4.9	151 ± 18	91.6	0.80
Yu-1-99	0.1456 ± 0.0036	2.039 ± 0.062	876.4 ± 21.5	1128 ± 34	77.7	0.10
Yu-1-100	0.0409 ± 0.0015	0.372 ± 0.041	258.4 ± 9.2	321 ± 36	80.4	0.79
Yu-1-101	0.2674 ± 0.0065	5.275 ± 0.144	1527.8 ± 37.0	1865 ± 51	81.9	0.53
Yu-1-102	0.0330 ± 0.0009	0.267 ± 0.018	209.4 ± 5.9	241 ± 17	87.0	0.48
Yu-1-103	0.3668 ± 0.0090	5.973 ± 0.177	2014.3 ± 49.4	1972 ± 58	102.2	0.37
Yu-1-104	0.1877 ± 0.0046	2.813 ± 0.085	1109.1 ± 27.1	1359 ± 41	81.6	0.23
Yu-1-105	0.0471 ± 0.0013	0.396 ± 0.028	296.8 ± 8.4	339 ± 24	87.6	0.48
Yu-1-106	0.0304 ± 0.0009	0.223 ± 0.016	193.3 ± 5.8	205 ± 15	94.5	0.35
Yu-1-107	0.1566 ± 0.0042	2.217 ± 0.083	937.9 ± 25.0	1186 ± 44	79.1	0.12

Sandstone of the middle part of the Yumoki Formation (Yu-2; 33° 42' 23.83" N, 133° 50' 13.85" E)						
Grain	$^{206}\text{Pb}/^{238}\text{U}$	$^{207}\text{Pb}/^{235}\text{U}$	$^{206}\text{Pb}/^{238}\text{U}$ age (Ma)	$^{207}\text{Pb}/^{235}\text{U}$ age (Ma)	%conc	Th/U
Yu-2-1	0.0717 ± 0.0017	0.561 ± 0.025	446.7 ± 10.8	452 ± 20	98.8	0.57
Yu-2-2	0.0188 ± 0.0005	0.148 ± 0.008	120.3 ± 3.0	140 ± 7	86.0	0.64
Yu-2-3	0.0252 ± 0.0009	0.126 ± 0.021	160.7 ± 5.9	120 ± 20	133.7	0.74
Yu-2-4	0.0437 ± 0.0019	0.313 ± 0.056	275.7 ± 12.1	277 ± 50	99.6	0.57
Yu-2-5	0.0184 ± 0.0005	0.132 ± 0.010	117.8 ± 3.3	126 ± 10	93.5	0.65
Yu-2-6	0.0353 ± 0.0009	0.246 ± 0.015	223.9 ± 5.7	223 ± 14	100.2	0.22
Yu-2-7	0.0267 ± 0.0009	0.180 ± 0.020	169.6 ± 5.4	168 ± 19	101.1	0.58
Yu-2-8	0.0269 ± 0.0007	0.255 ± 0.014	171.0 ± 4.5	231 ± 13	74.1	0.55
Yu-2-9	0.0675 ± 0.0021	0.566 ± 0.046	420.9 ± 13.2	455 ± 37	92.5	0.72
Yu-2-10	0.3047 ± 0.0082	4.820 ± 0.188	1714.6 ± 46.2	1788 ± 70	95.9	0.34
Yu-2-11	0.0506 ± 0.0021	0.389 ± 0.055	318.0 ± 13.0	334 ± 47	95.3	0.34
Yu-2-12	0.0221 ± 0.0008	0.224 ± 0.025	140.8 ± 5.3	205 ± 23	68.5	0.70
Yu-2-13	0.0251 ± 0.0007	0.235 ± 0.013	159.7 ± 4.5	215 ± 12	74.4	1.16
Yu-2-14	0.3176 ± 0.0083	5.016 ± 0.172	1777.8 ± 46.5	1822 ± 63	97.6	0.23
Yu-2-15	0.0188 ± 0.0005	0.146 ± 0.008	120.2 ± 3.4	138 ± 8	87.1	0.82
Yu-2-16	0.0662 ± 0.0019	0.511 ± 0.032	413.4 ± 11.9	419 ± 27	98.7	0.98
Yu-2-17	0.0634 ± 0.0019	0.518 ± 0.038	396.1 ± 12.0	424 ± 31	93.4	0.86
Yu-2-18	0.0183 ± 0.0005	0.115 ± 0.011	117.2 ± 2.9	110 ± 11	106.3	0.66
Yu-2-19	0.0240 ± 0.0043	4.095 ± 0.126	1459.1 ± 24.9	1633 ± 51	88.3	0.18
Yu-2-20	0.0411 ± 0.0015	0.504 ± 0.064	259.9 ± 9.7	414 ± 53	62.8	0.47
Yu-2-21	0.3198 ± 0.0056	5.002 ± 0.163	1789.0 ± 31.2	1820 ± 59	98.3	0.27
Yu-2-22	0.0181 ± 0.0006	0.135 ± 0.019	115.7 ± 3.9	129 ± 18	90.0	0.77
Yu-2-23	0.0721 ± 0.0018	0.565 ± 0.051	448.7 ± 11.4	454 ± 41	98.7	0.79
Yu-2-24	0.0683 ± 0.0013	0.537 ± 0.026	425.7 ± 8.0	437 ± 21	97.5	0.89
Yu-2-25	0.2473 ± 0.0042	3.799 ± 0.117	1424.7 ± 24.3	1592 ± 49	89.5	0.31

TABLE 1. (Continued)

Grain	$^{206}\text{Pb}/^{238}\text{U}$	$^{207}\text{Pb}/^{235}\text{U}$	$^{206}\text{Pb}/^{238}\text{U}$ age (Ma)	$^{207}\text{Pb}/^{235}\text{U}$ age (Ma)	%conc	Th/U	$^{206}\text{Pb}/^{238}\text{U}$	$^{207}\text{Pb}/^{235}\text{U}$	$^{206}\text{Pb}/^{238}\text{U}$ age (Ma)	$^{207}\text{Pb}/^{235}\text{U}$ age (Ma)	%conc	Th/U
Yu-2-26	0.0282 ± 0.0008	0.236 ± 0.024	179.1 ± 5.0	215 ± 22	83.2	0.46	0.0606 ± 0.0022	0.480 ± 0.074	379.4 ± 13.5	398 ± 61	95.3	0.51
Yu-2-27	0.0301 ± 0.0014	0.360 ± 0.100	191.2 ± 8.9	312 ± 87	61.2	1.41	0.0749 ± 0.0014	0.563 ± 0.042	465.9 ± 8.9	453 ± 34	102.8	0.93
Yu-2-28	0.0400 ± 0.0012	0.269 ± 0.035	252.7 ± 7.3	242 ± 32	104.5	0.30	0.0211 ± 0.0005	0.159 ± 0.016	134.8 ± 3.2	150 ± 15	89.8	0.99
Yu-2-29	0.0272 ± 0.0010	0.209 ± 0.054	173.1 ± 6.7	193 ± 50	89.8	0.63	0.0179 ± 0.0006	0.148 ± 0.022	114.5 ± 4.1	140 ± 21	81.7	1.23
Yu-2-30	0.0177 ± 0.0005	0.123 ± 0.018	113.0 ± 3.4	118 ± 18	95.9	0.70	0.0277 ± 0.0006	0.216 ± 0.013	176.0 ± 2.8	198 ± 12	88.8	0.42
Yu-2-31	0.0468 ± 0.0014	0.338 ± 0.050	294.6 ± 9.1	296 ± 44	99.7	0.56	0.0665 ± 0.0012	0.490 ± 0.036	414.8 ± 7.8	405 ± 30	102.4	0.75
Yu-2-32	0.0239 ± 0.0008	0.171 ± 0.029	152.2 ± 4.9	160 ± 27	95.2	0.64	0.0350 ± 0.0007	0.224 ± 0.018	221.8 ± 4.2	205 ± 16	108.0	0.44
Yu-2-33	0.0295 ± 0.0011	0.498 ± 0.066	187.5 ± 7.0	410 ± 54	45.7	0.71	0.0738 ± 0.0016	0.550 ± 0.047	458.9 ± 9.8	445 ± 38	103.1	0.76
Yu-2-34	0.0302 ± 0.0008	0.216 ± 0.021	191.6 ± 5.1	199 ± 19	96.5	0.54	0.4526 ± 0.0073	9.453 ± 0.409	2406.8 ± 39.0	2383 ± 103	101.0	0.60
Yu-2-35	0.0694 ± 0.0028	0.559 ± 0.066	432.4 ± 17.3	451 ± 54	95.8	0.46	0.0190 ± 0.0005	0.131 ± 0.014	121.4 ± 2.9	125 ± 13	97.3	0.66
Yu-2-36	0.0727 ± 0.0026	0.582 ± 0.050	452.1 ± 16.0	466 ± 40	97.1	0.71	0.0292 ± 0.0006	0.197 ± 0.016	185.4 ± 3.6	183 ± 15	101.6	0.41
Yu-2-37	0.0299 ± 0.0013	0.215 ± 0.032	189.9 ± 8.3	198 ± 29	95.9	0.62	0.0437 ± 0.0015	0.306 ± 0.048	275.7 ± 9.4	271 ± 43	101.8	0.48
Yu-2-38	0.0472 ± 0.0020	0.462 ± 0.060	297.6 ± 12.9	386 ± 50	77.2	0.66	0.0375 ± 0.0006	0.337 ± 0.016	237.6 ± 3.9	295 ± 14	80.6	0.47
Yu-2-39	0.0725 ± 0.0025	0.577 ± 0.048	451.4 ± 15.8	463 ± 39	97.6	0.62	0.3254 ± 0.0066	4.949 ± 0.223	1816.2 ± 36.9	1811 ± 81	100.3	1.49
Yu-2-40	0.0708 ± 0.0025	0.567 ± 0.050	441.1 ± 15.7	456 ± 40	96.7	0.70	0.0285 ± 0.0006	0.222 ± 0.014	180.9 ± 3.7	203 ± 13	88.9	0.80
Yu-2-41	0.0301 ± 0.0011	0.213 ± 0.020	191.2 ± 6.8	196 ± 18	97.3	0.49	0.0423 ± 0.0018	0.273 ± 0.054	267.2 ± 11.6	245 ± 48	109.1	0.58
Yu-2-42	0.0418 ± 0.0020	0.348 ± 0.056	264.1 ± 12.5	303 ± 49	87.1	0.46	0.0252 ± 0.0006	0.191 ± 0.014	160.7 ± 3.6	177 ± 13	90.6	0.46
Yu-2-43	0.0347 ± 0.0007	0.249 ± 0.019	219.6 ± 4.3	226 ± 17	97.3	0.94	0.0461 ± 0.0011	0.348 ± 0.031	290.4 ± 7.2	303 ± 27	95.7	0.41
Yu-2-44	0.0344 ± 0.0005	0.251 ± 0.009	218.3 ± 2.9	227 ± 8	96.0	0.89	0.3242 ± 0.0062	4.998 ± 0.198	1810.2 ± 34.3	1819 ± 72	99.5	0.90
Yu-2-45	0.0187 ± 0.0007	0.105 ± 0.020	119.2 ± 4.2	102 ± 19	117.3	0.57	0.0211 ± 0.0006	0.147 ± 0.016	134.6 ± 3.8	139 ± 16	96.7	0.59
Yu-2-46	0.0384 ± 0.0008	0.286 ± 0.025	243.0 ± 5.3	255 ± 22	95.2	0.62	0.2928 ± 0.0063	4.796 ± 0.235	1655.3 ± 35.6	1784 ± 87	92.8	0.13
Yu-2-47	0.0344 ± 0.0007	0.274 ± 0.022	218.0 ± 4.5	246 ± 20	88.6	0.67	0.0378 ± 0.0009	0.260 ± 0.023	239.4 ± 5.7	235 ± 21	101.9	0.18
Yu-2-48	0.0462 ± 0.0055	0.737 ± 0.201	2197.6 ± 29.9	2153 ± 59	102.1	0.21	0.3328 ± 0.0060	5.229 ± 0.165	1851.7 ± 33.6	1857 ± 59	99.7	0.29
Yu-2-49	0.3779 ± 0.0044	7.013 ± 0.124	2066.5 ± 24.1	2113 ± 37	97.8	0.46	0.0286 ± 0.0008	0.198 ± 0.023	181.5 ± 5.2	183 ± 21	98.9	0.93
Yu-2-50	0.2893 ± 0.0038	4.471 ± 0.117	1637.8 ± 21.4	1726 ± 45	94.9	0.23	0.0691 ± 0.0015	0.512 ± 0.036	430.5 ± 9.7	420 ± 30	102.6	0.92
Yu-2-51	0.0197 ± 0.0007	0.185 ± 0.025	125.6 ± 4.2	173 ± 23	72.7	0.45	0.0675 ± 0.0016	0.489 ± 0.040	421.2 ± 10.1	404 ± 33	104.1	0.85
Yu-2-52	0.0357 ± 0.0012	0.293 ± 0.040	226.1 ± 7.9	261 ± 35	86.6	0.25	0.0443 ± 0.0015	0.809 ± 0.078	279.1 ± 9.5	602 ± 58	46.4	0.18
Yu-2-53	0.0185 ± 0.0006	0.119 ± 0.016	118.0 ± 3.8	114 ± 15	103.6	0.28	0.0352 ± 0.0008	0.243 ± 0.016	223.3 ± 4.8	221 ± 15	101.1	0.59
Yu-2-54	0.0460 ± 0.0023	1.682 ± 0.191	290.2 ± 14.3	1002 ± 114	29.0	0.48	0.0190 ± 0.0009	0.136 ± 0.031	121.3 ± 5.5	130 ± 29	93.4	0.81
Yu-2-55	0.0280 ± 0.0007	0.207 ± 0.016	177.8 ± 4.3	191 ± 15	93.2	0.38	0.0349 ± 0.0007	0.260 ± 0.011	220.9 ± 4.2	234 ± 10	94.2	0.26
Yu-2-56	0.0280 ± 0.0007	0.210 ± 0.018	178.3 ± 4.6	193 ± 17	92.2	0.26	0.0267 ± 0.0006	0.181 ± 0.012	169.8 ± 4.0	169 ± 11	100.6	0.23
Yu-2-57	0.0978 ± 0.0019	1.265 ± 0.047	601.8 ± 11.9	830 ± 31	72.5	0.15	0.0276 ± 0.0007	0.206 ± 0.017	175.6 ± 4.7	190 ± 16	92.2	0.38
Yu-2-58	0.0272 ± 0.0005	0.195 ± 0.012	173.2 ± 3.1	181 ± 11	95.8	0.35	0.0447 ± 0.0016	0.334 ± 0.047	282.0 ± 10.0	293 ± 41	96.3	0.48
Yu-2-59	0.3174 ± 0.0060	4.970 ± 0.145	1772.3 ± 33.4	1814 ± 53	98.0	0.23	0.0304 ± 0.0011	0.203 ± 0.033	193.3 ± 7.2	188 ± 30	103.0	0.55
Yu-2-60	0.0441 ± 0.0011	0.332 ± 0.027	278.1 ± 6.9	291 ± 23	95.6	0.51	0.0271 ± 0.0008	0.195 ± 0.020	172.3 ± 5.1	181 ± 19	95.4	0.44
Yu-2-61	0.0272 ± 0.0005	0.195 ± 0.012	173.2 ± 3.1	181 ± 11	95.8	0.35	0.0472 ± 0.0029	0.384 ± 0.114	297.2 ± 18.1	330 ± 98	90.1	0.42
Yu-2-62	0.0364 ± 0.0010	0.246 ± 0.029	230.5 ± 6.3	224 ± 26	103.2	0.81	0.0559 ± 0.0017	1.100 ± 0.078	350.7 ± 10.5	753 ± 54	46.6	0.70
Yu-2-63	0.0200 ± 0.0007	0.143 ± 0.023	127.5 ± 4.7	135 ± 22	94.2	0.70	0.0728 ± 0.0019	0.781 ± 0.052	453.1 ± 11.7	586 ± 39	77.3	0.77
Yu-2-64	0.0230 ± 0.0005	0.145 ± 0.011	146.8 ± 3.0	137 ± 11	107.1	0.36	0.0168 ± 0.0005	0.117 ± 0.012	107.3 ± 3.1	112 ± 12	95.8	0.85
Yu-2-65	0.0372 ± 0.0008	0.375 ± 0.028	235.2 ± 5.3	324 ± 24	72.7	0.28	0.0369 ± 0.0011	0.331 ± 0.026	233.3 ± 6.7	290 ± 23	80.4	0.47
Yu-2-66	0.0433 ± 0.0015	0.288 ± 0.046	273.5 ± 9.6	257 ± 41	106.4	0.37	0.0429 ± 0.0016	0.283 ± 0.044	270.5 ± 10.3	255 ± 40	106.1	0.52
Yu-2-67	0.0267 ± 0.0006	0.180 ± 0.014	170.1 ± 3.6	168 ± 13	101.3	0.50	0.3285 ± 0.0077	5.167 ± 0.180	1830.9 ± 42.7	1847 ± 64	99.1	0.24
Yu-2-68	0.0433 ± 0.0014	0.306 ± 0.030	273.2 ± 9.1	271 ± 26	100.7	0.39	0.0213 ± 0.0007	0.156 ± 0.018	136.0 ± 4.5	147 ± 17	92.2	0.57
Yu-2-69	0.0735 ± 0.0023	0.612 ± 0.048	457.2 ± 14.4	485 ± 38	94.3	0.63	0.0686 ± 0.0019	0.550 ± 0.043	427.6 ± 11.9	445 ± 34	96.1	0.90
Yu-2-70	0.0172 ± 0.0006	0.127 ± 0.014	109.7 ± 3.9	122 ± 14	90.2	0.48	0.0419 ± 0.0018	0.322 ± 0.056	264.4 ± 11.4	284 ± 50	93.2	0.41
Yu-2-71	0.0276 ± 0.0009	0.223 ± 0.020	175.4 ± 5.8	204 ± 19	83.9	0.55	0.0419 ± 0.0014	0.339 ± 0.036	264.5 ± 8.6	297 ± 32	89.2	0.46
Yu-2-72	0.0341 ± 0.0010	0.239 ± 0.011	216.4 ± 6.0	218 ± 10	99.3	0.11	0.0845 ± 0.0023	1.150 ± 0.073	523.1 ± 14.5	777 ± 49	67.3	0.41
Yu-2-73	0.0343 ± 0.0011	0.268 ± 0.025	217.3 ± 7.3	241 ± 23	90.2	0.67	0.2967 ± 0.0071	4.615 ± 0.175	1675.0 ± 39.9	1752 ± 67	95.6	0.38
Yu-2-74	0.0289 ± 0.0009	0.207 ± 0.016	183.9 ± 5.7	191 ± 15	96.3	0.44						
Yu-2-75	0.0262 ± 0.0008	0.183 ± 0.013	166.5 ± 5.1	171 ± 12	97.4	0.50						
Yu-2-76	0.0335 ± 0.0009	0.240 ± 0.026	212.5 ± 5.4	219 ± 24	97.2	0.62						

TABLE 1. (Continued)

Grain	$^{206}\text{Pb}/^{238}\text{U}$	$^{207}\text{Pb}/^{235}\text{U}$	$^{206}\text{Pb}/^{238}\text{U}$ age (Ma)	$^{207}\text{Pb}/^{235}\text{U}$ age (Ma)	$^{206}\text{Pb}/^{238}\text{U}$ age (Ma)	$^{207}\text{Pb}/^{235}\text{U}$ age (Ma)	%conc	Th/U	Grain	$^{206}\text{Pb}/^{238}\text{U}$	$^{207}\text{Pb}/^{235}\text{U}$	$^{206}\text{Pb}/^{238}\text{U}$ age (Ma)	$^{207}\text{Pb}/^{235}\text{U}$ age (Ma)	$^{206}\text{Pb}/^{238}\text{U}$ age (Ma)	$^{207}\text{Pb}/^{235}\text{U}$ age (Ma)	%conc	Th/U
Sandstone of the Hibbala Formation (H1-1: 33° 42' 15.36" N, 133° 50' 34.28" E)																	
H1-1-1	0.0184 ± 0.0009	0.117 ± 0.021	117.4 ± 5.6	112 ± 20	104.8	0.62	0.43		H1-1-51	0.0197 ± 0.0009	0.137 ± 0.031	125.9 ± 5.9	148 ± 30	128 ± 11	122 ± 11	85.0	0.43
H1-1-2	0.0187 ± 0.0008	0.133 ± 0.018	119.2 ± 5.3	127 ± 17	94.2	0.55	1.09		H1-1-52	0.0176 ± 0.0005	0.128 ± 0.012	112.2 ± 3.2	122 ± 11	122 ± 11	92.0	0.38	
H1-1-3	0.0183 ± 0.0008	0.142 ± 0.020	116.7 ± 5.2	135 ± 19	86.4	0.53	0.38		H1-1-53	0.0165 ± 0.0006	0.133 ± 0.020	105.3 ± 4.1	127 ± 20	127 ± 20	83.3	0.38	
H1-1-4	0.0183 ± 0.0008	0.112 ± 0.018	117.0 ± 5.3	108 ± 17	108.7	0.56	0.62		H1-1-54	0.0179 ± 0.0008	0.127 ± 0.025	114.4 ± 5.1	121 ± 24	121 ± 24	94.1	0.62	
H1-1-5	0.0451 ± 0.0020	0.317 ± 0.043	284.5 ± 12.6	280 ± 38	101.8	0.66	0.19		H1-1-55	0.0928 ± 0.0020	0.823 ± 0.034	572.0 ± 12.5	610 ± 25	610 ± 25	93.8	0.46	
H1-1-6	0.0217 ± 0.0009	0.142 ± 0.018	138.4 ± 5.9	135 ± 17	102.5	0.53	0.46		H1-1-56	0.0296 ± 0.0007	0.209 ± 0.013	188.1 ± 4.5	193 ± 12	193 ± 12	97.5	0.46	
H1-1-7	0.0419 ± 0.0018	0.313 ± 0.037	264.4 ± 11.2	276 ± 32	95.7	0.43	0.58		H1-1-57	0.0208 ± 0.0008	0.122 ± 0.020	132.5 ± 4.8	117 ± 19	117 ± 19	113.7	0.48	
H1-1-8	0.0187 ± 0.0010	0.098 ± 0.023	119.2 ± 6.1	95 ± 22	125.7	0.45	0.59		H1-1-58	0.0173 ± 0.0006	0.124 ± 0.015	110.6 ± 4.1	119 ± 14	119 ± 14	93.1	0.48	
H1-1-9	0.0190 ± 0.0008	0.117 ± 0.017	121.0 ± 5.4	112 ± 16	107.7	0.93	0.97		H1-1-59	0.0434 ± 0.0015	0.322 ± 0.029	273.7 ± 9.2	283 ± 26	283 ± 26	96.2	0.59	
H1-1-10	0.0198 ± 0.0009	0.140 ± 0.021	126.5 ± 5.5	133 ± 20	95.1	0.41	0.97		H1-1-60	0.0625 ± 0.0021	0.493 ± 0.041	391.1 ± 12.9	407 ± 34	407 ± 34	96.7	0.97	
H1-1-11	0.0184 ± 0.0007	0.131 ± 0.015	117.8 ± 4.6	125 ± 14	94.4	0.65	0.46		H1-1-61	0.0178 ± 0.0007	0.103 ± 0.017	114.0 ± 4.7	100 ± 16	100 ± 16	114.3	0.46	
H1-1-12	0.0179 ± 0.0009	0.117 ± 0.022	114.5 ± 5.5	112 ± 21	101.9	0.47	0.62		H1-1-62	0.0174 ± 0.0008	0.143 ± 0.023	111.4 ± 5.1	135 ± 22	135 ± 22	95.2	0.62	
H1-1-13	0.0196 ± 0.0008	0.124 ± 0.017	124.8 ± 5.1	118 ± 16	105.4	0.51	0.44		H1-1-63	0.0175 ± 0.0008	0.123 ± 0.020	111.8 ± 4.9	117 ± 19	117 ± 19	92.2	0.62	
H1-1-14	0.0186 ± 0.0008	0.146 ± 0.022	118.7 ± 5.4	138 ± 21	86.0	0.49	0.41		H1-1-64	0.0159 ± 0.0007	0.110 ± 0.020	102.0 ± 4.8	106 ± 19	106 ± 19	96.2	0.44	
H1-1-15	0.0175 ± 0.0008	0.111 ± 0.017	112.1 ± 4.8	107 ± 16	105.0	0.81	0.45		H1-1-65	0.0186 ± 0.0007	0.120 ± 0.017	118.6 ± 4.7	115 ± 16	115 ± 16	102.9	0.41	
H1-1-16	0.0184 ± 0.0008	0.205 ± 0.026	172.8 ± 5.3	189 ± 24	62.4	0.78	0.48		H1-1-66	0.0287 ± 0.0009	0.249 ± 0.019	182.5 ± 5.8	225 ± 17	225 ± 17	81.0	0.45	

TABLE 1. (Continued)

Grain	$^{206}\text{Pb}/^{238}\text{U}$	$^{207}\text{Pb}/^{235}\text{U}$	$^{206}\text{Pb}/^{238}\text{U}$ age (Ma)	$^{207}\text{Pb}/^{235}\text{U}$ age (Ma)	%conc	Th/U	Grain	$^{206}\text{Pb}/^{238}\text{U}$	$^{207}\text{Pb}/^{235}\text{U}$	$^{206}\text{Pb}/^{238}\text{U}$ age (Ma)	$^{207}\text{Pb}/^{235}\text{U}$ age (Ma)	%conc	Th/U
Hi-1-102	0.0188 ± 0.0007	0.131 ± 0.019	119.9 ± 4.3	125 ± 18	96.3	0.41	Hi-1-153	0.0185 ± 0.0006	0.136 ± 0.012	118.0 ± 4.1	129 ± 11	91.2	0.64
Hi-1-103	0.0164 ± 0.0004	0.124 ± 0.010	104.6 ± 2.6	119 ± 9	88.2	0.99	Hi-1-154	0.0208 ± 0.0008	0.152 ± 0.016	132.6 ± 4.9	144 ± 15	92.3	0.91
Hi-1-104	0.0266 ± 0.0006	0.196 ± 0.013	169.2 ± 3.9	182 ± 12	93.2	0.50	Sandstone of the lower part of the Biraftu Formation (Bi-1; 33° 38' 55.27" N, 133° 47' 52.38" E)						
Hi-1-105	0.0171 ± 0.0005	0.115 ± 0.013	109.0 ± 3.1	111 ± 12	98.5	0.89							
Hi-1-106	0.3013 ± 0.0058	4.735 ± 0.148	1697.9 ± 32.4	1773 ± 55	95.7	0.16							
Hi-1-107	0.0294 ± 0.0014	0.615 ± 0.064	186.8 ± 9.1	487 ± 31	38.4	0.52							
Hi-1-108	0.0190 ± 0.0009	0.155 ± 0.023	121.5 ± 6.0	146 ± 22	83.0	0.37							
Hi-1-109	0.0185 ± 0.0008	0.139 ± 0.014	118.2 ± 5.0	133 ± 13	89.2	0.64							
Hi-1-110	0.0291 ± 0.0012	0.196 ± 0.017	185.0 ± 7.5	181 ± 16	102.0	0.37							
Hi-1-111	0.0273 ± 0.0011	0.213 ± 0.018	172.8 ± 7.0	196 ± 17	88.1	0.56							
Hi-1-112	0.0171 ± 0.0009	0.113 ± 0.021	109.4 ± 5.9	108 ± 20	100.9	0.57							
Hi-1-113	0.0297 ± 0.0012	0.215 ± 0.017	188.9 ± 7.5	197 ± 16	95.7	0.52							
Hi-1-114	0.0182 ± 0.0009	0.136 ± 0.019	116.1 ± 5.5	130 ± 18	89.5	0.57							
Hi-1-115	0.0190 ± 0.0010	0.154 ± 0.024	121.1 ± 6.2	145 ± 23	83.4	0.63							
Hi-1-116	0.0195 ± 0.0007	0.127 ± 0.020	124.2 ± 4.8	122 ± 19	102.0	0.65							
Hi-1-117	0.0319 ± 0.0009	0.336 ± 0.031	202.3 ± 5.8	294 ± 27	68.9	0.57							
Hi-1-118	0.0281 ± 0.0007	0.206 ± 0.019	178.7 ± 4.8	190 ± 18	94.1	0.31							
Hi-1-119	0.0187 ± 0.0005	0.106 ± 0.013	119.3 ± 3.4	102 ± 12	116.4	0.62							
Hi-1-120	0.0199 ± 0.0007	0.130 ± 0.021	127.0 ± 4.5	124 ± 20	102.2	0.42							
Hi-1-121	0.0241 ± 0.0009	0.139 ± 0.026	153.5 ± 5.7	132 ± 24	116.3	0.65							
Hi-1-122	0.0184 ± 0.0009	0.155 ± 0.018	117.8 ± 5.7	146 ± 17	80.5	0.76							
Hi-1-123	0.0201 ± 0.0009	0.137 ± 0.013	128.3 ± 5.8	130 ± 13	98.5	0.68							
Hi-1-124	0.0184 ± 0.0009	0.150 ± 0.020	117.3 ± 5.9	142 ± 19	82.9	0.85							
Hi-1-125	0.0181 ± 0.0010	0.126 ± 0.022	115.4 ± 6.3	120 ± 21	96.1	1.12							
Hi-1-126	0.3423 ± 0.0146	5.620 ± 0.340	1897.9 ± 80.8	1919 ± 116	98.9	0.27							
Hi-1-127	0.0432 ± 0.0019	0.328 ± 0.023	272.5 ± 11.8	288 ± 20	94.5	0.44							
Hi-1-128	0.0234 ± 0.0011	0.196 ± 0.023	149.0 ± 7.2	182 ± 22	82.0	0.62							
Hi-1-129	0.0200 ± 0.0010	0.147 ± 0.020	127.5 ± 6.5	139 ± 19	91.6	0.69							
Hi-1-130	0.0201 ± 0.0010	0.176 ± 0.022	128.5 ± 6.5	165 ± 21	78.0	0.54							
Hi-1-131	0.0199 ± 0.0012	0.141 ± 0.035	126.8 ± 7.5	134 ± 34	94.4	0.46							
Hi-1-132	0.0179 ± 0.0013	0.131 ± 0.039	116.6 ± 8.0	125 ± 37	91.4	1.03							
Hi-1-133	0.0200 ± 0.0024	0.116 ± 0.076	127.9 ± 15.6	111 ± 73	115.0	0.50							
Hi-1-134	0.0186 ± 0.0012	0.150 ± 0.038	119.1 ± 7.6	142 ± 36	83.9	0.59							
Hi-1-135	0.0457 ± 0.0012	0.414 ± 0.023	288.3 ± 7.4	352 ± 20	82.0	0.62							
Hi-1-136	0.0266 ± 0.0016	0.442 ± 0.063	169.1 ± 10.1	372 ± 53	45.5	0.51							
Hi-1-137	0.0321 ± 0.0012	0.222 ± 0.032	204.0 ± 7.8	203 ± 30	100.3	0.54							
Hi-1-138	0.0288 ± 0.0008	0.196 ± 0.012	183.0 ± 4.8	182 ± 11	100.6	0.23							
Hi-1-139	0.0200 ± 0.0007	0.172 ± 0.018	127.5 ± 4.3	161 ± 17	79.1	0.54							
Hi-1-140	0.0199 ± 0.0006	0.133 ± 0.014	127.1 ± 4.0	127 ± 13	99.9	0.47							
Hi-1-141	0.0201 ± 0.0008	0.144 ± 0.020	128.2 ± 4.8	137 ± 19	93.8	0.61							
Hi-1-142	0.0200 ± 0.0007	0.138 ± 0.018	127.9 ± 4.6	131 ± 17	97.4	0.53							
Hi-1-143	0.3609 ± 0.0087	5.594 ± 0.208	1986.5 ± 48.1	1915 ± 71	103.7	0.34							
Hi-1-144	0.0247 ± 0.0008	0.213 ± 0.019	157.6 ± 4.9	196 ± 18	80.3	0.59							
Hi-1-145	0.0345 ± 0.0013	0.307 ± 0.039	218.8 ± 8.2	272 ± 34	88.4	0.73							
Hi-1-146	0.0243 ± 0.0009	0.200 ± 0.027	154.5 ± 5.9	185 ± 25	83.3	0.40							
Hi-1-147	0.0263 ± 0.0011	0.208 ± 0.027	167.4 ± 6.9	192 ± 25	87.1	0.55							
Hi-1-148	0.0226 ± 0.0008	0.157 ± 0.013	143.8 ± 4.9	148 ± 12	97.1	0.74							
Hi-1-149	0.0420 ± 0.0014	0.312 ± 0.020	265.4 ± 8.6	276 ± 17	96.2	0.39							
Hi-1-150	0.0357 ± 0.0012	0.264 ± 0.021	226.1 ± 7.7	238 ± 19	94.9	0.48							
Hi-1-151	0.0299 ± 0.0011	0.256 ± 0.020	190.0 ± 6.7	215 ± 18	88.2	1.06							
Hi-1-152	0.0207 ± 0.0007	0.134 ± 0.012	132.1 ± 4.6	128 ± 12	103.2	0.63							

TABLE 1. (Continued)

Grain	$^{206}\text{Pb}/^{238}\text{U}$	$^{207}\text{Pb}/^{235}\text{U}$	$^{206}\text{Pb}/^{238}\text{U}$ age (Ma)	$^{207}\text{Pb}/^{235}\text{U}$ age (Ma)	Th/U	%conc	$^{206}\text{Pb}/^{238}\text{U}$	$^{207}\text{Pb}/^{235}\text{U}$	$^{206}\text{Pb}/^{238}\text{U}$ age (Ma)	$^{207}\text{Pb}/^{235}\text{U}$ age (Ma)	Th/U	%conc
Bi-1-48	0.0445 ± 0.0012	0.419 ± 0.032	280.5 ± 7.8	356 ± 27	78.9	0.49	0.0337 ± 0.0006	0.255 ± 0.013	213.9 ± 3.8	230 ± 12	92.8	0.46
Bi-1-49	0.0392 ± 0.0010	0.356 ± 0.024	247.9 ± 6.5	309 ± 21	80.3	0.54	0.0326 ± 0.0051	0.250 ± 0.012	185.1 ± 28.2	1861 ± 45	99.5	0.80
Bi-1-50	0.0389 ± 0.0009	0.343 ± 0.017	245.9 ± 5.8	299 ± 15	82.2	0.45	0.0327 ± 0.0006	0.259 ± 0.013	207.5 ± 3.8	234 ± 12	88.8	0.32
Bi-1-51	0.0273 ± 0.0006	0.239 ± 0.017	173.4 ± 4.0	218 ± 15	79.5	0.78	0.0298 ± 0.0042	0.209 ± 0.015	148.9 ± 23.8	1646 ± 47	90.5	0.25
Bi-1-52	0.0288 ± 0.0005	0.273 ± 0.012	183.0 ± 3.5	245 ± 11	74.8	0.38	0.0281 ± 0.0007	0.224 ± 0.019	178.5 ± 4.3	205 ± 18	87.0	0.62
Bi-1-53	0.0342 ± 0.0010	0.406 ± 0.042	216.5 ± 6.5	389 ± 35	55.7	1.01	0.0376 ± 0.0036	0.583 ± 0.184	2061.3 ± 19.7	1973 ± 61	104.5	0.27
Bi-1-54	0.0287 ± 0.0007	0.214 ± 0.020	182.4 ± 4.7	197 ± 18	92.8	0.78	0.0210 ± 0.0024	0.174 ± 0.017	123.1 ± 5.4	1451 ± 54	84.9	0.51
Bi-1-55	0.0635 ± 0.0012	0.492 ± 0.024	397.2 ± 7.7	406 ± 20	97.8	0.50	0.0406 ± 0.0009	0.338 ± 0.032	256.6 ± 5.8	295 ± 28	86.9	0.72
Bi-1-56	0.0277 ± 0.0006	0.198 ± 0.012	176.4 ± 3.7	183 ± 11	96.3	0.56	0.0282 ± 0.0004	0.192 ± 0.010	179.3 ± 2.2	178 ± 9	100.8	0.54
Bi-1-57	0.0349 ± 0.0007	0.578 ± 0.179	1932.0 ± 34.3	1913 ± 61	101.0	0.30	0.0396 ± 0.0004	0.326 ± 0.014	250.1 ± 2.8	287 ± 12	87.3	0.35
Bi-1-58	0.0342 ± 0.0008	0.368 ± 0.023	216.6 ± 4.9	318 ± 20	68.1	0.59	0.0369 ± 0.0032	0.326 ± 0.014	200.7 ± 17.8	1935 ± 55	103.4	0.57
Bi-1-59	0.0349 ± 0.0007	0.250 ± 0.014	221.2 ± 4.1	227 ± 12	97.5	0.42	0.0355 ± 0.0031	0.287 ± 0.016	186.5 ± 17.4	1876 ± 56	99.4	0.23
Bi-1-60	0.0310 ± 0.0005	0.221 ± 0.010	197.1 ± 3.5	202 ± 9	97.4	0.65	0.0381 ± 0.0005	0.347 ± 0.014	241.0 ± 2.9	256 ± 12	94.2	0.44
Bi-1-61	0.0300 ± 0.0007	0.214 ± 0.019	190.6 ± 4.7	197 ± 18	96.8	0.49	0.0325 ± 0.0006	0.269 ± 0.022	206.0 ± 4.0	242 ± 20	85.3	0.55
Bi-1-62	0.0322 ± 0.0055	0.153 ± 0.166	184.9 ± 30.7	1845 ± 59	100.2	0.38	0.0364 ± 0.0012	0.290 ± 0.024	230.2 ± 7.8	258 ± 22	89.1	0.37
Bi-1-63	0.0307 ± 0.0053	0.131 ± 0.148	184.1 ± 29.4	1841 ± 53	100.0	0.85	0.0394 ± 0.0012	0.311 ± 0.016	178.6 ± 52.9	1825 ± 69	97.9	0.30
Bi-1-64	0.0322 ± 0.0006	0.297 ± 0.016	204.3 ± 4.0	264 ± 14	77.4	0.90	0.0394 ± 0.0012	0.311 ± 0.016	249.2 ± 7.6	275 ± 14	90.6	0.48
Bi-1-65	0.0283 ± 0.0005	0.207 ± 0.010	180.1 ± 3.2	191 ± 9	94.4	0.92	0.0435 ± 0.0015	0.366 ± 0.034	274.4 ± 9.7	316 ± 29	86.7	0.45
Bi-1-66	0.0353 ± 0.0053	0.502 ± 0.151	1864.2 ± 29.7	1869 ± 53	99.7	0.36	0.0279 ± 0.0010	0.207 ± 0.021	177.4 ± 6.4	191 ± 20	92.9	0.57
Bi-1-67	0.0266 ± 0.0043	0.320 ± 0.121	1503.1 ± 24.5	1618 ± 50	92.9	0.27	0.0509 ± 0.0020	0.378 ± 0.048	320.2 ± 12.8	325 ± 42	98.4	0.57
Bi-1-68	0.0327 ± 0.0006	0.316 ± 0.018	207.6 ± 3.9	279 ± 16	74.5	0.51	0.0311 ± 0.0010	0.217 ± 0.016	197.6 ± 6.4	199 ± 15	99.2	0.60
Bi-1-69	0.0286 ± 0.0005	0.202 ± 0.011	181.5 ± 3.2	187 ± 10	97.2	0.32	0.0280 ± 0.0009	0.204 ± 0.014	178.1 ± 5.7	189 ± 13	94.4	0.51
Bi-1-70	0.0292 ± 0.0045	0.454 ± 0.149	1667.5 ± 25.6	1759 ± 57	95.9	0.35	0.0326 ± 0.0055	0.209 ± 0.026	179.6 ± 30.5	1861 ± 55	96.6	0.34
Bi-1-71	0.0350 ± 0.0055	0.553 ± 0.190	1936.3 ± 30.4	1909 ± 65	101.4	0.85	0.0360 ± 0.0055	0.506 ± 0.147	1818.8 ± 30.6	1830 ± 53	99.4	0.25
Bi-1-72	0.0463 ± 0.0008	0.351 ± 0.019	291.6 ± 5.2	306 ± 17	95.4	0.81	0.0344 ± 0.0058	0.344 ± 0.167	185.9 ± 32.0	1876 ± 58	99.1	0.36
Bi-1-73	0.0450 ± 0.0070	0.856 ± 0.273	2413.1 ± 37.0	2292 ± 73	105.3	0.39	0.1793 ± 0.0030	2.607 ± 0.077	1063.0 ± 17.9	1303 ± 38	81.6	0.20
Bi-1-74	0.0673 ± 0.0012	0.521 ± 0.030	419.7 ± 7.8	426 ± 25	98.6	0.78	0.0335 ± 0.0009	0.389 ± 0.030	212.7 ± 5.4	333 ± 26	63.8	0.72
Bi-1-75	0.3821 ± 0.0058	6.174 ± 0.193	2086.2 ± 31.5	2001 ± 63	104.3	0.19	0.0290 ± 0.0006	0.221 ± 0.013	184.4 ± 3.7	203 ± 12	90.8	0.48
Bi-1-76	0.0308 ± 0.0006	0.269 ± 0.014	195.3 ± 3.5	242 ± 13	80.8	0.60	0.0298 ± 0.0006	0.279 ± 0.014	189.0 ± 3.7	250 ± 12	75.6	1.15
Bi-1-77	0.0421 ± 0.0015	0.452 ± 0.040	265.5 ± 9.3	378 ± 33	70.2	0.59	0.0224 ± 0.0005	0.312 ± 0.020	142.9 ± 3.4	276 ± 18	51.8	0.97
Bi-1-78	0.3503 ± 0.0101	5.434 ± 0.225	1935.9 ± 35.6	1890 ± 78	102.4	0.27						
Bi-1-79	0.0450 ± 0.0014	0.507 ± 0.029	283.9 ± 8.7	417 ± 24	68.2	1.29						
Bi-1-80	0.0369 ± 0.0107	5.899 ± 0.251	2028.8 ± 58.6	1961 ± 83	103.5	0.26						
Bi-1-81	0.0527 ± 0.0017	0.528 ± 0.034	331.3 ± 10.4	430 ± 28	77.0	0.78						
Bi-1-82	0.0363 ± 0.0011	0.311 ± 0.017	230.2 ± 6.9	275 ± 15	83.8	0.38						
Bi-1-83	0.0460 ± 0.0015	0.411 ± 0.033	290.1 ± 9.6	349 ± 28	83.0	0.56						
Bi-1-84	0.3207 ± 0.0094	5.103 ± 0.228	1793.2 ± 52.4	1837 ± 82	97.6	0.62						
Bi-1-85	0.0331 ± 0.0010	0.259 ± 0.015	210.0 ± 6.3	234 ± 14	89.9	0.37						
Bi-1-86	0.0283 ± 0.0006	0.269 ± 0.012	179.9 ± 3.7	242 ± 11	74.4	0.63						
Bi-1-87	0.2901 ± 0.0056	4.630 ± 0.124	1641.8 ± 31.8	1755 ± 47	93.6	0.35						
Bi-1-88	0.0295 ± 0.0006	0.218 ± 0.012	187.1 ± 4.0	201 ± 11	93.3	0.29						
Bi-1-89	0.0389 ± 0.0010	0.285 ± 0.026	246.3 ± 6.6	255 ± 23	96.7	0.77						
Bi-1-90	0.0269 ± 0.0006	0.174 ± 0.009	171.3 ± 3.6	162 ± 8	105.4	0.43						
Bi-1-91	0.0408 ± 0.0008	0.295 ± 0.012	258.1 ± 5.2	262 ± 11	98.5	0.21						
Bi-1-92	0.0293 ± 0.0007	0.211 ± 0.014	186.4 ± 4.3	194 ± 13	95.9	0.39						
Bi-1-93	0.3334 ± 0.0064	5.635 ± 0.140	1855.1 ± 35.8	1921 ± 48	96.5	0.26						
Bi-1-94	0.0295 ± 0.0006	0.217 ± 0.009	187.6 ± 3.8	199 ± 8	94.2	0.35						
Bi-1-95	0.0483 ± 0.0009	0.378 ± 0.022	303.9 ± 5.8	326 ± 19	93.3	0.81						
Bi-1-96	0.0286 ± 0.0005	0.267 ± 0.011	181.5 ± 3.1	241 ± 10	75.5	0.30						
Bi-1-97	0.0288 ± 0.0005	0.251 ± 0.011	182.8 ± 3.1	227 ± 10	80.5	0.63						
Bi-1-98	0.0302 ± 0.0007	0.227 ± 0.018	191.6 ± 4.3	208 ± 17	92.2	0.47						

Sandstone of the middle part of the Bira Formation (Bi-2; 33° 38' 55.66" N, 133° 48' 07.93" E)

Bi-2-1	0.3873 ± 0.0065	6.645 ± 0.188	2110.2 ± 35.3	2065 ± 58	102.2	0.36
Bi-2-2	0.0384 ± 0.0007	0.265 ± 0.014	242.8 ± 4.6	238 ± 13	101.9	0.11
Bi-2-3	0.0292 ± 0.0009	0.209 ± 0.026	185.5 ± 5.6	193 ± 24	96.1	1.07
Bi-2-4	0.0211 ± 0.0005	0.155 ± 0.012	134.8 ± 3.0	146 ± 12	92.0	0.79
Bi-2-5	0.0268 ± 0.0006	0.194 ± 0.017	170.4 ± 4.1	180 ± 16	94.4	0.46
Bi-2-6	0.0270 ± 0.0005	0.248 ± 0.014	171.9 ± 3.5	225 ± 12	76.4	0.37
Bi-2-7	0.03079 ± 0.0035	4.733 ± 0.113	1730.4 ± 19.7	1773 ± 42	97.6	0.22
Bi-2-8	0.0373 ± 0.0009	0.262 ± 0.026	235.8 ± 5.4	237 ± 23	99.7	0.80
Bi-2-9	0.0297 ± 0.0005	0.204 ± 0.013	188.8 ± 3.2	189 ± 12	100.2	0.47
Bi-2-10	0.0302 ± 0.0005	0.202 ± 0.014	191.9 ± 3.4	187 ± 13	102.7	0.42
Bi-2-11	0.3425 ± 0.0040	5.372 ± 0.131	1898.8 ± 22.0	1880 ± 46	101.0	0.35
Bi-2-12	0.02834 ± 0.0032	4.472 ± 0.107	1608.4 ± 18.4	1726 ± 41	93.2	0.11
Bi-2-13	0.0265 ± 0.0006	0.216 ± 0.018	168.8 ± 3.6	198 ± 17	85.0	0.75
Bi-2-14	0.0271 ± 0.0004	0.207 ± 0.008	172.3 ± 2.2	191 ± 7	90.1	0.33
Bi-2-15	0.1513 ± 0.0017	2.732 ± 0.066	908.2 ± 10.4	1337 ± 32	67.9	0.10
Bi-2-16	0.0346 ± 0.0008	0.260 ± 0.020	219.1 ± 5.0	235 ± 18	93.4	0.56
Bi-2-17	0.3154 ± 0.0055	4.963 ± 0.142	1767.2 ± 30.7	1813 ± 52	97.5	0.75
Bi-2-18	0.0309 ± 0.0010	0.221 ± 0.029	196.2 ± 6.2	203 ± 27	96.6	0.39
Bi-2-19	0.0250 ± 0.0006	0.164 ± 0.015	159.5 ± 3.9	155 ± 15	103.2	0.90

TABLE 1. (Continued)

Grain	$^{206}\text{Pb}/^{238}\text{U}$	$^{207}\text{Pb}/^{235}\text{U}$	$^{206}\text{Pb}/^{238}\text{U}$ age (Ma)	$^{207}\text{Pb}/^{235}\text{U}$ age (Ma)	%conc	Th/U	Grain	$^{206}\text{Pb}/^{238}\text{U}$	$^{207}\text{Pb}/^{235}\text{U}$	$^{206}\text{Pb}/^{238}\text{U}$ age (Ma)	$^{207}\text{Pb}/^{235}\text{U}$ age (Ma)	%conc	Th/U
Bi-2-20	0.3020 ± 0.0051	4.687 ± 0.115	1701.0 ± 28.5	1765 ± 43	96.4	0.74	Bi-2-71	0.0243 ± 0.0010	0.163 ± 0.014	155.0 ± 6.4	153 ± 13	101.0	0.70
Bi-2-21	0.2818 ± 0.0047	4.367 ± 0.105	1600.6 ± 26.7	1706 ± 41	93.8	0.21	Bi-2-72	0.0215 ± 0.0009	0.159 ± 0.015	137.3 ± 5.8	150 ± 14	91.8	0.67
Bi-2-22	0.0300 ± 0.0008	0.231 ± 0.021	190.9 ± 4.8	211 ± 19	90.5	0.69	Bi-2-73	0.0271 ± 0.0011	0.181 ± 0.021	172.7 ± 6.8	169 ± 19	102.0	0.45
Bi-2-23	0.0304 ± 0.0007	0.204 ± 0.016	192.8 ± 4.3	189 ± 15	102.1	1.16	Bi-2-74	0.0272 ± 0.0009	0.193 ± 0.011	173.0 ± 5.8	179 ± 10	96.5	0.35
Bi-2-24	0.0306 ± 0.0007	0.195 ± 0.017	194.3 ± 4.6	181 ± 16	107.6	0.56	Bi-2-75	0.0274 ± 0.0010	0.189 ± 0.014	174.4 ± 6.1	176 ± 13	99.3	0.41
Bi-2-25	0.0230 ± 0.0005	0.175 ± 0.014	146.9 ± 3.5	164 ± 13	89.8	0.97	Bi-2-76	0.0212 ± 0.0007	0.131 ± 0.009	135.1 ± 4.7	125 ± 9	108.0	0.52
Bi-2-26	0.1873 ± 0.0032	2.902 ± 0.085	1107.0 ± 19.1	1382 ± 41	80.1	0.31	Bi-2-77	0.04076 ± 0.0134	7.802 ± 0.318	2203.8 ± 72.6	2208 ± 90	99.8	0.49
Bi-2-27	0.0299 ± 0.0007	0.381 ± 0.022	189.9 ± 4.1	328 ± 19	57.9	0.58	Bi-2-78	0.0275 ± 0.0009	0.199 ± 0.013	174.7 ± 6.0	184 ± 12	94.9	0.42
Bi-2-28	0.3355 ± 0.0055	5.256 ± 0.127	1864.9 ± 30.7	1857 ± 45	100.4	0.12	Bi-2-79	0.0308 ± 0.0011	0.257 ± 0.023	195.3 ± 7.3	232 ± 20	84.2	0.96
Bi-2-29	0.0384 ± 0.0008	0.266 ± 0.019	242.9 ± 5.3	239 ± 17	101.5	0.67	Bi-2-80	0.0275 ± 0.0010	0.181 ± 0.013	175.2 ± 6.1	169 ± 12	103.5	0.53
Bi-2-30	0.0309 ± 0.0007	0.221 ± 0.015	196.1 ± 4.2	203 ± 14	96.7	0.24	Bi-2-81	0.0276 ± 0.0010	0.190 ± 0.019	172.9 ± 6.5	177 ± 18	97.9	0.12
Bi-2-31	0.0489 ± 0.0019	0.346 ± 0.061	308.0 ± 11.9	302 ± 53	102.0	0.53	Bi-2-82	0.0394 ± 0.0014	0.288 ± 0.026	249.3 ± 8.9	257 ± 23	97.1	0.65
Bi-2-32	0.3479 ± 0.0061	5.425 ± 0.171	1924.7 ± 33.9	1889 ± 60	101.9	0.41	Bi-2-83	0.0273 ± 0.0009	0.356 ± 0.017	173.4 ± 5.5	309 ± 15	56.1	0.37
Bi-2-33	0.0282 ± 0.0007	0.203 ± 0.012	179.3 ± 4.6	188 ± 11	95.4	0.45	Bi-2-84	0.0274 ± 0.0009	0.193 ± 0.013	174.3 ± 5.8	179 ± 12	97.3	0.43
Bi-2-34	0.3596 ± 0.0088	5.560 ± 0.212	1980.4 ± 48.3	1910 ± 73	103.7	0.42	Bi-2-85	0.0279 ± 0.0009	0.212 ± 0.012	177.5 ± 5.7	195 ± 11	90.9	0.76
Bi-2-35	0.0285 ± 0.0007	0.193 ± 0.012	181.3 ± 4.7	179 ± 11	101.2	0.37	Bi-2-86	0.0338 ± 0.0107	5.227 ± 0.247	1856.9 ± 59.8	1857 ± 88	100.0	0.79
Bi-2-36	0.0504 ± 0.0019	0.381 ± 0.052	316.8 ± 11.9	328 ± 45	96.7	0.80	Bi-2-87	0.0381 ± 0.0013	0.364 ± 0.024	241.0 ± 8.1	315 ± 21	76.3	0.48
Bi-2-37	0.4079 ± 0.0095	8.678 ± 0.268	2205.2 ± 51.6	2305 ± 71	95.7	0.50	Bi-2-88	0.0294 ± 0.0010	0.205 ± 0.016	187.1 ± 6.3	190 ± 14	98.6	0.13
Bi-2-38	0.0322 ± 0.0009	0.284 ± 0.021	204.3 ± 5.8	254 ± 19	80.5	0.66	Bi-2-89	0.0279 ± 0.0009	0.199 ± 0.012	177.3 ± 5.8	185 ± 11	96.1	0.33
Bi-2-39	0.4530 ± 0.0109	9.845 ± 0.336	2408.6 ± 57.8	2420 ± 83	99.5	0.52	Bi-2-90	0.0329 ± 0.0014	0.263 ± 0.029	208.4 ± 8.8	237 ± 26	88.0	0.75
Bi-2-40	0.3437 ± 0.0081	5.367 ± 0.174	1904.2 ± 44.9	1880 ± 61	101.3	0.29	Bi-2-91	0.0272 ± 0.0010	0.191 ± 0.013	172.8 ± 6.4	177 ± 12	97.6	0.59
Bi-2-41	0.3268 ± 0.0078	5.163 ± 0.174	1822.6 ± 43.3	1846 ± 62	98.7	0.23	Bi-2-92	0.2588 ± 0.0092	4.131 ± 0.180	1483.8 ± 52.8	1660 ± 72	89.4	0.31
Bi-2-42	0.3579 ± 0.0059	5.660 ± 0.177	1972.0 ± 32.4	1925 ± 60	102.4	0.10	Bi-2-93	0.0350 ± 0.0013	0.247 ± 0.018	222.1 ± 8.3	224 ± 16	99.1	0.60
Bi-2-43	0.2143 ± 0.0036	3.250 ± 0.108	1251.6 ± 21.0	1469 ± 49	85.2	0.13	Bi-2-94	0.0259 ± 0.0010	0.176 ± 0.013	164.7 ± 6.2	164 ± 12	100.3	0.39
Bi-2-44	0.0238 ± 0.0005	0.154 ± 0.010	151.6 ± 3.0	146 ± 9	104.0	0.33	Bi-2-95	0.0282 ± 0.0010	0.198 ± 0.013	179.5 ± 6.6	184 ± 12	97.6	0.30
Bi-2-45	0.4489 ± 0.0074	9.610 ± 0.300	2390.2 ± 39.5	2398 ± 75	99.7	0.24	Bi-2-96	0.0268 ± 0.0008	0.189 ± 0.013	170.8 ± 5.3	176 ± 12	97.0	0.71
Bi-2-46	0.3456 ± 0.0057	5.421 ± 0.173	1913.6 ± 31.7	1888 ± 60	101.3	0.54	Bi-2-97	0.0201 ± 0.0007	0.149 ± 0.018	128.1 ± 4.7	141 ± 17	91.1	1.12
Bi-2-47	0.0291 ± 0.0006	0.224 ± 0.013	185.2 ± 3.7	205 ± 12	90.2	0.37	Bi-2-98	0.0403 ± 0.0012	0.277 ± 0.015	254.9 ± 7.5	248 ± 14	102.6	0.12
Bi-2-48	0.3198 ± 0.0053	5.010 ± 0.158	1789.0 ± 29.5	1821 ± 57	98.2	0.12	Bi-2-99	0.4818 ± 0.0137	13.250 ± 0.488	2535.3 ± 72.2	2698 ± 99	94.0	0.36
Bi-2-49	0.0285 ± 0.0007	0.194 ± 0.016	181.3 ± 4.2	180 ± 15	100.7	0.45	Bi-2-100	0.0350 ± 0.0011	0.234 ± 0.015	221.7 ± 6.7	213 ± 14	103.9	0.34
Bi-2-50	0.0212 ± 0.0005	0.159 ± 0.014	135.5 ± 3.4	150 ± 14	90.2	0.65	Bi-2-101	0.0256 ± 0.0008	0.167 ± 0.011	163.1 ± 4.9	156 ± 10	104.2	0.40
Bi-2-51	0.0287 ± 0.0010	0.211 ± 0.019	182.2 ± 6.5	194 ± 18	93.7	0.45	Bi-2-102	0.0271 ± 0.0008	0.200 ± 0.015	172.1 ± 5.4	185 ± 14	92.9	0.31
Bi-2-52	0.1944 ± 0.0062	2.915 ± 0.136	1145.0 ± 36.4	1386 ± 65	82.6	0.57	Bi-2-103	0.03277 ± 0.0093	5.170 ± 0.188	1827.3 ± 51.6	1848 ± 67	98.9	0.23
Bi-2-53	0.2714 ± 0.0085	4.238 ± 0.181	1548.1 ± 48.5	1681 ± 72	92.1	0.48	Bi-2-104	0.0258 ± 0.0008	0.178 ± 0.010	164.0 ± 4.8	166 ± 9	98.6	0.59
Bi-2-54	0.2984 ± 0.0093	4.684 ± 0.191	1683.2 ± 52.3	1764 ± 72	95.4	0.12	Bi-2-105	0.0220 ± 0.0008	0.155 ± 0.016	140.0 ± 5.2	147 ± 15	95.5	0.38
Bi-2-55	0.0460 ± 0.0018	0.346 ± 0.043	289.8 ± 11.5	302 ± 37	96.1	0.56	Bi-2-106	0.0273 ± 0.0010	0.204 ± 0.021	173.8 ± 6.5	189 ± 19	92.1	0.51
Bi-2-56	0.0296 ± 0.0010	0.199 ± 0.012	188.2 ± 6.1	184 ± 12	102.2	0.24	Bi-2-107	0.0215 ± 0.0008	0.240 ± 0.017	137.2 ± 4.8	219 ± 15	62.7	0.99
Bi-2-57	0.1748 ± 0.0057	2.492 ± 0.130	1038.5 ± 33.8	1270 ± 66	81.8	0.38	Bi-2-108	0.0272 ± 0.0009	0.173 ± 0.014	172.8 ± 6.0	162 ± 13	106.8	0.45
Bi-2-58	0.0286 ± 0.0013	0.189 ± 0.017	181.6 ± 4.2	176 ± 16	103.3	0.42	Bi-2-109	0.0219 ± 0.0008	0.139 ± 0.015	139.4 ± 5.2	132 ± 14	105.2	0.47
Bi-2-59	0.4931 ± 0.0208	11.868 ± 0.576	2584.3 ± 109.2	2594 ± 126	99.6	0.53	Bi-2-110	0.0216 ± 0.0008	0.136 ± 0.017	137.5 ± 5.3	130 ± 16	106.1	0.59
Bi-2-60	0.2436 ± 0.0103	3.724 ± 0.189	1405.5 ± 59.7	1577 ± 80	89.2	0.22	Bi-2-111	0.0253 ± 0.0007	0.197 ± 0.011	161.0 ± 4.7	182 ± 10	88.3	0.28
Bi-2-61	0.2503 ± 0.0106	3.851 ± 0.194	1440.1 ± 61.1	1603 ± 81	89.8	0.63	Bi-2-112	0.0228 ± 0.0009	0.158 ± 0.022	145.2 ± 5.8	149 ± 21	97.5	0.61
Bi-2-62	0.3067 ± 0.0130	4.786 ± 0.235	1724.3 ± 72.9	1782 ± 88	96.7	0.43	Bi-2-113	0.0368 ± 0.0092	6.849 ± 0.206	1871.3 ± 51.1	2092 ± 63	89.4	0.32
Bi-2-63	0.0290 ± 0.0013	0.204 ± 0.014	184.3 ± 8.0	188 ± 13	97.9	0.65	Bi-2-114	0.0396 ± 0.0012	0.274 ± 0.020	250.4 ± 7.7	245 ± 18	102.0	1.07
Bi-2-64	0.0340 ± 0.0015	0.235 ± 0.021	215.7 ± 9.7	214 ± 19	100.7	0.61	Bi-2-115	0.03463 ± 0.0096	5.482 ± 0.184	1916.7 ± 53.1	1898 ± 64	101.0	0.22
Bi-2-65	0.0299 ± 0.0013	0.215 ± 0.013	190.0 ± 8.1	198 ± 12	96.0	0.21	Bi-2-116	0.0278 ± 0.0008	0.196 ± 0.013	177.0 ± 5.4	182 ± 12	97.3	0.47
Bi-2-66	0.0217 ± 0.0009	0.150 ± 0.012	138.5 ± 5.7	142 ± 11	97.6	0.36	Bi-2-117	0.0290 ± 0.0009	0.216 ± 0.017	184.3 ± 5.8	199 ± 15	92.8	0.51
Bi-2-67	0.0274 ± 0.0011	0.187 ± 0.017	174.0 ± 7.3	174 ± 16	100.2	0.34	Bi-2-118	0.02637 ± 0.0074	3.939 ± 0.143	1508.7 ± 42.2	1622 ± 59	93.0	0.31
Bi-2-68	0.3358 ± 0.0130	5.337 ± 0.245	1866.5 ± 72.4	1875 ± 86	99.6	0.12	Bi-2-119	0.4978 ± 0.0085	12.241 ± 0.407	2604.5 ± 44.3	2623 ± 87	99.3	0.54
Bi-2-69	0.0264 ± 0.0011	0.177 ± 0.011	168.2 ± 6.7	166 ± 11	101.5	0.17	Bi-2-120	0.2562 ± 0.0044	4.019 ± 0.140	1470.2 ± 25.1	1638 ± 57	89.8	0.31
Bi-2-70	0.0277 ± 0.0013	0.180 ± 0.022	176.1 ± 8.0	168 ± 20	104.7	0.63	Bi-2-121	0.0288 ± 0.0007	0.212 ± 0.020	183.2 ± 4.6	195 ± 18	93.8	0.36

TABLE 1. (Continued)

Grain	$^{206}\text{Pb}/^{238}\text{U}$	$^{207}\text{Pb}/^{235}\text{U}$	$^{206}\text{Pb}/^{238}\text{U}$ age (Ma)	$^{207}\text{Pb}/^{235}\text{U}$ age (Ma)	Th/U	%conc	Grain	$^{206}\text{Pb}/^{238}\text{U}$	$^{207}\text{Pb}/^{235}\text{U}$	$^{206}\text{Pb}/^{238}\text{U}$ age (Ma)	$^{207}\text{Pb}/^{235}\text{U}$ age (Ma)	Th/U
Bi-2-122	0.3249 ± 0.0054	5.145 ± 0.169	1813.4 ± 30.2	1843 ± 61	98.4	102.3	Fu-1-45	0.0442 ± 0.0024	0.309 ± 0.052	279.0 ± 15.0	273 ± 46	102.1
Bi-2-123	0.0265 ± 0.0006	0.177 ± 0.014	168.9 ± 3.7	166 ± 13	101.9	91.0	Fu-1-46	0.0266 ± 0.0012	0.201 ± 0.016	169.4 ± 7.4	186 ± 15	91.0
Bi-2-124	0.3330 ± 0.0060	5.112 ± 0.201	1852.7 ± 33.2	1838 ± 72	100.8	99.5	Fu-1-47	0.0450 ± 0.0022	0.314 ± 0.039	283.7 ± 13.6	277 ± 35	102.3
Bi-2-125	0.1280 ± 0.0022	1.871 ± 0.070	776.4 ± 13.5	1071 ± 40	72.5	95.1	Fu-1-48	0.0257 ± 0.0011	0.185 ± 0.016	163.5 ± 7.2	172 ± 15	95.1
Bi-2-126	0.0279 ± 0.0006	0.201 ± 0.014	177.3 ± 3.8	186 ± 13	95.2	95.0	Fu-1-49	0.3799 ± 0.0161	7.607 ± 0.461	2076.0 ± 87.7	2186 ± 132	95.0
Sandstone of the Funadani Formation (Fu-1; 33° 37' 22.79" N, 133° 41' 59.69" E)												
Fu-1-1	0.3569 ± 0.0103	5.647 ± 0.238	1967.5 ± 37.0	1923 ± 81	102.3	0.17	Fu-1-50	0.0211 ± 0.0010	0.161 ± 0.018	134.8 ± 6.3	151 ± 17	89.2
Fu-1-2	0.0400 ± 0.0012	0.277 ± 0.019	252.7 ± 7.9	248 ± 17	101.9	0.65	Fu-1-51	0.0397 ± 0.0017	0.284 ± 0.024	251.1 ± 11.0	253 ± 22	99.1
Fu-1-3	0.0628 ± 0.0021	0.424 ± 0.036	392.6 ± 12.8	359 ± 30	109.3	0.54	Fu-1-52	0.0401 ± 0.0008	0.299 ± 0.020	253.3 ± 4.9	266 ± 18	95.4
Fu-1-4	0.0266 ± 0.0008	0.193 ± 0.014	169.0 ± 5.3	179 ± 13	94.5	0.29	Fu-1-53	0.3369 ± 0.0047	5.375 ± 0.149	1871.6 ± 26.2	1881 ± 52	99.5
Fu-1-5	0.0433 ± 0.0015	0.334 ± 0.032	273.2 ± 9.5	293 ± 28	93.4	0.61	Fu-1-54	0.0261 ± 0.0005	0.196 ± 0.014	166.3 ± 3.3	182 ± 13	91.3
Fu-1-6	0.0467 ± 0.0020	0.362 ± 0.045	294.1 ± 12.7	2757 ± 175	10.7	0.53	Fu-1-55	0.0225 ± 0.0005	0.165 ± 0.014	143.4 ± 3.2	155 ± 14	92.5
Fu-1-7	0.0442 ± 0.0018	0.362 ± 0.045	279.1 ± 11.2	314 ± 39	88.9	0.56	Fu-1-56	0.0403 ± 0.0007	0.290 ± 0.015	255.0 ± 4.2	258 ± 13	98.7
Fu-1-8	0.3111 ± 0.0091	4.905 ± 0.167	1746.1 ± 30.8	1803 ± 61	96.8	0.53	Fu-1-57	0.0340 ± 0.0010	0.261 ± 0.028	215.6 ± 5.8	235 ± 25	91.7
Fu-1-9	0.0461 ± 0.0018	0.337 ± 0.036	290.3 ± 11.5	295 ± 32	98.4	0.53	Fu-1-58	0.0380 ± 0.0010	0.308 ± 0.031	240.6 ± 6.3	273 ± 28	88.2
Fu-1-10	0.0435 ± 0.0015	0.296 ± 0.018	274.5 ± 9.3	264 ± 16	104.1	0.43	Fu-1-59	0.0293 ± 0.0005	0.216 ± 0.013	186.3 ± 3.3	199 ± 12	93.7
Fu-1-11	0.0423 ± 0.0016	0.296 ± 0.027	266.8 ± 9.9	264 ± 24	101.2	0.97	Fu-1-60	0.3041 ± 0.0044	4.818 ± 0.147	1711.4 ± 24.9	1788 ± 55	95.7
Fu-1-12	0.0315 ± 0.0011	0.214 ± 0.018	200.2 ± 7.3	197 ± 17	101.8	0.47	Fu-1-61	0.0466 ± 0.0020	0.419 ± 0.050	293.4 ± 72.8	355 ± 43	82.6
Fu-1-13	0.0463 ± 0.0017	0.327 ± 0.028	292.0 ± 10.7	287 ± 25	101.8	0.18	Fu-1-62	0.0388 ± 0.0014	0.679 ± 0.036	368.3 ± 8.8	526 ± 28	70.0
Fu-1-14	0.0749 ± 0.0026	0.531 ± 0.039	465.8 ± 16.5	433 ± 32	107.7	0.45	Fu-1-63	0.0440 ± 0.0014	0.366 ± 0.035	277.8 ± 9.1	317 ± 30	87.8
Fu-1-15	0.0325 ± 0.0012	0.218 ± 0.017	206.5 ± 7.4	200 ± 16	103.3	0.35	Fu-1-64	0.0440 ± 0.0015	0.344 ± 0.035	277.5 ± 9.5	300 ± 30	92.4
Fu-1-16	0.0459 ± 0.0017	0.307 ± 0.030	289.3 ± 10.6	272 ± 26	106.6	0.36	Fu-1-65	0.4564 ± 0.0104	10.005 ± 0.427	2423.6 ± 55.0	2435 ± 104	99.5
Fu-1-17	0.3978 ± 0.0196	7.602 ± 0.399	2158.9 ± 106.6	2185 ± 115	98.8	0.37	Fu-1-66	0.0473 ± 0.0019	0.394 ± 0.046	297.9 ± 12.0	337 ± 39	88.3
Fu-1-18	0.0528 ± 0.0026	0.406 ± 0.027	331.7 ± 16.6	346 ± 23	95.9	0.13	Fu-1-67	0.0432 ± 0.0013	0.341 ± 0.030	272.6 ± 8.3	298 ± 26	91.5
Fu-1-19	0.3391 ± 0.0168	5.278 ± 0.281	1882.6 ± 93.0	1865 ± 99	100.9	0.40	Fu-1-68	0.0480 ± 0.0035	0.342 ± 0.067	302.1 ± 21.9	299 ± 58	101.1
Fu-1-20	0.1455 ± 0.0076	0.435 ± 0.061	875.9 ± 46.0	367 ± 51	238.7	0.71	Fu-1-69	0.0322 ± 0.0010	0.234 ± 0.023	204.2 ± 6.7	213 ± 21	95.8
Fu-1-21	0.0427 ± 0.0023	0.347 ± 0.035	269.3 ± 14.3	303 ± 37	89.0	0.54	Fu-1-70	0.0491 ± 0.0017	0.364 ± 0.054	309.2 ± 10.4	315 ± 46	98.2
Fu-1-22	0.0419 ± 0.0023	0.313 ± 0.038	264.8 ± 14.5	276 ± 34	95.9	0.55	Fu-1-71	0.0295 ± 0.0006	0.212 ± 0.016	187.5 ± 3.7	196 ± 15	95.8
Fu-1-23	0.0567 ± 0.0033	0.454 ± 0.069	355.8 ± 20.8	380 ± 58	93.7	0.71	Fu-1-72	0.3447 ± 0.0049	5.457 ± 0.188	1909.4 ± 26.9	1894 ± 65	100.8
Fu-1-24	0.0455 ± 0.0024	0.315 ± 0.029	286.6 ± 14.8	278 ± 25	102.9	0.23	Fu-1-73	0.0480 ± 0.0021	0.387 ± 0.076	302.4 ± 13.5	332 ± 65	91.1
Fu-1-25	0.0279 ± 0.0015	0.193 ± 0.022	177.2 ± 9.5	179 ± 20	99.1	0.66	Fu-1-74	0.0398 ± 0.0009	0.310 ± 0.027	251.8 ± 5.7	275 ± 24	91.7
Fu-1-26	0.0338 ± 0.0008	0.249 ± 0.013	214.4 ± 5.2	225 ± 12	95.1	0.18	Fu-1-75	0.0373 ± 0.0012	0.267 ± 0.025	236.3 ± 7.7	241 ± 23	98.2
Fu-1-27	0.0481 ± 0.0015	0.297 ± 0.032	303.0 ± 9.3	264 ± 29	114.6	0.45	Fu-1-76	0.0426 ± 0.0015	0.287 ± 0.032	268.9 ± 9.3	256 ± 29	105.1
Fu-1-28	0.0409 ± 0.0012	0.341 ± 0.032	258.6 ± 7.8	298 ± 28	86.9	0.70	Fu-1-77	0.0426 ± 0.0016	0.300 ± 0.036	268.6 ± 9.8	266 ± 32	101.0
Fu-1-29	0.2757 ± 0.0064	4.417 ± 0.173	1569.5 ± 36.6	1715 ± 67	91.5	0.32	Fu-1-78	0.0459 ± 0.0013	0.329 ± 0.020	289.3 ± 8.3	289 ± 18	100.2
Fu-1-30	0.0466 ± 0.0013	0.365 ± 0.029	293.6 ± 8.1	316 ± 25	92.9	0.62	Fu-1-79	0.0424 ± 0.0012	0.320 ± 0.017	267.5 ± 7.5	282 ± 15	94.9
Fu-1-31	0.0462 ± 0.0018	0.321 ± 0.051	291.2 ± 11.5	283 ± 45	103.0	0.42	Fu-1-80	0.3949 ± 0.0106	6.666 ± 0.239	2145.5 ± 57.5	2068 ± 74	103.7
Fu-1-32	0.3324 ± 0.0076	5.766 ± 0.209	1850.1 ± 42.2	1941 ± 70	95.3	0.10	Fu-1-81	0.0477 ± 0.0015	0.398 ± 0.034	300.4 ± 9.7	340 ± 29	88.3
Fu-1-33	0.0496 ± 0.0017	0.425 ± 0.049	312.2 ± 10.7	360 ± 42	86.8	0.69	Fu-1-82	0.0699 ± 0.0019	0.575 ± 0.029	435.4 ± 12.1	461 ± 23	94.4
Fu-1-34	0.0676 ± 0.0021	0.571 ± 0.056	421.7 ± 13.1	458 ± 45	92.0	0.57	Fu-1-83	0.0471 ± 0.0014	0.435 ± 0.051	297.0 ± 8.9	367 ± 43	81.0
Fu-1-35	0.0499 ± 0.0018	0.379 ± 0.046	313.6 ± 11.2	326 ± 40	96.2	0.48	Fu-1-84	0.0403 ± 0.0010	0.311 ± 0.031	255.0 ± 6.2	275 ± 27	92.8
Fu-1-36	0.0663 ± 0.0026	0.679 ± 0.087	414.0 ± 16.4	526 ± 67	78.7	0.45	Fu-1-85	0.3196 ± 0.0049	5.067 ± 0.251	1788.0 ± 27.6	1831 ± 91	97.7
Fu-1-37	0.0304 ± 0.0016	0.462 ± 0.076	192.8 ± 10.3	386 ± 64	50.0	0.61	Fu-1-86	0.0346 ± 0.0006	0.241 ± 0.016	219.1 ± 3.7	219 ± 14	99.8
Fu-1-38	0.0229 ± 0.0007	0.151 ± 0.014	146.3 ± 4.5	143 ± 13	102.5	0.52	Fu-1-87	0.0418 ± 0.0011	0.296 ± 0.029	264.3 ± 6.7	263 ± 26	100.5
Fu-1-39	0.0457 ± 0.0019	0.315 ± 0.051	288.1 ± 11.9	278 ± 45	103.7	0.54	Fu-1-88	0.3288 ± 0.0050	5.373 ± 0.135	1832.4 ± 28.1	1881 ± 47	97.4
Fu-1-40	0.3435 ± 0.0088	5.517 ± 0.225	1903.4 ± 48.6	1903 ± 78	100.0	0.34	Fu-1-89	0.3384 ± 0.0084	5.529 ± 0.193	1879.0 ± 46.4	1905 ± 67	98.6
Fu-1-41	0.0412 ± 0.0014	0.329 ± 0.036	260.2 ± 8.9	289 ± 32	90.1	1.04	Fu-1-90	0.3597 ± 0.0088	5.860 ± 0.200	1980.7 ± 48.6	1955 ± 67	101.3
Fu-1-42	0.0367 ± 0.0012	0.262 ± 0.029	232.6 ± 7.7	236 ± 26	98.6	1.14	Fu-1-91	0.0601 ± 0.0020	0.546 ± 0.056	376.3 ± 12.7	442 ± 46	85.0
Fu-1-43	0.0396 ± 0.0012	0.276 ± 0.026	250.5 ± 7.7	248 ± 23	101.1	0.87	Fu-1-92	0.0449 ± 0.0011	0.342 ± 0.029	283.1 ± 8.4	299 ± 26	94.7
Fu-1-44	0.0425 ± 0.0019	0.285 ± 0.027	268.0 ± 12.0	254 ± 25	105.4	0.88	Fu-1-93	0.0419 ± 0.0011	0.335 ± 0.018	264.6 ± 6.8	293 ± 16	90.2
							Fu-1-94	0.0431 ± 0.0014	0.337 ± 0.035	272.2 ± 8.8	295 ± 30	92.3
							Fu-1-95	0.0277 ± 0.0008	0.200 ± 0.015	176.1 ± 4.9	185 ± 14	95.0

TABLE 1. (Continued)

Grain	$^{206}\text{Pb}/^{238}\text{U}$	$^{207}\text{Pb}/^{235}\text{U}$	$^{206}\text{Pb}/^{238}\text{U}$ age (Ma)	$^{207}\text{Pb}/^{235}\text{U}$ age (Ma)	%conc	Th/U	Grain	$^{206}\text{Pb}/^{238}\text{U}$	$^{207}\text{Pb}/^{235}\text{U}$	$^{206}\text{Pb}/^{238}\text{U}$ age (Ma)	$^{207}\text{Pb}/^{235}\text{U}$ age (Ma)	%conc	Th/U
Fu-1-96	0.0466 ± 0.0014	0.402 ± 0.032	293.8 ± 8.7	343 ± 38	83.7	0.63	Ha-1-22	0.2663 ± 0.0041	4.165 ± 0.147	1521.9 ± 23.6	1667 ± 59	91.3	0.54
Fu-1-97	0.0324 ± 0.0010	0.216 ± 0.016	205.7 ± 6.2	198 ± 15	103.8	0.51	Ha-1-23	0.0339 ± 0.0006	0.471 ± 0.019	215.1 ± 3.6	350 ± 16	61.5	0.41
Fu-1-98	0.0486 ± 0.0018	0.309 ± 0.042	306.0 ± 11.6	273 ± 38	112.0	0.55	Ha-1-24	0.2998 ± 0.0062	4.656 ± 0.142	1690.2 ± 35.2	1759 ± 54	96.1	0.31
Fu-1-99	0.0347 ± 0.0012	0.240 ± 0.023	220.1 ± 7.3	218 ± 21	100.9	0.40	Ha-1-25	0.0279 ± 0.0006	0.232 ± 0.012	177.5 ± 4.0	212 ± 11	83.7	0.41
Fu-1-100	0.3289 ± 0.0088	5.078 ± 0.150	1833.0 ± 49.2	1832 ± 54	100.0	0.10	Ha-1-26	0.0401 ± 0.0009	0.287 ± 0.012	253.1 ± 5.5	256 ± 11	98.8	0.49
Fu-1-101	0.0428 ± 0.0013	0.302 ± 0.024	270.5 ± 8.4	268 ± 21	101.0	0.71	Ha-1-27	0.0239 ± 0.0006	0.163 ± 0.013	152.5 ± 3.9	153 ± 12	99.4	0.68
Fu-1-102	0.0491 ± 0.0021	0.425 ± 0.063	308.9 ± 13.2	360 ± 55	85.9	0.33	Ha-1-28	0.0296 ± 0.0009	0.352 ± 0.028	188.3 ± 5.4	306 ± 25	61.5	0.76
Fu-1-103	0.4067 ± 0.0110	7.797 ± 0.233	2199.9 ± 59.3	2208 ± 66	99.6	0.70	Ha-1-29	0.0358 ± 0.0008	0.253 ± 0.012	226.5 ± 5.0	229 ± 11	98.8	0.42
Fu-1-104	0.0477 ± 0.0020	0.384 ± 0.055	300.1 ± 12.3	330 ± 48	91.0	0.59	Ha-1-30	0.0253 ± 0.0006	0.198 ± 0.012	161.3 ± 3.8	183 ± 11	88.0	0.97
Fu-1-105	0.3555 ± 0.0097	5.468 ± 0.188	1960.9 ± 53.8	1896 ± 65	103.4	0.21	Ha-1-31	0.3359 ± 0.0071	5.420 ± 0.179	1866.8 ± 59.6	1888 ± 62	98.9	0.34
Fu-1-106	0.0462 ± 0.0016	0.329 ± 0.052	291.3 ± 10.2	289 ± 45	100.8	0.66	Ha-1-32	0.0303 ± 0.0007	0.286 ± 0.017	192.2 ± 4.7	255 ± 15	75.4	0.81
Fu-1-107	0.0429 ± 0.0011	0.317 ± 0.035	270.8 ± 7.0	279 ± 31	96.9	0.87	Ha-1-33	0.0397 ± 0.0009	0.296 ± 0.018	250.9 ± 5.9	263 ± 16	95.4	0.81
Fu-1-108	0.0307 ± 0.0005	0.221 ± 0.013	195.1 ± 3.1	203 ± 12	96.3	0.26	Ha-1-34	0.0396 ± 0.0009	0.293 ± 0.012	250.2 ± 5.4	261 ± 11	96.0	0.38
Fu-1-109	0.3308 ± 0.0044	5.324 ± 0.176	1842.0 ± 24.8	1873 ± 62	98.4	0.37	Ha-1-35	0.0298 ± 0.0007	0.226 ± 0.016	189.0 ± 4.7	207 ± 15	91.4	0.55
Fu-1-110	0.0458 ± 0.0010	0.389 ± 0.084	288.5 ± 6.6	334 ± 29	86.5	0.66	Ha-1-36	0.0208 ± 0.0005	0.198 ± 0.014	132.6 ± 3.5	183 ± 13	72.4	0.58
Fu-1-111	0.0549 ± 0.0019	0.476 ± 0.068	344.3 ± 12.0	396 ± 57	87.0	0.64	Ha-1-37	0.0267 ± 0.0006	0.199 ± 0.012	170.0 ± 4.0	184 ± 11	92.3	0.67
Fu-1-112	0.4100 ± 0.0052	6.503 ± 0.196	2215.0 ± 38.2	2046 ± 62	108.2	0.44	Ha-1-38	0.0339 ± 0.0007	0.432 ± 0.017	214.7 ± 4.7	365 ± 14	58.9	0.36
Fu-1-113	0.0332 ± 0.0006	0.249 ± 0.016	210.4 ± 3.6	226 ± 14	93.3	0.48	Ha-1-39	0.0471 ± 0.0011	0.361 ± 0.019	296.6 ± 6.8	313 ± 17	94.7	0.57
Fu-1-114	0.0470 ± 0.0007	0.324 ± 0.015	296.0 ± 4.1	285 ± 13	104.0	0.25	Ha-1-40	0.0280 ± 0.0007	0.201 ± 0.014	178.3 ± 4.4	186 ± 13	95.7	0.40
Fu-1-115	0.0396 ± 0.0010	0.281 ± 0.024	250.3 ± 6.3	252 ± 22	99.5	1.09	Ha-1-41	0.0298 ± 0.0006	0.205 ± 0.009	189.0 ± 4.0	189 ± 8	99.9	0.55
Fu-1-116	0.0405 ± 0.0011	0.305 ± 0.031	255.6 ± 7.1	270 ± 27	94.6	0.88	Ha-1-42	0.0285 ± 0.0006	0.365 ± 0.019	181.4 ± 3.9	316 ± 16	57.4	0.76
Fu-1-117	0.0422 ± 0.0009	0.311 ± 0.029	266.4 ± 5.9	419 ± 24	63.6	0.62	Ha-1-43	0.0126 ± 0.0070	9.458 ± 0.206	2226.9 ± 37.7	2383 ± 52	93.4	0.36
Fu-1-118	0.0439 ± 0.0017	0.296 ± 0.050	276.8 ± 10.7	264 ± 44	105.0	0.68	Ha-1-44	0.0280 ± 0.0005	0.260 ± 0.010	178.1 ± 3.3	235 ± 9	75.9	0.43
Fu-1-119	0.0377 ± 0.0010	0.268 ± 0.024	238.7 ± 6.1	241 ± 22	99.2	0.28	Ha-1-45	0.0287 ± 0.0007	0.843 ± 0.043	182.5 ± 4.5	621 ± 32	29.4	1.28
Fu-1-120	0.0338 ± 0.0010	0.257 ± 0.027	214.3 ± 6.2	232 ± 25	92.2	0.55	Ha-1-46	0.3243 ± 0.0055	5.166 ± 0.119	1810.5 ± 30.8	1847 ± 43	98.0	0.14
Fu-1-121	0.0438 ± 0.0014	0.280 ± 0.036	276.1 ± 8.5	250 ± 32	110.3	0.64	Ha-1-47	0.0318 ± 0.0006	0.241 ± 0.011	201.8 ± 3.8	219 ± 10	92.1	0.38
Fu-1-122	0.0774 ± 0.0019	0.592 ± 0.049	480.5 ± 11.9	472 ± 39	101.7	0.54	Ha-1-48	0.0440 ± 0.0017	0.492 ± 0.037	277.7 ± 7.0	406 ± 30	68.4	0.83
Fu-1-123	0.0422 ± 0.0015	0.307 ± 0.045	266.5 ± 9.6	272 ± 40	98.0	0.52	Ha-1-49	0.0276 ± 0.0006	0.197 ± 0.010	175.5 ± 3.9	183 ± 9	96.0	0.42
Ha-1-1	0.0232 ± 0.0005	0.154 ± 0.009	148.1 ± 3.5	146 ± 8	101.7	0.56	Ha-1-50	0.3269 ± 0.0066	5.100 ± 0.144	1823.2 ± 37.0	1836 ± 52	99.3	0.20
Ha-1-2	0.2518 ± 0.0054	3.978 ± 0.125	1447.7 ± 31.1	1630 ± 51	88.8	0.17	Ha-1-51	0.0613 ± 0.0016	0.610 ± 0.044	383.5 ± 10.0	484 ± 35	79.3	0.44
Ha-1-3	0.0205 ± 0.0007	0.213 ± 0.021	130.6 ± 4.2	196 ± 19	66.7	1.71	Ha-1-52	0.0336 ± 0.0008	0.289 ± 0.020	213.1 ± 5.3	258 ± 17	82.6	0.66
Ha-1-4	0.0335 ± 0.0010	0.328 ± 0.027	212.5 ± 6.1	288 ± 24	73.7	0.40	Ha-1-53	0.0414 ± 0.0010	0.331 ± 0.019	261.8 ± 6.1	290 ± 17	90.1	0.81
Ha-1-5	0.0344 ± 0.0009	0.282 ± 0.019	218.1 ± 5.5	252 ± 17	86.6	0.76	Ha-1-54	0.4052 ± 0.0082	8.989 ± 0.248	2192.8 ± 44.6	2337 ± 64	93.8	0.91
Ha-1-6	0.0447 ± 0.0016	0.465 ± 0.052	281.9 ± 10.0	388 ± 44	72.7	0.31	Ha-1-55	0.0360 ± 0.0009	0.316 ± 0.019	228.2 ± 5.4	278 ± 17	82.0	0.62
Ha-1-7	0.0206 ± 0.0006	0.220 ± 0.018	131.6 ± 3.9	202 ± 17	63.3	1.39	Ha-1-56	0.0375 ± 0.0011	0.361 ± 0.035	237.3 ± 7.2	313 ± 30	75.8	0.64
Ha-1-8	0.0304 ± 0.0007	0.282 ± 0.015	193.1 ± 4.4	252 ± 14	76.5	0.37	Ha-1-57	0.0376 ± 0.0006	0.274 ± 0.010	238.0 ± 3.8	246 ± 9	96.9	0.40
Ha-1-9	0.0212 ± 0.0006	0.226 ± 0.017	135.3 ± 3.6	207 ± 15	65.5	0.87	Ha-1-58	0.0261 ± 0.0005	0.219 ± 0.011	166.0 ± 3.0	201 ± 10	82.6	0.26
Ha-1-10	0.0292 ± 0.0007	0.272 ± 0.017	185.8 ± 4.4	244 ± 15	76.1	0.66	Ha-1-59	0.2474 ± 0.0040	3.867 ± 0.120	1425.2 ± 22.8	1607 ± 50	88.7	0.51
Ha-1-11	0.0534 ± 0.0016	0.627 ± 0.055	335.3 ± 10.1	494 ± 43	67.9	0.51	Ha-1-60	0.0227 ± 0.0005	0.218 ± 0.016	144.9 ± 3.3	200 ± 15	72.3	0.50
Ha-1-12	0.2897 ± 0.0059	4.587 ± 0.154	1640.1 ± 33.5	1747 ± 59	93.9	0.38	Ha-1-61	0.0192 ± 0.0004	0.165 ± 0.011	122.6 ± 2.5	155 ± 10	79.0	0.79
Ha-1-13	0.0247 ± 0.0005	0.201 ± 0.010	157.2 ± 3.4	186 ± 9	84.4	0.28	Ha-1-62	0.0273 ± 0.0005	0.232 ± 0.013	173.4 ± 3.3	212 ± 12	81.9	0.32
Ha-1-14	0.0391 ± 0.0009	0.332 ± 0.022	247.1 ± 5.9	291 ± 19	84.8	0.53	Ha-1-63	0.0282 ± 0.0005	0.215 ± 0.013	179.3 ± 3.5	198 ± 12	90.7	0.57
Ha-1-15	0.0292 ± 0.0007	0.228 ± 0.015	185.7 ± 4.4	209 ± 14	89.0	0.79	Ha-1-64	0.0430 ± 0.0008	0.355 ± 0.020	271.7 ± 5.1	308 ± 17	88.1	0.24
Ha-1-16	0.0462 ± 0.0012	0.445 ± 0.040	291.2 ± 7.3	374 ± 33	78.0	0.36	Ha-1-65	0.0235 ± 0.0008	0.903 ± 0.071	149.9 ± 5.2	653 ± 51	22.9	1.00
Ha-1-17	0.3097 ± 0.0053	5.454 ± 0.221	1739.4 ± 29.7	1893 ± 77	91.9	0.40	Ha-1-66	0.0332 ± 0.0007	0.257 ± 0.012	210.3 ± 4.7	232 ± 10	90.6	0.53
Ha-1-18	0.0393 ± 0.0010	0.454 ± 0.037	248.4 ± 6.1	380 ± 31	63.4	0.77	Ha-1-67	0.0388 ± 0.0009	0.295 ± 0.014	245.7 ± 5.5	263 ± 12	93.5	0.51
Ha-1-19	0.0250 ± 0.0004	0.181 ± 0.009	159.2 ± 2.5	169 ± 8	94.3	0.52	Ha-1-68	0.0331 ± 0.0007	0.254 ± 0.010	209.8 ± 4.5	230 ± 9	91.2	0.47
Ha-1-20	0.0306 ± 0.0006	0.221 ± 0.015	194.1 ± 3.7	203 ± 14	95.8	0.56	Ha-1-69	0.2941 ± 0.0063	4.667 ± 0.146	1662.1 ± 35.3	1761 ± 55	94.4	0.91
Ha-1-21	0.0291 ± 0.0006	0.210 ± 0.016	185.1 ± 3.8	194 ± 15	95.6	0.44	Ha-1-70	0.0446 ± 0.0010	0.439 ± 0.022	281.2 ± 6.5	369 ± 19	76.1	0.44
							Ha-1-71	0.0346 ± 0.0009	0.327 ± 0.022	219.2 ± 5.6	287 ± 19	76.4	0.65
							Ha-1-72	0.0289 ± 0.0007	0.204 ± 0.016	183.5 ± 4.7	189 ± 14	97.3	1.12

Sandstone of the Hagino Formation from Sano (Ha-1; 33° 37' 16.89" N, 133° 42' 42.87" E)

TABLE 1. (Continued)

Grain	$^{206}\text{Pb}/^{238}\text{U}$	$^{207}\text{Pb}/^{235}\text{U}$	$^{206}\text{Pb}/^{238}\text{U}$ age (Ma)	$^{207}\text{Pb}/^{235}\text{U}$ age (Ma)	$^{207}\text{Pb}/^{235}\text{U}$ age (%conc)	Th/U	Grain	$^{206}\text{Pb}/^{238}\text{U}$	$^{207}\text{Pb}/^{235}\text{U}$	$^{206}\text{Pb}/^{238}\text{U}$ age (Ma)	$^{207}\text{Pb}/^{235}\text{U}$ age (Ma)	$^{207}\text{Pb}/^{235}\text{U}$ age (%conc)	Th/U
<i>Ha-1-73</i>	0.0209 ± 0.0006	0.158 ± 0.016	133.6 ± 4.0	149 ± 13	89.7	1.33	<i>Ha-2-9</i>	0.0298 ± 0.0010	0.204 ± 0.020	189.2 ± 6.1	189 ± 19	100.2	0.45
<i>Ha-1-74</i>	0.2843 ± 0.0060	4.462 ± 0.149	1612.9 ± 34.2	1724 ± 58	93.6	0.31	<i>Ha-2-10</i>	0.0239 ± 0.0009	0.191 ± 0.016	152.1 ± 5.4	177 ± 15	85.9	0.56
<i>Ha-1-75</i>	0.0400 ± 0.0013	0.386 ± 0.039	252.8 ± 8.0	332 ± 34	76.3	0.64	<i>Ha-2-11</i>	0.0282 ± 0.0011	0.515 ± 0.045	179.6 ± 7.2	422 ± 37	42.6	0.53
<i>Ha-1-76</i>	0.0465 ± 0.0014	0.555 ± 0.047	292.8 ± 8.7	449 ± 38	65.3	0.56	<i>Ha-2-12</i>	0.0222 ± 0.0009	0.144 ± 0.020	141.3 ± 5.9	137 ± 19	103.3	0.69
<i>Ha-1-77</i>	0.0253 ± 0.0006	0.217 ± 0.013	161.1 ± 3.8	199 ± 12	80.9	0.83	<i>Ha-2-13</i>	0.0256 ± 0.0009	0.179 ± 0.012	163.2 ± 5.5	167 ± 12	97.7	0.41
<i>Ha-1-78</i>	0.3033 ± 0.0065	4.780 ± 0.165	1707.7 ± 36.5	1781 ± 62	95.9	0.32	<i>Ha-2-14</i>	0.0284 ± 0.0010	0.194 ± 0.018	180.4 ± 6.5	180 ± 16	100.0	0.36
<i>Ha-1-79</i>	0.0404 ± 0.0011	0.376 ± 0.027	255.4 ± 6.7	324 ± 24	78.7	0.59	<i>Ha-2-15</i>	0.0139 ± 0.0136	8.029 ± 0.391	2232.9 ± 73.2	2234 ± 109	99.9	0.11
<i>Ha-1-80</i>	0.0291 ± 0.0009	0.288 ± 0.030	184.6 ± 6.0	257 ± 27	71.8	0.72	<i>Ha-2-16</i>	0.0187 ± 0.0007	0.131 ± 0.013	119.5 ± 4.4	125 ± 12	95.6	0.66
<i>Ha-1-81</i>	0.0359 ± 0.0009	0.343 ± 0.034	227.3 ± 5.9	300 ± 21	75.8	0.84	<i>Ha-2-17</i>	0.0280 ± 0.0011	0.163 ± 0.020	178.1 ± 6.9	154 ± 19	115.8	0.51
<i>Ha-1-82</i>	0.0371 ± 0.0011	0.312 ± 0.030	234.9 ± 6.8	276 ± 27	83.2	0.90	<i>Ha-2-18</i>	0.0265 ± 0.0010	0.172 ± 0.016	168.9 ± 6.1	161 ± 15	104.8	0.53
<i>Ha-1-83</i>	0.0273 ± 0.0007	0.213 ± 0.018	173.6 ± 4.6	196 ± 17	88.5	0.42	<i>Ha-2-19</i>	0.0320 ± 0.0011	0.221 ± 0.021	203.3 ± 6.9	202 ± 19	100.5	0.58
<i>Ha-1-84</i>	0.3165 ± 0.0063	5.069 ± 0.171	1772.8 ± 35.1	1831 ± 62	96.8	0.47	<i>Ha-2-20</i>	0.0209 ± 0.0007	0.142 ± 0.013	133.6 ± 4.4	135 ± 12	99.1	0.85
<i>Ha-1-85</i>	0.0408 ± 0.0010	0.443 ± 0.031	257.8 ± 6.6	372 ± 26	69.3	0.73	<i>Ha-2-21</i>	0.0279 ± 0.0008	0.195 ± 0.012	177.5 ± 5.4	181 ± 12	98.1	0.45
<i>Ha-1-86</i>	0.0277 ± 0.0006	0.204 ± 0.010	176.4 ± 3.7	189 ± 10	93.4	0.42	<i>Ha-2-22</i>	0.0183 ± 0.0007	0.122 ± 0.014	117.1 ± 4.2	117 ± 14	100.2	0.86
<i>Ha-1-87</i>	0.0320 ± 0.0007	0.289 ± 0.013	203.1 ± 4.2	257 ± 12	78.9	0.80	<i>Ha-2-23</i>	0.0268 ± 0.0009	0.196 ± 0.021	170.7 ± 6.0	181 ± 19	94.1	0.52
<i>Ha-1-88</i>	0.0267 ± 0.0006	0.190 ± 0.009	170.0 ± 3.6	177 ± 8	96.3	0.37	<i>Ha-2-24</i>	0.0421 ± 0.0014	0.413 ± 0.031	265.7 ± 8.6	351 ± 26	75.8	0.52
<i>Ha-1-89</i>	0.0211 ± 0.0007	0.182 ± 0.019	134.8 ± 4.2	170 ± 18	79.5	0.61	<i>Ha-2-25</i>	0.0292 ± 0.0010	0.205 ± 0.018	185.8 ± 6.1	189 ± 16	98.0	0.44
<i>Ha-1-90</i>	0.0247 ± 0.0005	0.195 ± 0.013	157.5 ± 3.3	181 ± 12	87.3	0.34	<i>Ha-2-26</i>	0.0300 ± 0.0012	0.225 ± 0.028	190.6 ± 7.4	206 ± 26	92.7	0.66
<i>Ha-1-91</i>	0.0277 ± 0.0006	0.225 ± 0.016	176.2 ± 3.9	206 ± 14	85.5	0.51	<i>Ha-2-27</i>	0.0350 ± 0.0012	0.245 ± 0.023	221.5 ± 7.4	222 ± 21	99.7	0.52
<i>Ha-1-92</i>	0.3149 ± 0.0051	4.904 ± 0.123	1764.7 ± 28.8	1803 ± 45	97.9	0.32	<i>Ha-2-28</i>	0.0287 ± 0.0012	0.199 ± 0.019	182.3 ± 7.5	184 ± 18	99.1	0.41
<i>Ha-1-93</i>	0.0323 ± 0.0007	0.273 ± 0.017	204.7 ± 4.3	245 ± 15	83.6	0.52	<i>Ha-2-29</i>	0.0375 ± 0.0016	0.275 ± 0.026	182.6 ± 7.0	184 ± 117	99.2	0.18
<i>Ha-1-94</i>	0.3078 ± 0.0052	4.805 ± 0.133	1729.8 ± 29.1	1786 ± 50	96.9	0.37	<i>Ha-2-30</i>	0.0418 ± 0.0019	0.315 ± 0.041	264.1 ± 12.0	278 ± 36	94.9	0.25
<i>Ha-1-95</i>	0.0267 ± 0.0005	0.194 ± 0.012	170.1 ± 3.5	180 ± 12	94.4	0.60	<i>Ha-2-31</i>	0.0273 ± 0.0011	0.194 ± 0.018	173.7 ± 7.1	180 ± 17	96.6	0.60
<i>Ha-1-96</i>	0.0295 ± 0.0007	0.223 ± 0.018	187.3 ± 4.4	204 ± 16	91.6	0.37	<i>Ha-2-32</i>	0.0199 ± 0.0009	0.135 ± 0.016	127.1 ± 5.5	128 ± 15	99.0	0.60
<i>Ha-1-97</i>	0.0385 ± 0.0007	0.305 ± 0.013	243.5 ± 3.4	270 ± 12	90.1	0.51	<i>Ha-2-33</i>	0.0212 ± 0.0012	0.161 ± 0.031	135.3 ± 7.3	152 ± 29	89.1	0.59
<i>Ha-1-98</i>	0.0301 ± 0.0005	0.223 ± 0.011	191.2 ± 2.9	204 ± 10	93.5	0.55	<i>Ha-2-34</i>	0.0191 ± 0.0008	0.138 ± 0.008	122.2 ± 5.4	131 ± 16	93.1	1.72
<i>Ha-1-99</i>	0.0662 ± 0.0010	0.538 ± 0.025	413.0 ± 6.2	437 ± 21	94.5	0.75	<i>Ha-2-35</i>	0.0344 ± 0.0014	0.237 ± 0.021	218.3 ± 8.8	216 ± 19	101.0	0.68
<i>Ha-1-100</i>	0.0303 ± 0.0006	0.233 ± 0.017	192.4 ± 3.7	212 ± 16	90.6	0.60	<i>Ha-2-36</i>	0.1579 ± 0.0060	2.373 ± 0.150	945.3 ± 36.2	1234 ± 78	76.6	0.26
<i>Ha-1-101</i>	0.0202 ± 0.0004	0.360 ± 0.020	128.9 ± 2.6	312 ± 17	41.3	0.73	<i>Ha-2-37</i>	0.0326 ± 0.0054	5.090 ± 0.180	1817.2 ± 29.9	1834 ± 65	99.1	0.45
<i>Ha-1-102</i>	0.2997 ± 0.0036	4.804 ± 0.116	1689.8 ± 20.2	1786 ± 43	94.6	0.44	<i>Ha-2-38</i>	0.0315 ± 0.0008	0.238 ± 0.024	200.1 ± 5.3	217 ± 22	92.2	0.47
<i>Ha-1-103</i>	0.0340 ± 0.0007	0.416 ± 0.029	215.5 ± 4.7	353 ± 25	61.0	1.29	<i>Ha-2-39</i>	0.0384 ± 0.0008	0.256 ± 0.017	242.8 ± 4.9	231 ± 16	104.9	0.63
<i>Ha-1-104</i>	0.0367 ± 0.0006	0.307 ± 0.019	232.2 ± 4.1	272 ± 17	83.4	0.28	<i>Ha-2-40</i>	0.0392 ± 0.0012	0.276 ± 0.033	248.1 ± 7.4	247 ± 30	100.3	0.71
<i>Ha-1-105</i>	0.0348 ± 0.0005	0.268 ± 0.012	220.6 ± 3.1	241 ± 11	91.4	0.83	<i>Ha-2-41</i>	0.3077 ± 0.0050	4.714 ± 0.164	1729.3 ± 28.2	1770 ± 62	97.7	0.39
<i>Ha-1-106</i>	0.0280 ± 0.0006	0.208 ± 0.013	178.3 ± 3.8	191 ± 12	93.1	0.59	<i>Ha-2-42</i>	0.0426 ± 0.0013	0.314 ± 0.040	268.9 ± 8.4	278 ± 35	96.9	0.61
<i>Ha-1-107</i>	0.0377 ± 0.0007	0.281 ± 0.011	238.5 ± 4.5	252 ± 10	94.7	0.87	<i>Ha-2-43</i>	0.0190 ± 0.0005	0.127 ± 0.012	121.3 ± 2.9	122 ± 11	99.6	1.54
<i>Ha-1-108</i>	0.0339 ± 0.0006	0.246 ± 0.011	214.9 ± 3.1	224 ± 10	96.1	0.95	<i>Ha-2-44</i>	0.0270 ± 0.0010	0.206 ± 0.020	172.0 ± 6.1	190 ± 18	90.3	0.58
<i>Ha-1-109</i>	0.0272 ± 0.0005	0.222 ± 0.010	173.1 ± 3.4	204 ± 9	85.0	0.58	<i>Ha-2-45</i>	0.0320 ± 0.0011	0.247 ± 0.023	202.8 ± 7.1	224 ± 20	90.5	0.62
<i>Ha-1-110</i>	0.0372 ± 0.0008	0.344 ± 0.021	235.6 ± 5.2	300 ± 19	78.4	0.86	<i>Ha-2-46</i>	0.0203 ± 0.0008	0.158 ± 0.018	129.2 ± 4.9	149 ± 17	86.6	1.32
<i>Ha-1-111</i>	0.0319 ± 0.0006	0.246 ± 0.009	202.6 ± 3.8	223 ± 8	90.8	0.47	<i>Ha-2-47</i>	0.0246 ± 0.0013	0.569 ± 0.077	156.6 ± 8.5	457 ± 62	34.3	1.32
<i>Ha-1-112</i>	0.0270 ± 0.0006	0.301 ± 0.019	171.7 ± 4.0	267 ± 17	64.3	1.14	<i>Ha-2-48</i>	0.0265 ± 0.0009	0.175 ± 0.017	168.7 ± 5.9	164 ± 16	103.0	0.54
<i>Ha-1-113</i>	0.0421 ± 0.0009	0.378 ± 0.021	265.6 ± 5.6	326 ± 18	81.5	0.70	<i>Ha-2-49</i>	0.0265 ± 0.0009	0.183 ± 0.015	168.6 ± 5.6	170 ± 14	98.9	0.45
							<i>Ha-2-50</i>	0.0260 ± 0.0008	0.194 ± 0.013	165.2 ± 5.3	180 ± 12	91.6	0.25
							<i>Ha-2-51</i>	0.0288 ± 0.0010	0.217 ± 0.018	182.9 ± 6.2	199 ± 16	91.9	0.46
<i>Ha-2-1</i>	0.0385 ± 0.0015	0.305 ± 0.041	243.7 ± 5.4	270 ± 36	90.2	0.63	<i>Ha-2-52</i>	0.3075 ± 0.0098	4.747 ± 0.261	1728.2 ± 54.9	1776 ± 98	97.3	0.43
<i>Ha-2-2</i>	0.0253 ± 0.0009	0.217 ± 0.026	161.1 ± 5.9	199 ± 24	80.8	0.58	<i>Ha-2-53</i>	0.0401 ± 0.0028	0.305 ± 0.028	253.7 ± 12.3	271 ± 25	93.7	0.52
<i>Ha-2-3</i>	0.0214 ± 0.0006	0.140 ± 0.011	136.5 ± 3.9	133 ± 10	102.3	0.72	<i>Ha-2-54</i>	0.0212 ± 0.0010	0.138 ± 0.014	135.1 ± 6.6	131 ± 13	103.2	0.58
<i>Ha-2-4</i>	0.0403 ± 0.0011	0.273 ± 0.017	254.6 ± 6.9	245 ± 15	103.9	0.22	<i>Ha-2-55</i>	0.0302 ± 0.0015	0.208 ± 0.024	191.8 ± 9.7	192 ± 22	100.0	0.39
<i>Ha-2-5</i>	0.0293 ± 0.0011	0.202 ± 0.028	186.1 ± 7.0	186 ± 26	99								

TABLE 1. (Continued)

Grain	$^{206}\text{Pb}/^{238}\text{U}$	$^{207}\text{Pb}/^{235}\text{U}$	$^{206}\text{Pb}/^{238}\text{U}$ age (Ma)	$^{207}\text{Pb}/^{235}\text{U}$ age (Ma)	%conc	Th/U	Grain	$^{206}\text{Pb}/^{238}\text{U}$	$^{207}\text{Pb}/^{235}\text{U}$	$^{206}\text{Pb}/^{238}\text{U}$ age (Ma)	$^{207}\text{Pb}/^{235}\text{U}$ age (Ma)	%conc	Th/U
Ha-2-60	0.0259 \pm 0.0012	0.167 \pm 0.015	164.7 \pm 7.9	157 \pm 14	104.9	0.32	Ha-2-111	0.0285 \pm 0.0009	0.188 \pm 0.016	180.9 \pm 5.5	175 \pm 15	103.5	0.38
Ha-2-61	0.0291 \pm 0.0014	0.206 \pm 0.021	184.9 \pm 9.2	190 \pm 20	97.2	0.32	Ha-2-112	0.0215 \pm 0.0009	0.163 \pm 0.027	137.3 \pm 6.0	153 \pm 25	89.7	0.73
Ha-2-62	0.0201 \pm 0.0007	0.134 \pm 0.015	128.3 \pm 4.3	127 \pm 14	100.8	0.84	Ha-2-113	0.0278 \pm 0.0013	0.209 \pm 0.018	176.6 \pm 8.4	193 \pm 16	91.4	0.65
Ha-2-63	0.0186 \pm 0.0007	0.124 \pm 0.019	118.9 \pm 4.7	119 \pm 18	100.1	0.68	Ha-2-114	0.0179 \pm 0.0009	0.113 \pm 0.013	114.4 \pm 5.7	109 \pm 13	105.3	1.06
Ha-2-64	0.0287 \pm 0.0009	0.206 \pm 0.018	182.7 \pm 5.5	190 \pm 17	96.0	0.53	Ha-2-115	0.0279 \pm 0.0014	0.203 \pm 0.023	177.6 \pm 8.9	188 \pm 21	94.7	0.39
Ha-2-65	0.0286 \pm 0.0009	0.959 \pm 0.064	181.8 \pm 6.0	683 \pm 46	26.6	0.40	Ha-2-116	0.0205 \pm 0.0011	0.150 \pm 0.023	131.1 \pm 7.3	142 \pm 22	92.3	1.25
Ha-2-66	0.0194 \pm 0.0007	0.115 \pm 0.017	124.0 \pm 4.6	111 \pm 16	111.8	0.67	Ha-2-117	0.0297 \pm 0.0137	4.619 \pm 0.300	1676.5 \pm 77.4	1753 \pm 114	95.7	0.40
Ha-2-67	0.0324 \pm 0.0009	0.222 \pm 0.018	205.3 \pm 5.9	204 \pm 16	100.7	0.55	Ha-2-118	0.0230 \pm 0.0013	0.243 \pm 0.037	146.8 \pm 8.5	221 \pm 33	66.4	1.07
Ha-2-68	0.0185 \pm 0.0006	0.123 \pm 0.014	118.4 \pm 3.9	118 \pm 13	100.6	0.89	Ha-2-119	0.0248 \pm 0.0013	0.228 \pm 0.028	157.8 \pm 8.3	208 \pm 26	75.8	0.65
Ha-2-69	0.0279 \pm 0.0008	0.193 \pm 0.014	177.7 \pm 4.9	179 \pm 13	99.0	0.33	Ha-2-120	0.0270 \pm 0.0013	0.188 \pm 0.017	171.9 \pm 8.3	175 \pm 16	98.2	0.45
Ha-2-70	0.0324 \pm 0.0009	0.195 \pm 0.020	178.5 \pm 5.7	180 \pm 18	98.9	0.48	Ha-2-121	0.0268 \pm 0.0009	0.182 \pm 0.018	170.2 \pm 5.5	170 \pm 12	100.1	0.52
Ha-2-71	0.0257 \pm 0.0009	0.168 \pm 0.012	163.8 \pm 5.6	157 \pm 12	104.0	0.43	Ha-2-122	0.0280 \pm 0.0010	0.196 \pm 0.018	177.9 \pm 6.1	182 \pm 16	97.8	0.39
Ha-2-72	0.0236 \pm 0.0008	0.176 \pm 0.013	150.3 \pm 5.1	165 \pm 12	91.1	0.66	Ha-2-123	0.0209 \pm 0.0007	0.148 \pm 0.011	133.5 \pm 4.4	141 \pm 11	95.0	0.50
Ha-2-73	0.3191 \pm 0.0104	5.024 \pm 0.235	1785.1 \pm 58.2	1823 \pm 85	97.9	2.34	Ha-2-124	0.0382 \pm 0.0012	0.242 \pm 0.016	241.6 \pm 7.6	220 \pm 15	109.7	0.50
Ha-2-74	0.0262 \pm 0.0010	0.207 \pm 0.024	166.5 \pm 5.6	191 \pm 22	87.2	0.78	Ha-2-125	0.0292 \pm 0.0012	0.171 \pm 0.025	185.8 \pm 7.6	161 \pm 24	115.7	0.60
Ha-2-75	0.0302 \pm 0.0010	0.217 \pm 0.016	192.1 \pm 5.5	199 \pm 14	96.4	0.42	Ha-2-126	0.0275 \pm 0.0009	0.208 \pm 0.017	175.0 \pm 5.9	192 \pm 16	91.3	0.53
Ha-2-76	0.0463 \pm 0.0020	0.312 \pm 0.046	292.0 \pm 12.6	276 \pm 41	105.9	0.45	Ha-2-127	0.0201 \pm 0.0007	0.201 \pm 0.018	128.4 \pm 4.7	186 \pm 17	69.2	0.89
Ha-2-77	0.0347 \pm 0.0012	0.259 \pm 0.020	219.9 \pm 7.7	234 \pm 18	94.2	0.74	Ha-2-128	0.2986 \pm 0.0089	4.718 \pm 0.183	1684.1 \pm 50.3	1770 \pm 69	95.1	0.76
Ha-2-78	0.4794 \pm 0.0150	11.153 \pm 0.398	2524.7 \pm 78.9	2536 \pm 91	99.6	0.48	Ha-2-129	0.3688 \pm 0.0083	5.800 \pm 0.214	2023.8 \pm 45.4	1946 \pm 72	104.0	0.17
Ha-2-79	0.0623 \pm 0.0025	0.704 \pm 0.075	389.9 \pm 15.8	541 \pm 58	72.0	0.43	Ha-2-130	0.3388 \pm 0.0077	5.346 \pm 0.205	1880.9 \pm 42.6	1876 \pm 72	100.2	0.16
Ha-2-80	0.0316 \pm 0.0012	0.234 \pm 0.026	200.3 \pm 7.7	213 \pm 24	93.9	0.50	Ha-2-131	0.0345 \pm 0.0010	0.406 \pm 0.032	218.4 \pm 6.3	346 \pm 27	63.1	0.45
Ha-2-81	0.0323 \pm 0.0011	0.216 \pm 0.017	205.1 \pm 7.0	199 \pm 15	103.2	0.68	Ha-2-132	0.0493 \pm 0.0014	0.438 \pm 0.037	310.0 \pm 8.8	369 \pm 31	84.0	0.57
Ha-2-82	0.3494 \pm 0.0110	5.470 \pm 0.237	1931.8 \pm 60.6	1896 \pm 82	101.9	0.32	Ha-2-133	0.0275 \pm 0.0007	0.192 \pm 0.014	175.0 \pm 4.5	179 \pm 13	97.9	0.37
Ha-2-83	0.0352 \pm 0.0013	0.298 \pm 0.028	223.3 \pm 8.2	265 \pm 25	84.2	1.14	Ha-2-134	0.1607 \pm 0.0037	2.507 \pm 0.101	960.5 \pm 22.0	1274 \pm 51	75.4	0.31
Ha-2-84	0.0192 \pm 0.0008	0.130 \pm 0.020	122.5 \pm 5.4	124 \pm 19	98.5	0.89	Ha-2-135	0.0276 \pm 0.0008	0.209 \pm 0.021	175.6 \pm 5.3	192 \pm 19	91.3	0.95
Ha-2-85	0.0177 \pm 0.0006	0.117 \pm 0.010	112.9 \pm 3.9	112 \pm 9	100.5	1.57	Ha-2-136	0.0286 \pm 0.0010	0.170 \pm 0.023	182.0 \pm 6.1	159 \pm 21	114.3	0.79
Ha-2-86	0.0265 \pm 0.0010	0.194 \pm 0.022	168.7 \pm 6.6	180 \pm 21	93.8	0.42	Ha-2-137	0.0284 \pm 0.0007	0.202 \pm 0.013	180.2 \pm 4.5	187 \pm 12	96.4	0.38
Ha-2-87	0.3380 \pm 0.0107	5.339 \pm 0.240	1876.9 \pm 59.3	1875 \pm 84	100.1	0.52	A sandstone cobble from the Ryosaki Formation (RySs-1; 33° 38' 17.23" N, 133° 45' 23.01" E)						
Ha-2-88	0.0344 \pm 0.0009	0.237 \pm 0.012	218.2 \pm 5.4	216 \pm 11	101.0	0.58							
Ha-2-89	0.0276 \pm 0.0008	0.185 \pm 0.018	175.6 \pm 5.4	172 \pm 17	101.8	0.52	RySs-1-1	0.0391 \pm 0.0008	0.290 \pm 0.017	247.4 \pm 5.2	259 \pm 16	95.6	0.48
Ha-2-90	0.0422 \pm 0.0012	0.289 \pm 0.026	266.2 \pm 7.9	258 \pm 23	103.4	0.51	RySs-1-2	0.0399 \pm 0.0008	0.276 \pm 0.014	252.4 \pm 4.9	248 \pm 13	101.9	0.27
Ha-2-91	0.0291 \pm 0.0008	0.201 \pm 0.016	185.2 \pm 5.2	186 \pm 14	99.5	0.47	RySs-1-3	0.0394 \pm 0.0008	0.270 \pm 0.014	249.4 \pm 4.9	242 \pm 13	102.9	0.43
Ha-2-92	0.0215 \pm 0.0009	0.173 \pm 0.026	137.3 \pm 5.7	162 \pm 25	84.5	0.52	RySs-1-4	0.0442 \pm 0.0012	0.463 \pm 0.041	278.5 \pm 7.8	386 \pm 35	72.1	0.34
Ha-2-93	0.0296 \pm 0.0008	0.194 \pm 0.016	188.2 \pm 5.3	180 \pm 15	104.4	0.58	RySs-1-5	0.0527 \pm 0.0012	0.424 \pm 0.029	331.0 \pm 7.5	359 \pm 24	92.2	0.50
Ha-2-94	0.0196 \pm 0.0007	0.131 \pm 0.016	125.2 \pm 4.3	125 \pm 15	100.0	0.73	RySs-1-6	0.0679 \pm 0.0015	0.510 \pm 0.032	423.3 \pm 9.1	419 \pm 26	101.1	0.55
Ha-2-95	0.0273 \pm 0.0008	0.185 \pm 0.015	173.6 \pm 5.0	172 \pm 14	100.7	0.73	RySs-1-7	0.0474 \pm 0.0014	0.348 \pm 0.038	298.4 \pm 8.6	304 \pm 33	98.3	0.44
Ha-2-96	0.0252 \pm 0.0008	0.226 \pm 0.020	160.7 \pm 5.0	207 \pm 18	77.8	0.92	RySs-1-8	0.0417 \pm 0.0008	0.302 \pm 0.015	263.6 \pm 5.2	268 \pm 13	98.4	0.37
Ha-2-97	0.0261 \pm 0.0006	0.178 \pm 0.014	165.9 \pm 5.8	166 \pm 13	99.8	0.44	RySs-1-9	0.0395 \pm 0.0009	0.288 \pm 0.021	249.8 \pm 5.7	257 \pm 19	97.3	0.95
Ha-2-98	0.0367 \pm 0.0010	0.265 \pm 0.027	232.1 \pm 6.3	239 \pm 24	97.3	0.74	RySs-1-10	0.0495 \pm 0.0011	0.375 \pm 0.022	311.2 \pm 6.8	323 \pm 19	96.4	0.38
Ha-2-99	0.0405 \pm 0.0009	0.296 \pm 0.020	256.2 \pm 5.5	263 \pm 18	97.3	0.50	RySs-1-11	0.0414 \pm 0.0009	0.284 \pm 0.018	261.3 \pm 5.8	253 \pm 16	103.1	0.20
Ha-2-100	0.3273 \pm 0.0062	5.210 \pm 0.202	1825.3 \pm 34.8	1854 \pm 72	98.4	1.13	RySs-1-12	0.0435 \pm 0.0012	0.324 \pm 0.033	274.6 \pm 7.8	285 \pm 29	96.4	0.24
Ha-2-101	0.0301 \pm 0.0008	0.218 \pm 0.023	191.4 \pm 5.4	200 \pm 22	95.5	0.52	RySs-1-13	0.0416 \pm 0.0010	0.301 \pm 0.021	262.8 \pm 6.0	267 \pm 18	98.5	0.56
Ha-2-102	0.0283 \pm 0.0006	0.200 \pm 0.014	180.1 \pm 3.9	185 \pm 13	97.4	0.62	RySs-1-14	0.0395 \pm 0.0009	0.411 \pm 0.026	249.6 \pm 5.9	349 \pm 22	71.4	0.71
Ha-2-103	0.0271 \pm 0.0007	0.192 \pm 0.016	172.1 \pm 4.2	179 \pm 15	96.4	0.42	RySs-1-15	0.0403 \pm 0.0008	0.292 \pm 0.010	254.5 \pm 4.8	260 \pm 9	97.8	0.40
Ha-2-104	0.0206 \pm 0.0008	0.247 \pm 0.025	131.5 \pm 4.8	224 \pm 23	58.8	0.51	RySs-1-16	0.0440 \pm 0.0011	0.312 \pm 0.021	277.3 \pm 6.0	276 \pm 19	100.6	0.32
Ha-2-105	0.0243 \pm 0.0008	0.171 \pm 0.016	154.9 \pm 4.9	161 \pm 15	96.5	0.38	RySs-1-17	0.0407 \pm 0.0008	0.303 \pm 0.013	256.9 \pm 5.1	269 \pm 11	95.5	0.74
Ha-2-106	0.0216 \pm 0.0007	0.156 \pm 0.017	137.7 \pm 4.7	147 \pm 16	93.8	0.59	RySs-1-18	0.0429 \pm 0.0010	0.308 \pm 0.022	270.5 \pm 6.3	273 \pm 19	99.2	0.57
Ha-2-107	0.0232 \pm 0.0007	0.149 \pm 0.010	147.9 \pm 4.2	141 \pm 10	104.6	0.36	RySs-1-19	0.0409 \pm 0.0012	0.280 \pm 0.016	258.2 \pm 6.0	251 \pm 15	102.9	0.67
Ha-2-108	0.0259 \pm 0.0007	0.175 \pm 0.011	165.1 \pm 4.7	164 \pm 11	100.7	0.42	RySs-1-20	0.0397 \pm 0.0012	0.338 \pm 0.016	251.0 \pm 7.3	296 \pm 14	84.8	0.51
Ha-2-109	0.0188 \pm 0.0007	0.152 \pm 0.017	119.8 \pm 4.2	144 \pm 16	83.2	0.83	RySs-1-21	0.0380 \pm 0.0012	0.257 \pm 0.021	240.2 \pm 7.			

TABLE 1. (Continued)

Grain	$^{206}\text{Pb}/^{238}\text{U}$	$^{207}\text{Pb}/^{235}\text{U}$	$^{206}\text{Pb}/^{238}\text{U}$ age (Ma)	$^{207}\text{Pb}/^{235}\text{U}$ age (Ma)	%conc	Th/U	Grain	$^{206}\text{Pb}/^{238}\text{U}$	$^{207}\text{Pb}/^{235}\text{U}$	$^{206}\text{Pb}/^{238}\text{U}$ age (Ma)	$^{207}\text{Pb}/^{235}\text{U}$ age (Ma)	%conc	Th/U
RySs-1-23	0.0479 \pm 0.0015	0.348 \pm 0.026	301.8 \pm 9.5	303 \pm 22	99.6	0.29	RySs-1-74	0.0419 \pm 0.0014	0.293 \pm 0.016	264.3 \pm 8.6	261 \pm 14	101.4	0.25
RySs-1-24	0.0425 \pm 0.0014	0.288 \pm 0.024	268.2 \pm 8.7	257 \pm 22	104.5	0.72	RySs-1-75	0.0425 \pm 0.0014	0.325 \pm 0.021	268.4 \pm 9.0	285 \pm 18	94.0	0.36
RySs-1-25	0.0459 \pm 0.0015	0.322 \pm 0.030	289.2 \pm 9.6	284 \pm 26	102.0	0.66	RySs-1-76	0.0635 \pm 0.0018	0.397 \pm 0.027	336.2 \pm 11.4	339 \pm 23	99.1	0.58
RySs-1-26	0.0390 \pm 0.0012	0.257 \pm 0.018	246.9 \pm 7.6	232 \pm 17	106.4	0.39	RySs-1-77	0.0428 \pm 0.0015	0.302 \pm 0.026	270.4 \pm 9.6	268 \pm 23	101.0	0.71
RySs-1-27	0.0405 \pm 0.0013	0.289 \pm 0.025	255.7 \pm 8.4	258 \pm 22	99.2	0.40	RySs-1-78	0.0419 \pm 0.0011	0.290 \pm 0.019	264.6 \pm 6.9	259 \pm 17	102.3	0.60
RySs-1-28	0.0601 \pm 0.0016	2.038 \pm 0.109	376.3 \pm 10.3	1128 \pm 60	33.4	0.82	RySs-1-79	0.0454 \pm 0.0013	0.443 \pm 0.035	286.3 \pm 8.3	373 \pm 29	76.8	1.30
RySs-1-29	0.0421 \pm 0.0011	0.294 \pm 0.023	265.9 \pm 6.9	262 \pm 21	101.6	0.38	RySs-1-80	0.0414 \pm 0.0010	0.301 \pm 0.017	261.4 \pm 6.5	267 \pm 15	97.8	0.46
RySs-1-30	0.0428 \pm 0.0013	0.267 \pm 0.030	270.0 \pm 7.9	240 \pm 27	112.3	0.63	RySs-1-81	0.0407 \pm 0.0010	0.456 \pm 0.021	257.2 \pm 6.3	382 \pm 18	67.4	0.70
RySs-1-31	0.3179 \pm 0.0071	5.080 \pm 0.203	1779.4 \pm 39.6	1833 \pm 73	91.1	0.36	RySs-1-82	0.0480 \pm 0.0016	0.387 \pm 0.041	302.2 \pm 9.8	332 \pm 36	91.1	0.36
RySs-1-32	0.0435 \pm 0.0014	0.350 \pm 0.042	274.2 \pm 8.9	305 \pm 36	90.0	0.37	RySs-1-83	0.0418 \pm 0.0012	0.330 \pm 0.026	263.8 \pm 7.4	290 \pm 23	91.0	0.57
RySs-1-33	0.0424 \pm 0.0010	0.301 \pm 0.020	267.6 \pm 6.5	267 \pm 18	100.1	0.63	RySs-1-84	0.0400 \pm 0.0010	0.281 \pm 0.016	252.9 \pm 6.3	252 \pm 14	100.4	0.49
RySs-1-34	0.0424 \pm 0.0011	0.295 \pm 0.023	267.9 \pm 6.8	262 \pm 20	102.2	0.83	RySs-1-85	0.0461 \pm 0.0012	0.337 \pm 0.021	290.3 \pm 7.4	295 \pm 18	98.4	0.33
RySs-1-35	0.0428 \pm 0.0011	0.323 \pm 0.026	270.1 \pm 7.1	284 \pm 23	95.0	0.58	RySs-1-86	0.0424 \pm 0.0015	2.775 \pm 0.134	267.8 \pm 9.4	1349 \pm 65	19.9	0.44
RySs-1-36	0.0392 \pm 0.0010	0.265 \pm 0.018	247.8 \pm 6.0	239 \pm 16	103.7	0.67	RySs-1-87	0.0816 \pm 0.0027	0.633 \pm 0.036	505.7 \pm 16.6	498 \pm 28	101.5	0.34
RySs-1-37	0.0488 \pm 0.0010	0.370 \pm 0.028	307.4 \pm 6.2	320 \pm 24	96.1	0.65	RySs-1-88	0.0411 \pm 0.0015	0.309 \pm 0.027	259.4 \pm 9.3	273 \pm 24	94.9	0.64
RySs-1-38	0.0724 \pm 0.0012	0.579 \pm 0.031	450.4 \pm 7.3	464 \pm 24	97.1	0.45	RySs-1-89	0.0564 \pm 0.0020	0.493 \pm 0.036	353.5 \pm 12.3	400 \pm 30	88.4	0.47
RySs-1-39	0.0437 \pm 0.0009	0.313 \pm 0.027	275.8 \pm 5.9	277 \pm 24	99.7	0.44	RySs-1-90	0.0444 \pm 0.0016	0.324 \pm 0.027	280.2 \pm 9.9	285 \pm 23	98.2	0.43
RySs-1-40	0.0429 \pm 0.0009	0.310 \pm 0.025	271.0 \pm 5.7	274 \pm 23	98.7	0.51	RySs-1-91	0.0414 \pm 0.0014	0.342 \pm 0.022	261.3 \pm 8.8	298 \pm 20	87.6	0.61
RySs-1-41	0.0470 \pm 0.0009	0.356 \pm 0.026	295.8 \pm 5.8	309 \pm 23	95.8	0.68	RySs-1-92	0.0392 \pm 0.0013	0.278 \pm 0.015	248.1 \pm 8.0	249 \pm 13	99.5	0.60
RySs-1-42	0.0458 \pm 0.0008	0.334 \pm 0.021	288.8 \pm 5.0	292 \pm 18	98.8	0.25	RySs-1-93	0.0407 \pm 0.0014	0.279 \pm 0.020	257.2 \pm 8.8	250 \pm 18	103.0	0.43
RySs-1-43	0.0612 \pm 0.0011	0.422 \pm 0.027	382.9 \pm 6.8	358 \pm 23	107.1	0.41	RySs-1-94	0.0470 \pm 0.0016	0.346 \pm 0.026	295.9 \pm 10.3	302 \pm 23	98.1	0.34
RySs-1-44	0.0440 \pm 0.0007	0.320 \pm 0.019	277.7 \pm 4.7	282 \pm 16	98.5	0.41	RySs-1-95	0.0456 \pm 0.0026	0.314 \pm 0.062	287.5 \pm 16.6	277 \pm 54	103.8	0.55
RySs-1-45	0.1020 \pm 0.0039	0.944 \pm 0.083	626.3 \pm 24.0	675 \pm 59	92.8	1.14	RySs-1-96	0.0471 \pm 0.0025	0.307 \pm 0.060	296.7 \pm 15.8	340 \pm 51	87.3	0.47
RySs-1-46	0.0533 \pm 0.0020	0.379 \pm 0.034	334.7 \pm 12.6	326 \pm 29	102.7	0.59	RySs-1-97	0.0454 \pm 0.0023	0.332 \pm 0.045	286.1 \pm 14.2	291 \pm 40	98.3	0.40
RySs-1-47	0.0469 \pm 0.0019	0.393 \pm 0.044	295.5 \pm 12.1	337 \pm 37	87.7	0.46	RySs-1-98	0.0531 \pm 0.0028	0.340 \pm 0.058	333.4 \pm 17.8	297 \pm 50	112.3	0.58
RySs-1-48	0.0428 \pm 0.0015	0.400 \pm 0.028	270.1 \pm 9.7	341 \pm 24	79.1	0.51	RySs-1-99	0.0431 \pm 0.0019	0.327 \pm 0.029	272.2 \pm 12.1	287 \pm 26	94.7	1.05
RySs-1-49	0.0415 \pm 0.0015	0.289 \pm 0.024	262.4 \pm 9.7	258 \pm 21	101.7	0.86	RySs-1-100	0.0413 \pm 0.0019	0.527 \pm 0.042	260.7 \pm 11.7	430 \pm 34	60.7	1.23
RySs-1-50	0.0427 \pm 0.0015	0.309 \pm 0.021	269.8 \pm 9.5	273 \pm 18	98.7	0.65	RySs-1-101	0.0462 \pm 0.0019	0.383 \pm 0.023	291.1 \pm 12.2	330 \pm 20	88.3	0.36
RySs-1-51	0.0430 \pm 0.0015	0.321 \pm 0.023	271.2 \pm 9.7	283 \pm 20	96.0	0.57	RySs-1-102	0.0399 \pm 0.0017	0.293 \pm 0.021	252.3 \pm 10.7	261 \pm 18	96.7	0.90
RySs-1-52	0.0504 \pm 0.0018	0.403 \pm 0.030	316.8 \pm 11.5	344 \pm 25	92.1	0.47	RySs-1-103	0.0410 \pm 0.0017	0.307 \pm 0.021	258.7 \pm 11.0	272 \pm 18	95.2	0.36
RySs-1-53	0.0490 \pm 0.0024	0.367 \pm 0.060	308.2 \pm 14.8	318 \pm 52	97.0	0.40	RySs-1-104	0.0753 \pm 0.0013	0.609 \pm 0.032	468.0 \pm 8.4	483 \pm 25	96.8	0.61
RySs-1-54	0.0496 \pm 0.0011	0.360 \pm 0.017	311.9 \pm 6.7	312 \pm 15	99.8	0.58	RySs-1-105	0.0510 \pm 0.0010	0.442 \pm 0.027	320.8 \pm 6.3	372 \pm 23	86.3	0.53
RySs-1-55	0.0414 \pm 0.0009	0.312 \pm 0.015	261.6 \pm 5.7	275 \pm 13	95.0	0.35	RySs-1-106	0.0414 \pm 0.0007	0.429 \pm 0.019	261.3 \pm 4.5	363 \pm 16	72.1	0.47
RySs-1-56	0.0407 \pm 0.0008	0.291 \pm 0.012	256.9 \pm 5.4	260 \pm 10	98.9	0.32	RySs-1-107	0.0414 \pm 0.0008	0.299 \pm 0.020	261.2 \pm 5.2	266 \pm 18	98.4	0.61
RySs-1-57	0.0439 \pm 0.0011	0.323 \pm 0.025	277.2 \pm 7.1	284 \pm 22	97.6	0.58	RySs-1-108	0.0522 \pm 0.0013	0.382 \pm 0.039	327.8 \pm 8.5	328 \pm 33	99.8	0.28
RySs-1-58	0.0795 \pm 0.0020	0.651 \pm 0.048	493.0 \pm 12.5	509 \pm 37	96.8	0.84	RySs-1-109	0.0417 \pm 0.0009	0.328 \pm 0.026	263.5 \pm 5.9	288 \pm 23	91.5	0.49
RySs-1-59	0.0451 \pm 0.0014	0.348 \pm 0.036	284.6 \pm 8.6	303 \pm 32	93.9	0.39	RySs-1-110	0.0394 \pm 0.0008	0.270 \pm 0.020	248.9 \pm 5.2	242 \pm 18	102.6	0.46
RySs-1-60	0.0410 \pm 0.0009	0.294 \pm 0.018	259.1 \pm 6.0	261 \pm 16	99.1	0.49	A sandstone cobble from the Yumoki Formation (YuSs-1; 33° 42' 43.20" N, 133° 50' 06.09" E)						
RySs-1-61	0.0426 \pm 0.0011	0.307 \pm 0.015	268.9 \pm 6.7	272 \pm 13	98.9	0.28	YuSs-1-1	0.3330 \pm 0.0082	5.292 \pm 0.198	1852.7 \pm 45.5	1868 \pm 70	99.2	0.47
RySs-1-62	0.0459 \pm 0.0016	0.393 \pm 0.044	289.2 \pm 9.9	337 \pm 38	85.9	0.60	YuSs-1-2	0.0410 \pm 0.0014	0.274 \pm 0.031	259.2 \pm 8.6	246 \pm 28	105.3	0.74
RySs-1-63	0.0607 \pm 0.0015	0.492 \pm 0.024	379.8 \pm 9.6	406 \pm 20	93.5	0.65	YuSs-1-3	0.0357 \pm 0.0013	0.275 \pm 0.034	225.8 \pm 8.0	247 \pm 30	91.4	0.49
RySs-1-64	0.0421 \pm 0.0013	0.307 \pm 0.029	266.1 \pm 8.1	272 \pm 25	97.8	0.58	YuSs-1-4	0.0571 \pm 0.0016	0.444 \pm 0.031	357.7 \pm 9.9	373 \pm 26	96.0	0.45
RySs-1-65	0.0479 \pm 0.0017	0.367 \pm 0.046	301.9 \pm 10.8	317 \pm 40	95.2	0.51	YuSs-1-5	0.5044 \pm 0.0121	10.940 \pm 0.364	2632.5 \pm 63.2	2518 \pm 84	104.5	0.12
RySs-1-66	0.0753 \pm 0.0019	0.593 \pm 0.028	468.1 \pm 11.7	473 \pm 23	99.0	0.33	YuSs-1-6	0.0388 \pm 0.0010	0.282 \pm 0.017	245.4 \pm 6.4	252 \pm 15	97.4	0.47
RySs-1-67	0.0451 \pm 0.0011	0.316 \pm 0.016	284.4 \pm 7.1	279 \pm 14	101.9	0.19	YuSs-1-7	0.0464 \pm 0.0012	0.356 \pm 0.023	292.2 \pm 7.8	310 \pm 20	94.4	0.47
RySs-1-68	0.0416 \pm 0.0012	0.328 \pm 0.027	262.9 \pm 7.7	288 \pm 24	91.3	0.67	YuSs-1-8	0.0476 \pm 0.0020	0.404 \pm 0.063	299.7 \pm 12.9	345 \pm 54	87.0	0.47
RySs-1-69	0.0418 \pm 0.0014	0.335 \pm 0.021	264.2 \pm 8.9	293 \pm 19	90.2	0.54	YuSs-1-9	0.0465 \pm 0.0019	0.317 \pm 0.050	292.9 \pm 11.8	280 \pm 44	104.7	0.35
RySs-1-70	0.0430 \pm 0.0015	0.324 \pm 0.027	271.6 \pm 9.7	285 \pm 24	95.2	0.97	YuSs-1-10	0.3059 \pm 0.0055	4.681 \pm 0.149	1720.6 \pm 31.1	1764 \pm 56	97.6	0.83
RySs-1-71	0.0438 \pm 0.0014	0.307 \pm 0.015	276.2 \pm 8.9	271 \pm 13	101.7	0.44	YuSs-1-11	0.0447 \pm 0.0014	0.420 \pm 0.045	282.1 \pm 8.7	356 \pm 39	79.2	0.30
RySs-1-72	0.0532 \pm 0.0018	0.391 \pm 0.026	334.2 \pm 11.3	335 \pm 23	99.7	0.58	YuSs-1-12	0.3297 \pm 0.0058	5.210 \pm 0.153	1837.0 \pm 32.5	1854 \pm 55	99.1	0.14
RySs-1-73	0.0441 \pm 0.0015	0.307 \pm 0.023	278.0 \pm 9.6	272 $\pm</$									

TABLE 1. (Continued)

Grain	$^{206}\text{Pb}/^{238}\text{U}$	$^{207}\text{Pb}/^{235}\text{U}$	$^{206}\text{Pb}/^{238}\text{U}$ age (Ma)	$^{207}\text{Pb}/^{235}\text{U}$ age (Ma)	%conc	Th/U	Grain	$^{206}\text{Pb}/^{238}\text{U}$	$^{207}\text{Pb}/^{235}\text{U}$	$^{206}\text{Pb}/^{238}\text{U}$ age (Ma)	$^{207}\text{Pb}/^{235}\text{U}$ age (Ma)	%conc	Th/U
YuSs1-13	0.0452 ± 0.0020	0.391 ± 0.071	284.7 ± 12.8	335 ± 61	85.0	0.56	YuSs1-64	0.3375 ± 0.0046	5.352 ± 0.168	1874.8 ± 25.4	1877 ± 59	99.9	0.20
YuSs1-14	0.0407 ± 0.0011	0.315 ± 0.030	257.3 ± 6.8	278 ± 26	92.5	0.53	YuSs1-65	0.0427 ± 0.0009	0.396 ± 0.031	269.8 ± 5.9	339 ± 26	79.6	0.49
YuSs1-15	0.0445 ± 0.0010	0.313 ± 0.025	280.6 ± 6.6	277 ± 22	101.5	0.29	YuSs1-66	0.0375 ± 0.0008	0.306 ± 0.024	237.3 ± 5.0	271 ± 21	87.5	0.64
YuSs1-16	0.0417 ± 0.0009	0.279 ± 0.019	263.2 ± 5.6	250 ± 17	105.2	0.35	YuSs1-67	0.0473 ± 0.0012	0.358 ± 0.038	298.1 ± 7.8	310 ± 33	96.0	0.44
YuSs1-17	0.0418 ± 0.0016	0.351 ± 0.052	263.8 ± 10.0	305 ± 45	86.5	0.75	YuSs1-68	0.0500 ± 0.0025	0.398 ± 0.091	314.3 ± 15.7	340 ± 78	92.5	0.37
YuSs1-18	0.0339 ± 0.0007	0.233 ± 0.013	214.9 ± 4.3	213 ± 12	100.9	0.56	YuSs1-69	0.0427 ± 0.0006	0.304 ± 0.014	269.7 ± 4.1	269 ± 12	100.2	0.37
YuSs1-19	0.0442 ± 0.0014	0.525 ± 0.048	279.1 ± 8.9	428 ± 39	65.2	0.62	YuSs1-70	0.0418 ± 0.0012	0.640 ± 0.060	264.2 ± 7.8	502 ± 47	52.6	0.49
YuSs1-20	0.0461 ± 0.0012	0.334 ± 0.023	290.3 ± 7.5	292 ± 20	99.3	0.63	YuSs1-71	0.3787 ± 0.0087	5.623 ± 0.204	2070.3 ± 47.6	1920 ± 69	107.9	0.57
YuSs1-21	0.3392 ± 0.0077	5.372 ± 0.189	1882.7 ± 42.8	1880 ± 66	100.1	0.46	YuSs1-72	0.0332 ± 0.0010	0.258 ± 0.023	210.8 ± 6.0	233 ± 20	90.3	0.38
YuSs1-22	0.3395 ± 0.0077	5.282 ± 0.186	1884.1 ± 42.8	1866 ± 66	101.0	0.44	YuSs1-73	0.0724 ± 0.0026	0.771 ± 0.086	450.4 ± 15.9	581 ± 65	77.6	0.48
YuSs1-23	0.0678 ± 0.0025	0.784 ± 0.092	422.8 ± 15.8	588 ± 69	71.9	0.59	YuSs1-74	0.0432 ± 0.0012	0.337 ± 0.030	272.5 ± 7.8	295 ± 26	92.4	0.80
YuSs1-24	0.0467 ± 0.0012	0.346 ± 0.023	294.2 ± 7.5	302 ± 20	97.5	0.96	YuSs1-75	0.0397 ± 0.0011	0.288 ± 0.022	251.1 ± 6.7	257 ± 20	97.8	0.89
YuSs1-25	0.0315 ± 0.0008	0.235 ± 0.016	199.6 ± 5.2	214 ± 14	93.1	0.48	YuSs1-76	0.0333 ± 0.0008	0.234 ± 0.013	211.2 ± 5.1	213 ± 12	99.0	0.56
YuSs1-26	0.0432 ± 0.0024	0.298 ± 0.073	272.6 ± 15.2	265 ± 65	103.0	0.35	YuSs1-77	0.3483 ± 0.0078	5.563 ± 0.172	1926.5 ± 43.0	1910 ± 59	100.9	0.36
YuSs1-27	0.0448 ± 0.0020	0.353 ± 0.056	282.6 ± 12.8	307 ± 48	92.2	0.41	YuSs1-78	0.0471 ± 0.0013	0.362 ± 0.029	296.9 ± 8.1	314 ± 25	94.6	0.57
YuSs1-28	0.0441 ± 0.0016	0.333 ± 0.032	277.9 ± 9.9	292 ± 28	95.1	0.63	YuSs1-79	0.0366 ± 0.0011	0.270 ± 0.026	232.0 ± 6.9	243 ± 24	95.6	0.33
YuSs1-29	0.0592 ± 0.0021	0.453 ± 0.042	371.0 ± 13.0	379 ± 35	97.8	0.58	A sandstone cobble from the Funadani Formation (FuSs-1; 33° 37' 21.28" N, 133° 42' 02.22" E)						
YuSs1-30	0.0304 ± 0.0011	0.335 ± 0.032	193.0 ± 7.3	294 ± 28	65.7	0.79	FuSs-1-1	0.0432 ± 0.0017	0.335 ± 0.046	272.9 ± 10.9	293 ± 40	93.0	0.65
YuSs1-31	0.0447 ± 0.0017	0.336 ± 0.038	281.6 ± 10.6	294 ± 33	95.7	0.48	FuSs-1-2	0.0503 ± 0.0021	0.306 ± 0.049	316.6 ± 12.9	271 ± 44	116.7	0.45
YuSs1-32	0.3698 ± 0.0110	6.163 ± 0.224	2028.3 ± 60.4	1999 ± 73	101.5	0.26	FuSs-1-3	0.3511 ± 0.0100	5.503 ± 0.218	1940.0 ± 55.2	1901 ± 75	102.1	0.26
YuSs1-33	0.0322 ± 0.0011	0.255 ± 0.020	204.6 ± 6.9	229 ± 18	89.2	0.75	FuSs-1-4	0.0447 ± 0.0014	0.335 ± 0.028	281.6 ± 9.1	293 ± 25	96.0	0.94
YuSs1-34	0.0468 ± 0.0016	0.329 ± 0.028	294.7 ± 10.0	289 ± 24	102.1	0.48	FuSs-1-5	0.0470 ± 0.0019	0.389 ± 0.051	296.3 ± 11.8	334 ± 44	88.8	0.56
YuSs1-35	0.0465 ± 0.0019	0.419 ± 0.051	293.1 ± 11.9	356 ± 43	82.4	0.75	FuSs-1-6	0.0507 ± 0.0021	0.378 ± 0.056	319.1 ± 13.1	325 ± 48	98.1	0.69
YuSs1-36	0.0413 ± 0.0009	0.315 ± 0.025	261.2 ± 5.9	278 ± 22	93.9	0.59	FuSs-1-7	0.0423 ± 0.0021	0.335 ± 0.069	266.9 ± 13.4	294 ± 60	90.9	0.67
YuSs1-37	0.0301 ± 0.0006	0.219 ± 0.014	191.2 ± 3.8	201 ± 13	94.9	0.79	FuSs-1-8	0.0685 ± 0.0028	0.343 ± 0.058	427.2 ± 17.2	299 ± 51	142.9	0.55
YuSs1-38	0.0365 ± 0.0007	0.272 ± 0.018	230.9 ± 4.7	244 ± 16	94.6	0.49	FuSs-1-9	0.0463 ± 0.0017	0.307 ± 0.036	291.7 ± 10.5	272 ± 31	107.3	0.35
YuSs1-39	0.0468 ± 0.0014	0.354 ± 0.042	294.6 ± 8.8	307 ± 37	95.9	0.46	FuSs-1-10	0.0579 ± 0.0016	0.430 ± 0.049	362.6 ± 10.1	363 ± 42	99.8	0.47
YuSs1-40	0.3653 ± 0.0057	5.770 ± 0.158	2007.1 ± 31.2	1942 ± 53	103.4	0.24	FuSs-1-11	0.0458 ± 0.0015	0.388 ± 0.052	288.4 ± 9.7	333 ± 45	86.6	0.68
YuSs1-41	0.3545 ± 0.0055	5.548 ± 0.151	1955.9 ± 30.3	1908 ± 52	102.5	0.44	FuSs-1-12	0.0489 ± 0.0022	0.389 ± 0.072	307.9 ± 13.6	333 ± 62	92.3	0.62
YuSs1-42	0.0356 ± 0.0007	0.252 ± 0.017	225.2 ± 4.6	229 ± 15	98.5	0.39	FuSs-1-13	0.0436 ± 0.0013	0.332 ± 0.039	275.3 ± 7.9	291 ± 34	94.5	0.98
YuSs1-43	0.3676 ± 0.0057	6.146 ± 0.170	2018.2 ± 31.5	1997 ± 55	101.1	0.31	FuSs-1-14	0.0451 ± 0.0019	0.280 ± 0.055	284.3 ± 11.9	251 ± 49	113.4	0.64
YuSs1-44	0.0479 ± 0.0009	0.437 ± 0.024	301.8 ± 5.8	368 ± 20	82.0	0.24	FuSs-1-15	0.0494 ± 0.0015	0.390 ± 0.049	311.1 ± 9.6	334 ± 42	93.1	0.32
YuSs1-45	0.0357 ± 0.0011	0.301 ± 0.018	226.1 ± 7.3	267 ± 16	84.6	0.58	FuSs-1-16	0.0443 ± 0.0022	0.445 ± 0.086	279.4 ± 14.1	374 ± 72	74.8	0.55
YuSs1-46	0.0426 ± 0.0019	0.356 ± 0.052	269.0 ± 12.0	309 ± 46	87.0	0.41	FuSs-1-17	0.0532 ± 0.0012	0.434 ± 0.037	333.9 ± 7.6	366 ± 32	91.3	1.20
YuSs1-47	0.0419 ± 0.0013	0.314 ± 0.018	264.8 ± 8.4	277 ± 16	95.4	0.29	FuSs-1-18	0.0432 ± 0.0012	0.318 ± 0.038	272.3 ± 7.7	280 ± 33	97.1	0.33
YuSs1-48	0.0408 ± 0.0014	0.408 ± 0.032	263.5 ± 9.1	348 ± 27	75.8	0.39	FuSs-1-19	0.0492 ± 0.0013	0.355 ± 0.028	309.4 ± 8.1	309 ± 25	100.3	0.45
YuSs1-49	0.0457 ± 0.0021	0.381 ± 0.059	288.3 ± 13.3	328 ± 51	88.0	0.34	FuSs-1-20	0.0494 ± 0.0018	0.380 ± 0.052	311.0 ± 11.2	327 ± 44	95.0	0.69
YuSs1-50	0.0345 ± 0.0011	0.260 ± 0.017	218.9 ± 7.1	235 ± 15	93.2	1.00	FuSs-1-21	0.0469 ± 0.0020	0.362 ± 0.062	295.8 ± 12.5	314 ± 53	94.3	0.58
YuSs1-51	0.0311 ± 0.0010	0.222 ± 0.013	197.1 ± 5.3	204 ± 12	96.7	0.53	FuSs-1-22	0.0486 ± 0.0022	0.389 ± 0.070	305.9 ± 13.7	334 ± 60	91.7	0.72
YuSs1-52	0.0344 ± 0.0012	0.258 ± 0.022	218.1 ± 7.5	233 ± 20	93.6	0.43	FuSs-1-23	0.0456 ± 0.0017	0.355 ± 0.052	287.4 ± 10.9	309 ± 45	93.1	0.68
YuSs1-53	0.0420 ± 0.0013	0.300 ± 0.019	265.1 ± 8.5	267 ± 17	99.4	0.43	FuSs-1-24	0.0411 ± 0.0011	0.316 ± 0.028	259.7 ± 7.2	279 ± 24	93.2	0.63
YuSs1-54	0.3229 ± 0.0037	5.070 ± 0.175	1803.8 ± 20.8	1831 ± 63	98.5	0.39	FuSs-1-25	0.0520 ± 0.0017	0.395 ± 0.048	326.8 ± 10.9	338 ± 41	96.7	0.55
YuSs1-55	0.0375 ± 0.0005	0.270 ± 0.014	237.4 ± 3.2	243 ± 12	97.7	0.94	FuSs-1-26	0.0561 ± 0.0017	0.408 ± 0.045	351.9 ± 11.0	347 ± 39	101.3	0.69
YuSs1-56	0.0369 ± 0.0009	0.304 ± 0.029	233.9 ± 5.4	269 ± 26	86.8	0.57	FuSs-1-27	0.0445 ± 0.0019	0.371 ± 0.057	280.7 ± 11.8	320 ± 49	87.7	0.67
YuSs1-57	0.0473 ± 0.0011	0.384 ± 0.036	297.9 ± 6.7	330 ± 31	90.3	0.61	FuSs-1-28	0.0442 ± 0.0019	0.396 ± 0.059	279.1 ± 11.8	339 ± 51	82.4	0.60
YuSs1-58	0.0289 ± 0.0004	0.200 ± 0.011	183.6 ± 2.6	185 ± 10	99.0	0.69	FuSs-1-29	0.0445 ± 0.0015	0.331 ± 0.036	280.4 ± 9.2	290 ± 32	96.6	0.49
YuSs1-59	0.0418 ± 0.0018	0.303 ± 0.061	264.0 ± 11.3	269 ± 54	98.2	0.54	FuSs-1-30	0.0421 ± 0.0017	0.338 ± 0.050	265.6 ± 10.8	295 ± 44	89.9	0.53
YuSs1-60	0.0420 ± 0.0006	0.300 ± 0.015	265.2 ± 3.5	266 ± 13	99.6	0.59	FuSs-1-31	0.0447 ± 0.0018	0.350 ± 0.050	281.8 ± 11.1	305 ± 44	92.5	0.72
YuSs1-61	0.0606 ± 0.0008	0.451 ± 0.024	379.5 ± 5.3	378 ± 20	100.3	0.64	FuSs-1-32	0.0475 ± 0.0016	0.358 ± 0.039	299.0 ± 9.8	310 ± 34	96.3	0.49
YuSs1-62	0.0416 ± 0.0007	0.303 ± 0.022	262.8 ± 4.6	269 ± 19	97.8	0.59	FuSs-1-33	0.0485 ± 0.0020	0.441 ± 0.065	305.0 ± 12.8	371 ± 55	82.2	0.45
YuSs1-63	0.3208 ± 0.0046	5.177 ± 0.179	1793.6 ± 25.6	1849 ± 64	97.0	0.21							

TABLE 1. (Continued)

Grain	$^{206}\text{Pb}/^{238}\text{U}$	$^{207}\text{Pb}/^{235}\text{U}$	$^{206}\text{Pb}/^{238}\text{U}$ age (Ma)	$^{207}\text{Pb}/^{235}\text{U}$ age (Ma)	%conc	Th/U
FuSs-1-34	0.0459 ± 0.0015	0.310 ± 0.035	289.0 ± 9.3	274 ± 31	105.3	0.60
FuSs-1-35	0.0430 ± 0.0020	0.519 ± 0.080	271.7 ± 12.9	425 ± 65	64.0	0.48
FuSs-1-36	0.0481 ± 0.0020	0.441 ± 0.073	302.6 ± 12.9	371 ± 62	81.6	0.45
FuSs-1-37	0.0455 ± 0.0017	0.424 ± 0.061	287.0 ± 10.9	359 ± 52	80.0	0.60
FuSs-1-38	0.0433 ± 0.0011	0.321 ± 0.030	273.2 ± 6.9	283 ± 26	96.6	0.98
FuSs-1-39	0.0493 ± 0.0019	0.308 ± 0.054	310.0 ± 11.9	272 ± 48	113.8	0.37
FuSs-1-40	0.0531 ± 0.0012	0.390 ± 0.030	333.3 ± 7.5	334 ± 26	99.7	0.76
FuSs-1-41	0.0518 ± 0.0023	0.329 ± 0.067	325.5 ± 14.3	289 ± 59	112.7	0.58
FuSs-1-42	0.0432 ± 0.0010	0.297 ± 0.024	272.5 ± 6.1	264 ± 21	103.1	0.72
FuSs-1-43	0.0439 ± 0.0017	0.360 ± 0.055	276.7 ± 10.6	312 ± 48	88.6	0.81
FuSs-1-44	0.0497 ± 0.0020	0.400 ± 0.065	312.4 ± 12.5	341 ± 56	91.5	0.51
FuSs-1-45	0.0524 ± 0.0019	0.391 ± 0.059	329.4 ± 11.9	335 ± 51	98.3	0.86
FuSs-1-46	0.0508 ± 0.0020	0.396 ± 0.064	319.6 ± 12.3	339 ± 55	94.4	0.52
FuSs-1-47	0.0437 ± 0.0015	0.290 ± 0.043	275.7 ± 9.5	258 ± 38	106.7	0.60
FuSs-1-48	0.0476 ± 0.0015	0.356 ± 0.044	299.9 ± 9.5	309 ± 38	97.0	0.49
FuSs-1-49	0.0469 ± 0.0014	0.377 ± 0.040	295.8 ± 8.8	325 ± 35	91.0	1.03
FuSs-1-50	0.0439 ± 0.0023	0.422 ± 0.098	276.7 ± 14.8	358 ± 83	77.4	0.61
FuSs-1-51	0.0513 ± 0.0018	0.412 ± 0.057	322.7 ± 11.3	350 ± 48	92.2	0.47
FuSs-1-52	0.0530 ± 0.0024	0.422 ± 0.086	332.7 ± 15.1	358 ± 73	93.0	0.59
FuSs-1-53	0.0526 ± 0.0016	0.380 ± 0.043	330.6 ± 9.9	327 ± 37	101.0	0.46
FuSs-1-54	0.0477 ± 0.0014	0.386 ± 0.045	300.1 ± 8.9	331 ± 38	90.6	0.52
FuSs-1-55	0.0454 ± 0.0016	0.329 ± 0.050	286.5 ± 10.1	288 ± 44	99.3	0.43
FuSs-1-56	0.0475 ± 0.0012	0.311 ± 0.034	299.2 ± 7.8	275 ± 30	108.7	0.60
FuSs-1-57	0.0472 ± 0.0017	0.358 ± 0.054	297.5 ± 10.7	311 ± 47	95.7	0.32
FuSs-1-58	0.0526 ± 0.0010	0.391 ± 0.024	330.3 ± 6.3	335 ± 21	98.5	0.88
FuSs-1-59	0.0511 ± 0.0017	0.399 ± 0.054	321.1 ± 10.7	341 ± 46	94.3	0.46
FuSs-1-60	0.0473 ± 0.0018	0.374 ± 0.059	297.9 ± 11.3	323 ± 51	92.4	0.72
FuSs-1-61	0.0468 ± 0.0011	0.359 ± 0.032	294.5 ± 7.1	312 ± 28	94.5	0.77
FuSs-1-62	0.0462 ± 0.0011	0.368 ± 0.032	291.3 ± 6.9	318 ± 28	91.5	0.46
FuSs-1-63	0.0463 ± 0.0020	0.391 ± 0.074	291.8 ± 12.7	335 ± 63	87.2	0.49
FuSs-1-64	0.0461 ± 0.0016	0.392 ± 0.054	290.7 ± 10.3	336 ± 47	86.6	0.45
FuSs-1-65	0.0449 ± 0.0012	0.463 ± 0.040	283.0 ± 7.8	386 ± 33	73.3	0.65
FuSs-1-66	0.0483 ± 0.0016	0.323 ± 0.046	304.1 ± 10.1	284 ± 41	107.0	0.46
FuSs-1-67	0.0515 ± 0.0015	0.390 ± 0.041	323.8 ± 9.3	334 ± 35	96.9	0.43
FuSs-1-68	0.0490 ± 0.0018	0.392 ± 0.060	308.3 ± 11.4	336 ± 52	91.8	0.66
FuSs-1-69	0.0444 ± 0.0011	0.339 ± 0.028	280.3 ± 7.1	297 ± 24	94.5	0.51
FuSs-1-70	0.0481 ± 0.0017	0.317 ± 0.049	302.6 ± 10.5	280 ± 43	108.2	0.39
FuSs-1-71	0.0427 ± 0.0017	0.371 ± 0.060	269.8 ± 10.7	321 ± 52	84.2	0.48
FuSs-1-72	0.0455 ± 0.0016	0.341 ± 0.053	287.0 ± 10.3	298 ± 46	96.4	0.50
FuSs-1-73	0.0447 ± 0.0014	0.341 ± 0.045	281.9 ± 8.8	298 ± 39	94.6	0.60
FuSs-1-74	0.0422 ± 0.0012	0.368 ± 0.041	266.2 ± 7.6	318 ± 36	83.7	0.57
FuSs-1-75	0.3944 ± 0.0051	7.620 ± 0.169	2143.0 ± 27.5	2187 ± 48	98.0	0.46
FuSs-1-76	0.0596 ± 0.0019	0.677 ± 0.074	373.4 ± 11.6	525 ± 57	71.1	0.41
FuSs-1-77	0.0681 ± 0.0017	0.823 ± 0.067	424.5 ± 10.5	609 ± 49	69.7	0.51
FuSs-1-78	0.0497 ± 0.0014	0.473 ± 0.052	312.5 ± 9.1	393 ± 43	79.5	0.45
FuSs-1-79	0.0505 ± 0.0015	0.453 ± 0.046	317.5 ± 9.6	379 ± 39	83.8	0.65
FuSs-1-80	0.0451 ± 0.0012	0.333 ± 0.038	284.3 ± 7.3	292 ± 24	97.5	0.79
FuSs-1-81	0.0465 ± 0.0012	0.341 ± 0.031	293.0 ± 7.8	298 ± 27	98.5	0.44
FuSs-1-82	0.0428 ± 0.0016	0.330 ± 0.049	269.9 ± 10.2	290 ± 43	93.2	0.51
FuSs-1-83	0.0506 ± 0.0014	0.368 ± 0.037	318.2 ± 9.1	318 ± 32	100.1	0.35
FuSs-1-84	0.0473 ± 0.0023	0.374 ± 0.074	298.2 ± 14.6	322 ± 64	92.5	0.43

TABLE 1. (Continued)

Grain	$^{206}\text{Pb}/^{238}\text{U}$	$^{207}\text{Pb}/^{235}\text{U}$	$^{206}\text{Pb}/^{238}\text{U}$ age (Ma)	$^{207}\text{Pb}/^{235}\text{U}$ age (Ma)	%conc	Th/U	Grain	$^{206}\text{Pb}/^{238}\text{U}$	$^{207}\text{Pb}/^{235}\text{U}$	$^{206}\text{Pb}/^{238}\text{U}$ age (Ma)	$^{207}\text{Pb}/^{235}\text{U}$ age (Ma)	%conc	Th/U
Hilg-1-11	0.0191 \pm 0.0005	0.138 \pm 0.015	122.0 \pm 3.2	131 \pm 15	93.1	0.55	13072103-36	0.0712 \pm 0.0026	0.570 \pm 0.036	443.6 \pm 15.9	458 \pm 29	96.9	0.59
Hilg-1-12	0.0194 \pm 0.0007	0.136 \pm 0.023	123.7 \pm 7.7	129 \pm 22	95.9	0.52	13072103-37	0.0793 \pm 0.0029	0.734 \pm 0.052	492.0 \pm 18.1	559 \pm 40	88.0	0.41
Hilg-1-13	0.0208 \pm 0.0006	0.383 \pm 0.033	132.7 \pm 4.0	329 \pm 29	40.3	0.47	13072103-38	0.1673 \pm 0.0059	1.631 \pm 0.092	997.3 \pm 35.2	982 \pm 55	101.5	0.16
Hilg-1-14	0.0209 \pm 0.0005	0.146 \pm 0.014	133.3 \pm 3.1	138 \pm 14	96.3	0.64	13072103-39	0.0433 \pm 0.0018	0.386 \pm 0.047	273.2 \pm 11.9	332 \pm 40	82.4	0.50
Hilg-1-15	0.0193 \pm 0.0006	0.145 \pm 0.018	123.2 \pm 3.5	137 \pm 17	89.9	0.55	13072103-40	0.0430 \pm 0.0018	0.366 \pm 0.039	271.3 \pm 11.1	317 \pm 34	85.6	0.50
Hilg-1-16	0.0198 \pm 0.0005	0.142 \pm 0.015	126.2 \pm 3.1	135 \pm 14	93.7	0.53	13072103-41	0.0422 \pm 0.0014	0.292 \pm 0.036	266.2 \pm 9.1	260 \pm 32	102.3	0.83
Hilg-1-17	0.0205 \pm 0.0005	0.144 \pm 0.016	130.5 \pm 3.3	137 \pm 15	95.6	0.57	13072103-42	0.0431 \pm 0.0013	0.365 \pm 0.030	272.0 \pm 7.9	316 \pm 26	86.2	0.33
Hilg-1-18	0.0199 \pm 0.0005	0.164 \pm 0.017	126.9 \pm 3.3	155 \pm 16	88.2	0.52	13072103-43	0.0776 \pm 0.0021	0.653 \pm 0.048	482.0 \pm 13.3	511 \pm 38	94.4	0.21
Hilg-1-19	0.0190 \pm 0.0005	0.151 \pm 0.015	121.1 \pm 3.0	143 \pm 14	84.9	0.66	13072103-44	0.0413 \pm 0.0012	0.318 \pm 0.028	260.9 \pm 7.6	280 \pm 25	93.1	0.53
Hilg-1-20	0.0207 \pm 0.0008	0.127 \pm 0.024	132.4 \pm 5.1	122 \pm 23	108.7	0.47	13072103-45	0.0404 \pm 0.0011	0.318 \pm 0.025	255.5 \pm 7.2	280 \pm 22	91.2	0.46
Hilg-1-21	0.0193 \pm 0.0005	0.135 \pm 0.017	123.5 \pm 3.2	147 \pm 16	84.2	0.53	13072103-46	0.0388 \pm 0.0011	0.276 \pm 0.023	245.2 \pm 7.0	247 \pm 21	99.1	1.19
Hilg-1-22	0.0194 \pm 0.0004	0.133 \pm 0.013	124.1 \pm 2.7	126 \pm 12	98.2	0.69	13072103-47	0.0419 \pm 0.0011	0.321 \pm 0.024	264.4 \pm 7.2	283 \pm 21	93.5	0.38
Hilg-1-23	0.0187 \pm 0.0004	0.112 \pm 0.012	119.7 \pm 3.8	108 \pm 12	111.0	0.54	13072103-48	0.0414 \pm 0.0014	0.402 \pm 0.044	261.8 \pm 9.0	343 \pm 38	76.2	0.57
Hilg-1-24	0.0208 \pm 0.0006	0.144 \pm 0.018	133.0 \pm 3.6	137 \pm 17	97.3	0.56	13072103-49	0.0397 \pm 0.0014	0.294 \pm 0.037	250.7 \pm 8.8	262 \pm 33	95.8	0.76
							13072103-50	0.0570 \pm 0.0018	0.467 \pm 0.043	357.2 \pm 11.6	389 \pm 36	91.7	0.99
							13072103-51	0.1442 \pm 0.0040	1.431 \pm 0.076	868.2 \pm 24.1	902 \pm 48	96.3	0.70
							13072103-52	0.0399 \pm 0.0013	0.326 \pm 0.032	252.2 \pm 8.5	287 \pm 28	88.0	0.55
							13072103-53	0.0428 \pm 0.0014	0.359 \pm 0.031	270.3 \pm 8.6	311 \pm 27	86.8	0.55
							13072103-54	0.2221 \pm 0.0060	2.655 \pm 0.120	1293.0 \pm 34.8	1316 \pm 60	98.3	0.32
							13072103-55	0.0399 \pm 0.0012	0.288 \pm 0.024	252.4 \pm 7.7	257 \pm 21	98.2	0.52
							13072103-56	0.0494 \pm 0.0020	0.397 \pm 0.054	310.7 \pm 12.3	339 \pm 46	91.6	0.54
							13072103-57	0.0423 \pm 0.0012	0.323 \pm 0.023	266.9 \pm 7.8	284 \pm 20	94.0	0.45
							13072103-58	0.0416 \pm 0.0014	0.383 \pm 0.035	263.0 \pm 9.0	329 \pm 30	79.9	0.68
							13072103-59	0.0479 \pm 0.0022	0.714 \pm 0.093	301.8 \pm 14.0	547 \pm 71	55.2	0.40
							13072103-60	0.0436 \pm 0.0015	0.344 \pm 0.034	275.2 \pm 9.6	299 \pm 30	92.0	0.46
							13072103-61	0.0445 \pm 0.0015	0.343 \pm 0.031	280.5 \pm 9.4	300 \pm 27	93.4	0.38
							13072103-62	0.0433 \pm 0.0015	0.346 \pm 0.037	273.4 \pm 9.8	302 \pm 32	90.5	0.63
							13072103-63	0.0469 \pm 0.0018	0.407 \pm 0.047	295.4 \pm 11.2	347 \pm 40	85.2	0.62
							13072103-64	0.0459 \pm 0.0019	0.408 \pm 0.055	289.3 \pm 12.0	348 \pm 47	83.2	0.48
							13072103-65	0.0397 \pm 0.0015	0.321 \pm 0.037	250.8 \pm 9.4	282 \pm 33	88.8	0.61
							13072103-66	0.0425 \pm 0.0017	0.342 \pm 0.044	268.4 \pm 10.6	299 \pm 39	89.8	0.51
							13072103-67	0.0398 \pm 0.0018	0.305 \pm 0.025	251.8 \pm 11.4	270 \pm 22	93.1	0.57
							13072103-68	0.0410 \pm 0.0019	0.288 \pm 0.023	259.1 \pm 11.8	257 \pm 21	100.7	0.74
							13072103-69	0.5178 \pm 0.0240	13.337 \pm 0.864	2690.0 \pm 124.7	2704 \pm 175	99.5	1.46
							13072103-70	0.0511 \pm 0.0033	0.503 \pm 0.103	321.5 \pm 20.8	414 \pm 85	77.7	0.48
							13072103-71	0.0404 \pm 0.0018	0.295 \pm 0.023	255.6 \pm 11.6	262 \pm 21	97.4	0.29
							13072103-72	0.0445 \pm 0.0023	0.413 \pm 0.064	280.7 \pm 15.7	351 \pm 55	80.0	0.38
							13072103-73	0.0420 \pm 0.0021	0.307 \pm 0.038	265.0 \pm 13.2	272 \pm 34	97.4	0.99
							13072103-74	0.1567 \pm 0.0069	1.494 \pm 0.088	938.2 \pm 41.3	928 \pm 55	101.1	0.72
							13072103-75	0.0484 \pm 0.0022	0.354 \pm 0.029	304.4 \pm 13.9	308 \pm 26	98.8	1.01
							13072103-76	0.0584 \pm 0.0027	0.555 \pm 0.070	366.1 \pm 17.2	448 \pm 57	81.7	0.66
							13072103-77	0.0399 \pm 0.0017	0.297 \pm 0.029	252.2 \pm 10.5	264 \pm 25	95.4	0.74
							13072103-78	0.0467 \pm 0.0023	0.365 \pm 0.056	294.3 \pm 14.3	330 \pm 48	89.1	0.40
							13072103-79	0.0409 \pm 0.0019	0.323 \pm 0.043	258.1 \pm 12.0	284 \pm 38	90.7	0.65
							13072103-80	0.0428 \pm 0.0018	0.326 \pm 0.035	270.1 \pm 11.6	287 \pm 31	94.2	0.51
							13072103-81	0.0456 \pm 0.0020	0.303 \pm 0.038	287.5 \pm 12.8	269 \pm 34	107.0	0.51
							13072103-82	0.0432 \pm 0.0019	0.304 \pm 0.034	272.5 \pm 11.8	269 \pm 30	101.2	0.73
							13072103-83	0.0424 \pm 0.0019	0.375 \pm 0.041	267.8 \pm 11.8	324 \pm 35	82.8	0.48
							13072103-84	0.0450 \pm 0.0019	0.337 \pm 0.035	283.9 \pm 12.1	295 \pm 31	96.4	0.56
							13072103-85	0.0456 \pm 0.0022	0.385 \pm 0.060	287.3 \pm 14.0	331 \pm 51	86.9	0.55
							13072103-86	0.0418 \pm 0.0016	0.300 \pm 0.027	263.9 \pm 10.1	266 \pm 24	99.0	0.83
Sandstone of the Shingai Unit (13072103; 33° 36' 16.44" N, 133° 28' 22.83" E)													
13072103-1	0.0377 \pm 0.0009	0.336 \pm 0.020	238.4 \pm 5.4	294 \pm 17	81.1	1.22	13072103-51	0.1442 \pm 0.0040	1.431 \pm 0.076	868.2 \pm 24.1	902 \pm 48	96.3	0.70
13072103-2	0.0411 \pm 0.0012	0.325 \pm 0.032	259.4 \pm 7.5	286 \pm 28	90.7	1.13	13072103-52	0.0399 \pm 0.0013	0.326 \pm 0.032	252.2 \pm 8.5	287 \pm 28	88.0	0.55
13072103-3	0.0543 \pm 0.0014	0.402 \pm 0.033	341.0 \pm 8.8	343 \pm 28	99.4	0.66	13072103-53	0.0428 \pm 0.0014	0.359 \pm 0.031	270.3 \pm 8.6	311 \pm 27	86.8	0.55
13072103-4	0.0433 \pm 0.0011	0.346 \pm 0.029	273.1 \pm 7.2	302 \pm 25	90.6	0.39	13072103-54	0.2221 \pm 0.0060	2.655 \pm 0.120	1293.0 \pm 34.8	1316 \pm 60	98.3	0.32
13072103-5	0.1965 \pm 0.0043	2.143 \pm 0.103	1156.3 \pm 25.3	1163 \pm 56	99.4	1.09	13072103-55	0.0399 \pm 0.0012	0.288 \pm 0.024	252.4 \pm 7.7	257 \pm 21	98.2	0.52
13072103-6	0.0426 \pm 0.0014	0.517 \pm 0.054	268.8 \pm 9.1	423 \pm 44	63.5	0.58	13072103-56	0.0494 \pm 0.0020	0.397 \pm 0.054	310.7 \pm 12.3	339 \pm 46	91.6	0.54
13072103-7	0.0820 \pm 0.0017	0.690 \pm 0.023	508.2 \pm 10.3	533 \pm 18	95.4	0.34	13072103-57	0.0423 \pm 0.0012	0.323 \pm 0.023	266.9 \pm 7.8	284 \pm 20	94.0	0.45
13072103-8	0.0440 \pm 0.0011	0.368 \pm 0.028	277.8 \pm 7.2	318 \pm 24	87.3	0.66	13072103-58	0.0416 \pm 0.0014	0.383 \pm 0.035	263.0 \pm 9.0	329 \pm 30	79.9	0.68
13072103-9	0.1226 \pm 0.0031	1.155 \pm 0.052	745.7 \pm 18.6	780 \pm 35	95.6	0.19	13072103-59	0.0479 \pm 0.0022	0.714 \pm 0.093	301.8 \pm 14.0	547 \pm 71	55.2	0.40
13072103-10	0.0409 \pm 0.0012	0.323 \pm 0.026	258.7 \pm 7.5	284 \pm 23	91.0	0.54	13072103-60	0.0445 \pm 0.0015	0.344 \pm 0.031	275.2 \pm 9.6	299 \pm 30	92.0	0.46
13072103-11	0.2826 \pm 0.0069	4.053 \pm 0.147	1604.										

Grain	$^{206}\text{Pb}/^{235}\text{U}$	$^{207}\text{Pb}/^{235}\text{U}$	$^{206}\text{Pb}/^{238}\text{U}$ (Ma)	$^{40}\text{Ar}/^{39}\text{Ar}$ U age (Ma)	%conc	Th/U	Grain	$^{206}\text{Pb}/^{238}\text{U}$	$^{207}\text{Pb}/^{235}\text{U}$	$^{206}\text{Pb}/^{235}\text{U}$ age (Ma)	$^{40}\text{Ar}/^{39}\text{Ar}$ U age (Ma)	%conc	Th/U
13072103-87	0.0417 ± 0.0017	0.311 ± 0.034	263.6 ± 10.8	275 ± 30	95.8	0.63	16091701-26	0.0506 ± 0.0024	0.294 ± 0.072	318.2 ± 15.4	262 ± 64	121.6	0.49
13072103-88	0.1623 ± 0.0058	1.633 ± 0.092	969.7 ± 34.4	991 ± 55	97.9	0.17	16091701-27	0.0473 ± 0.0015	0.312 ± 0.038	297.8 ± 9.4	276 ± 34	107.9	0.25
13072103-89	0.0418 ± 0.0016	0.315 ± 0.029	264.1 ± 10.2	278 ± 25	95.1	0.83	16091701-28	0.0408 ± 0.0015	0.308 ± 0.045	257.7 ± 9.6	273 ± 40	94.5	0.56
13072103-90	0.0396 ± 0.0015	0.322 ± 0.027	250.6 ± 9.6	284 ± 24	88.4	0.79	16091701-29	0.0434 ± 0.0023	0.324 ± 0.072	273.7 ± 14.6	285 ± 64	96.0	0.41
13072103-91	0.1325 ± 0.0048	1.121 ± 0.075	802.1 ± 28.9	806 ± 50	99.5	0.92	16091701-30	0.0419 ± 0.0033	0.317 ± 0.107	264.7 ± 21.1	280 ± 95	94.6	0.47
13072103-92	0.2466 ± 0.0087	3.155 ± 0.139	1420.9 ± 50.6	1446 ± 64	98.3	0.49	16091701-31	0.0452 ± 0.0021	0.443 ± 0.067	284.7 ± 13.2	372 ± 64	76.5	0.38
13072103-93	0.0430 ± 0.0017	0.330 ± 0.030	271.3 ± 10.0	289 ± 26	93.7	0.53	16091701-32	0.0453 ± 0.0019	0.392 ± 0.074	283.7 ± 12.5	336 ± 54	83.0	0.53
13072103-94	0.0442 ± 0.0022	0.472 ± 0.068	278.9 ± 14.1	393 ± 57	71.0	0.98	16091701-33	0.0431 ± 0.0016	0.306 ± 0.046	271.9 ± 10.2	271 ± 41	100.2	0.79
13072103-95	0.0654 ± 0.0031	0.465 ± 0.070	408.3 ± 19.5	388 ± 58	105.4	0.82	16091701-34	0.0411 ± 0.0017	0.334 ± 0.052	259.4 ± 7.5	293 ± 46	88.6	0.42
13072103-96	0.0403 ± 0.0015	0.294 ± 0.021	254.6 ± 9.8	262 ± 19	97.4	0.28	16091701-35	0.3251 ± 0.0070	0.4983 ± 0.196	1814.7 ± 38.9	1816 ± 72	98.9	0.64
13072103-97	0.0417 ± 0.0019	0.304 ± 0.039	263.4 ± 11.9	269 ± 35	97.8	0.90	16091701-36	0.0393 ± 0.0020	0.238 ± 0.060	248.7 ± 12.9	217 ± 55	114.7	0.69
13072103-98	0.0401 ± 0.0021	0.317 ± 0.034	253.7 ± 10.7	280 ± 30	90.8	0.59	16091701-37	0.0460 ± 0.0015	0.286 ± 0.041	289.9 ± 9.2	256 ± 37	713.4	0.34
13072103-99	0.0439 ± 0.0021	0.385 ± 0.056	277.0 ± 13.5	331 ± 48	83.7	0.60	16091701-38	0.0405 ± 0.0013	0.325 ± 0.043	285.9 ± 8.4	286 ± 38	89.4	0.72
13072103-100	0.1669 ± 0.0064	1.639 ± 0.112	995.1 ± 38.2	985 ± 67	101.0	0.77	16091701-39	0.0407 ± 0.0019	0.304 ± 0.062	257.0 ± 12.0	270 ± 55	95.3	0.66
13072103-101	0.0870 ± 0.0034	0.706 ± 0.052	537.8 ± 20.8	542 ± 40	99.1	0.51	16091701-40	0.0399 ± 0.0018	0.426 ± 0.066	305.6 ± 11.8	360 ± 56	84.9	0.51
13072103-102	0.0417 ± 0.0016	0.302 ± 0.022	263.1 ± 10.1	268 ± 19	98.1	0.32	16091701-41	0.0486 ± 0.0019	0.439 ± 0.071	269.1 ± 14.3	267 ± 63	100.7	0.69
13072103-103	0.0408 ± 0.0034	0.408 ± 0.054	255.1 ± 8.5	347 ± 29	73.5	0.65	16091701-42	0.0419 ± 0.0025	0.301 ± 0.083	264.5 ± 16.1	267 ± 74	99.1	0.63
13072103-104	0.298 ± 0.018	2.573 ± 7.6	265 ± 16	265 ± 16	97.3	0.48	16091701-43	0.0435 ± 0.0013	0.299 ± 0.038	274.5 ± 8.0	265 ± 33	103.5	0.87
13072103-105	1.601 ± 0.094	925.1 ± 27.7	970 ± 57	970 ± 57	95.3	0.21	16091701-44	0.0408 ± 0.0019	0.340 ± 0.065	257.6 ± 11.7	297 ± 56	86.7	0.52
13072103-106	0.368 ±												

TABLE 1. (Continued)

Grain	$^{206}\text{Pb}/^{238}\text{U}$	$^{207}\text{Pb}/^{235}\text{U}$	$^{206}\text{Pb}/^{238}\text{U}$ age (Ma)	$^{207}\text{Pb}/^{235}\text{U}$ age (Ma)	%conc	Th/U
16091701-77	0.0402 ± 0.0017	0.352 ± 0.061	254.3 ± 10.8	306 ± 53	83.1	0.53
16091701-78	0.0426 ± 0.0015	0.328 ± 0.050	268.8 ± 9.6	288 ± 44	93.3	0.41
16091701-79	0.0415 ± 0.0014	0.318 ± 0.046	262.0 ± 8.9	281 ± 40	93.3	0.56
16091701-80	0.0401 ± 0.0019	0.331 ± 0.064	253.6 ± 12.1	291 ± 56	87.3	0.53
16091701-81	0.0400 ± 0.0013	0.307 ± 0.040	252.9 ± 8.5	272 ± 36	93.0	0.65
16091701-82	0.0422 ± 0.0024	0.793 ± 0.133	266.3 ± 15.3	593 ± 99	44.9	0.65
16091701-83	0.0443 ± 0.0014	0.355 ± 0.042	279.6 ± 8.7	308 ± 36	90.7	0.38
16091701-84	0.0386 ± 0.0007	0.277 ± 0.014	243.9 ± 4.7	248 ± 13	98.3	1.28
16091701-85	0.0447 ± 0.0011	0.338 ± 0.029	282.2 ± 7.0	296 ± 25	95.4	0.52
16091701-86	0.0412 ± 0.0009	0.292 ± 0.020	260.4 ± 5.6	260 ± 18	100.0	0.96
16091701-87	0.0441 ± 0.0014	0.350 ± 0.041	278.5 ± 8.6	305 ± 36	91.4	0.60
16091701-88	0.0434 ± 0.0018	0.342 ± 0.057	273.8 ± 11.3	298 ± 50	91.8	0.67
16091701-89	0.0472 ± 0.0030	0.285 ± 0.109	297.4 ± 19.1	255 ± 97	116.8	0.53
16091701-90	0.0464 ± 0.0016	0.378 ± 0.040	292.6 ± 9.9	325 ± 35	89.9	0.48
16091701-91	0.0433 ± 0.0017	0.285 ± 0.045	273.5 ± 10.7	255 ± 40	107.4	0.74
16091701-92	0.0484 ± 0.0020	0.371 ± 0.058	304.4 ± 12.4	320 ± 50	95.0	0.71
16091701-93	0.0436 ± 0.0016	0.300 ± 0.042	274.9 ± 10.2	266 ± 37	103.3	0.66
16091701-94	0.0422 ± 0.0015	0.336 ± 0.041	266.3 ± 9.5	294 ± 36	90.4	0.95
16091701-95	0.0488 ± 0.0022	0.402 ± 0.072	307.3 ± 13.9	343 ± 61	89.6	0.61
16091701-96	0.0485 ± 0.0019	0.371 ± 0.052	305.3 ± 11.7	321 ± 45	95.2	0.52